MODELLING OF MICRO ELECTRO DISCHARGE MACHINING IN AEROSPACE MATERIAL

A Thesis Submitted to

National Institute of Technology, Rourkela

(Deemed University)

In Partial fulfilment of the requirement for the degree of

Master of Technology
In
Mechanical Engineering

By
VED PRAKASH KISHOR
(211 ME 2350)
Under The Guidance of
(Prof . K . P. Maity)

Department of Mechanical Engineering

National Institute of Technology

Rourkela -769 008 (India)

2013

MODELLING OF MICRO ELECTRO DISCHARGE MACHINING IN AEROSPACE MATERIAL

A Thesis Submitted to

National Institute of Technology, Rourkela

(Deemed University)

In Partial fulfilment of the requirement for the degree of

Master of Technology
In
Mechanical Engineering

By
VED PRAKASH KISHOR

Department of Mechanical Engineering

National Institute of Technology

Rourkela -769 008 (India)

2013

Dedicated to

My Most

Loving Family

National Institute of Technology

Rourkela

CERTIFICATE

This is to certify that the thesis entitled **—Modelling of Micro Electro Discharge Machining in Aerospace material** submitted to the National Institute of Technology, Rourkela (Deemed University) by **Ved Prakash Kishor** Roll No. 211 ME 2350 for the award of the Degree of **Master of Technology** in Mechanical Engineering with specialization in **—Production Engineering** is a record of bonafide research work carried out by him under my supervision and guidance. The results presented in this thesis has not been, to the best of my knowledge, submitted to any other University or Institute for the award of any degree or diploma. The thesis, in my opinion, has reached the standards fulfilling the requirement for the award of the degree of Master of technology in accordance with regulations of the Institute.

Place: Rourkela

Date

Dr. K. P. Maity
Professor
Department of Mechanical Engineering
National Institute of Technology, Rourkela

ACKNOWLEDGEMENT

I express my deep sense of gratitude and indebtedness to my thesis supervisor Dr. K. P. Maity, Professor and Head of Department of Mechanical Engineering for providing precious guidance, inspiring discussions and constant supervision throughout the course of this work. His timely help, constructive criticism, and conscientious efforts made it possible to present the work contained in this thesis.

This work is also the outcome of the blessing, guidance, love and support of my family, I express my sincere thanks to Mr. Himansu and Anshuman Kumar, PhD Research Scholars. . I am also thankful to all the staff members of the department of Mechanical Engineering and to all my well wishers for their inspiration and help.

I feel pleased and privileged to fulfil my parent‘s ambition and I am greatly indebted to them for bearing the inconvenience during my M-Tech course. I express my appreciation to my friends Shakti , Neelam, Sanjay, Chandu, Sandeep, Reliance and Kanhu sir for their understanding, patience and active co-operation throughout my M-Tech course finally.

Date: (Ved Prakash Kishor)

Mechanical Engineering -211ME2350

NIT Rourkela

Abstract

Micro EDM is a non-conventional, non-contact machining process where the material is melted and removed from the work surface by the sparks produced between anode and cathode immersed inside the dielectric medium. In the present day scenario the micro products play a crucial role in the field of biomedical, nuclear, defense, transportation and space application so its necessary to produce such components with desired precision and accuracy on the same ground my thesis revolve around the same concept of advanced and precision manufacturing. EDM has been used for decades for machining pieces for the aeronautical industry, but surface integrity, and consequently the reliability of the machined parts have been questioned for long time due to the thermal nature of this machining process. In recent years, efforts have been put on modeling of the EDM process, being thermal modeling of the process one promising alternative. Used for machining micro features like through, blind and tapered micro holes, straight, circular and spiral micro channels which are used in MEMS devices. Micro EDM is a better alternative to micro fabrication techniques for production of some of the 3Dmicrostructure.In the present investigation optimization of micro EDM has been carried out by considering process parameters like voltage, current and pulse-on time and responses machining time, circularity error and recast layer thickness using L9 orthogonal array and it has been optimized by grey based taguchi method. FEA modelling of micro EDM process has also been carried out to predict the MRR and residual stress for single discharge.

Keywords- Micro EDM, Metal removal rate, Residual stress analysis, Thermal modelling.

Contents

List of figure

List of Tables

1. Introduction

1.1 Introduction of Micro EDM

Micro EDM is a non-conventional, non-contact machining process which has been used for machining micro features like through, blind and tapered micro holes, straight, circular and spiral micro channels which are used in MEMS devices, produce dies, molds and metalworking industries. In this modern day scenario every industries like biomedical, nuclear, defense, transportation and space needs micro product in all their industrial application because they consumes less energy and also beneficial for the environment .Micro-EDM is becoming more frequently used for the machining of complex micro-parts that traditional processes are unable to create[1,2]. By electric discharge machining (EDM) [3], material with electric conductivity can be machined in complicated shapes with high accuracy regardless of the material hardness. Especially, micro-EDM [4-5] is applied to the machining of holes, such as nozzles, orifices and slits, and dies for micro-components for dimensions ranging from a few micrometers to hundreds of micrometers. It is an ideal process to obtain burr-free micron-size apertures with high aspect ratios in most metals. Similar to conventional EDM, material is removed in micro-EDM by a series of rapidly recurring electric spark discharges between the cutting tool (the tool electrode) and the work piece. Typical micro-EDM tool electrode ranges in size between 5 and 300 mm diameter. During the process, the work piece is immersed in a dielectric fluid and a voltage is applied between a tool electrode and work piece. When the tool electrode is brought close to the work piece, sparks will arc across the inter electrode gap, melting and vaporizing microscopic bits of the work piece. The molten work piece particles harden and are washed away by the continuously flushing dielectric fluid. The area and the movement of the tool determine the shape of the cavity created in the work piece (6).

Micro Electro Discharge Machining is a market emergent processing technology due to the industrial attention and the increasing number of applications. Its process concept is not very different to conventional EDM. This fact makes easier to know the features that can be machined. In spite of this, the process similarities, the process and the applied systems present some important differences with respect to conventional EDM. Compared to many current methods of conventional machining which are limited to two-dimensions, micro-EDM is capable of creating complex three-dimensional shapes with high aspect ratios. Micro-electro-discharge machining is an striking micro machining technique that is used to

cut electrically conductive material, like steel, graphite, silicon [7], and magnetic materials [8], [9], as well as permanent magnets [10].

Differences between micro EDM and conventional EDM:-

1. The main significant difference between micro EDM and EDM is the dimension of the plasma channel radius that arises, much smaller than the electrode in conventional EDM during the spark: but the size is equivalent for micro EDM [11].

(Such type of small electrodes presents a limited heat conduction and low mass to dissipate the spark heat.)

2. In case of energy effects, the Flushing pressure acting on the electrode varies much with respect to the conventional EDM process. In conventional EDM, the higher precision is achieved only if electrode vibrations and wear are limited. This implies an important inadequacy for conventional EDM that turns out to be more preventive in micro EDM.

3. In case of discharge for each discharge, the electrode wear in micro EDM is proportionally higher than conventional EDM. The electrode is softened, which depends on the section reduction on the spark energy.

In micro EDM, to control the unit removal rate per spark the Peak energy (Maximum value) must be limited [12, 13]. It's also recommended to use small electrodes and wires.

For micro EDM, the entire machine, the programme, the control, the measuring instruments, the electrodes, and the operators plays an important role in the process [14]. Micro EDM is a better alternative to micro fabrication techniques for production of some of the 3DMicrostructure in silicon.

Micro EDM has gained reputation for the production of microstructures because of its low set-up costs, high precision, and large design freedom. Precise positioning and machining accuracy along with CAD/CAM software enable the micro-EDM machine to produce complex shapes with a high degree of precision. The reality that micro-EDM is a non-contact process makes high precision machining on curved surfaces, inclined surfaces, and very thin sheet materials possible.

Conventional EDM is a thermal process that involves melting and vaporization of the work piece electrode by using electrical energy. This method was able to produce any intricate shape with exceptionally hard metals and other materials that were complex to machine with conventional methods. As this process is accurate and trustworthy, it has becoming an increasingly popular choice for many industries [15,16]. The finished part from EDM is burr-free and safe from thermal damage [17, 18]. When the same principle of EDM is applied at the micro meter level for micro machining and the process was called as micro-EDM. In case of conventional EDM, higher energy resulted in a higher removal rate but a rougher surface. In micro-EDM, the key aspect is to limit the energy discharge in the order of micro-Joule at higher frequency. It results is about 50 nm Ra of surface finish and 2-3 μm of accuracy [19].

As it has found earlier that basic principle of micro EDM is same as that of the conventional EDM process. In EDM, a particular amount of potential difference is applied between the tool and work piece. It is necessary that both the tool and the work material are to be electrically conductive; both are submerged in the dielectric fluid. As dielectric fluid deionised water and kerosene oil are used generally.

Main axis (Z axis) control for micro-EDM is generally made by servo system control using average discharge gap voltage accuracy of ±0.5 μm [20] which is needed to control the positions of electrodes against a machining object, i.e. gap distances, so that it gives higher effective pulse frequency or the number of discharges per unit time. Conventionally, AC/DC servo motors had been used, but the use of stepping motors for main axis (Z axis) control is more economical. For controlling the inter electrode gape a tool feed controller is also used. Depending upon the applied voltage and the gap between the tool and work piece, an electric field would be established. voltage applied to them should be enough to create an electric field higher than the dielectric rigidity of the fluid used in the process .when two electrodes is estranged by a dielectric medium, come nearer to each other, the dielectric medium that is at first non conductive breaks down and becomes conductive. In between this period sparks will be generated between the electrodes. The thermal energy released will be used to remove material by melting and evaporation. By specifically controlling the amount of energy released, it is possible to machine micro features on any electrically conductive material. In the inter electrode gap filled with insulating medium most preferably a dielectric liquid such as kerosene oil or de-ionized water between the tool and electrode, occurs the discharging of the pulsed arc. The insulating medium is to evade the electrolysis effects on the electrodes during the EDM process [21]. The shape of the electrode is copied with an offset equal to the

liquid and the gap size will be selected to minimize the inter electrode gap in order to obtain precise machining. For making sure it is safe, a certain gap width is required to avoid short circuiting especially for electrodes that are responsive to vibration or deformation. At first a high voltage current is necessary to discharge in order to rise above the dielectric breakdown strength of the small inter electrode gap formed between the electrodes is a channel of plasma (electrically conductive and ionized gas with temperature of very high) and its further development depends upon the discharge durations. Electrical resistance of such plasma channel would be very less. Then suddenly, a huge number of electrons will start flowing from the tool to the job and ions from the job to the tool this type of motion of electron is called avalanche motion of electrons. This movement of ions and electrons are shown as spark. Then these high speed electrons are strikes on the job and ions on the tool, and create a localized heat flux. Such severe contained heat flux leads to extreme instantaneous restrained rise in temperature which would be in excess of $10{,}000^{0}$C. Because of such instance rise in temperature it leads to material removal. Material removed because of the immediate vaporization of the material as well as due to melting. The molten metal is removed only partially. As the potential difference has introverted the plasma channel collapse, it generates pressure or shock waves, because of this a crater is formed by by molten metal around the spark. The physical model developed for micro-EDM is faintly different from that of conventional EDM. It uses resistance capacitance pulse generator, an advanced controller for machining in smaller inter electrode gaps and with lower discharge energies than in conventional EDM, to make the material removal characteristics of a single discharge in micro-EDM different from that of the EDM [22]. In Figure 1.2, the breakdown phase of single discharge model in micro-EDM is shown. In EDM, breakdown of dielectric fluid leads to the formation of a plasma channel between the electrodes. The plasma expands further and interacts with electrodes to remove material from the respective electrodes.

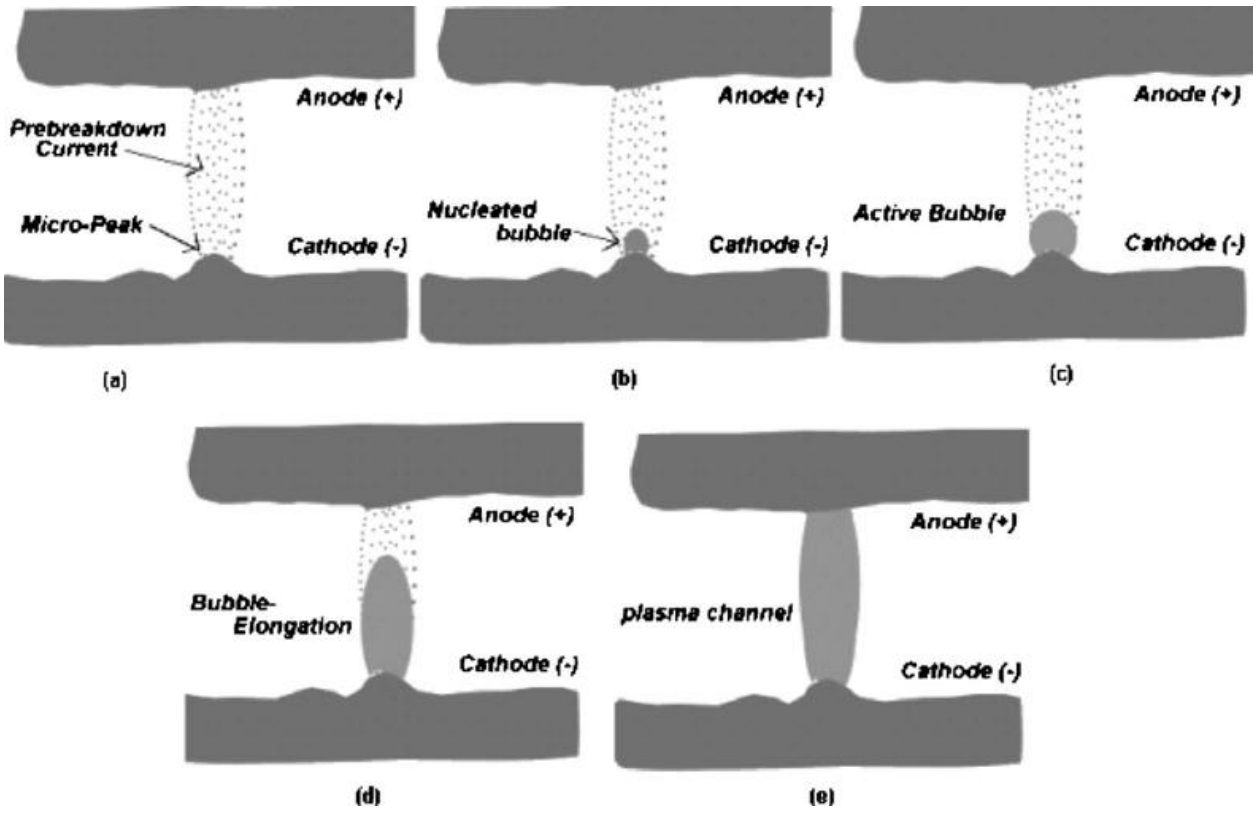

Fig.1 [23]

Figure 1 the model of breakdown stage. (a) Secretion of pre breakdown current and heating at micro peaks. (b) The nucleation of bubbles at micro-peak. (c) At the bubble interface electron impact criteria is reached. (d) Elongation of the bubbles towards anode. (e) Bubble reduced the gap between the electrodes and plasma channel at the end of the breakdown phase [22].

In micro EDM discharge occurs at very high frequencies between 10^3 and 10^6 hertz so metal removal per discharge is very small. For each pulse, discharge occurs at a particular position where the electrode materials are evaporated or ejected in the molten phase then a small crater shaped cavity is generated both on the tool electrode and work piece surfaces. In the dielectric liquid the removed material are cooled and re-solidified and forms a number of hundreds of spherical debris particles which are flushed away from the inter electrode gap by the dielectric flow. At the end of the discharge duration, the temperature of the electrode surfaces and the plasma that is in contact of the plasma quickly drops, which results in the recombination of ions and electrons, also the recovery of the dielectric breakdown strength.[21] To obtain stable condition in EDM, it is essential for the next pulse discharge to occur at a spot distanced adequately far from the previous discharge location because as the

previous location will result in having a small gap so it is infected with debris particles which may decline the dielectric breakdown strength of the liquid. Richardson et al. [23] has developed a wireless monitoring system to sense the debris accumulation. The interval for the next pulse should be so long that the plasma which is generated by the previous discharge will be fully de-ionized and the dielectric breakdown strength can be recovered around the previous discharge location by the time the next voltage is applied. If discharges occurs at the same location, resulting in thermal non-uniform erosion and overheating of the work piece.

An important point of micro-EDM is the inverted polarity of the tool electrode. Because of the polarity effect in conventional EDM with long pulse duration, the tool electrode is usually charged as anode to increase material removal rate and to reduce electrode wear. But in micro EDM as it has been used short pulse durations, this effect is reversed. Therefore, in micro-EDM, the tool electrode is usually charged as cathode [21].

1.2 Fabrication of micro EDM set up

Micro Electro Discharge Machining is one of the capable techniques where a tool of micrometer in size is used to fabricate 3-D microstructures on any electrically conducting materials. In Micro EDM, the workpiece and the tool are immersed in the dielectric medium so forms the two electrodes having different polarity. A adequately small gap is to be maintained between these electrode a pulse voltage is to be applied between them and with the application of a pulsed voltage a spark is produced which results into the melting and evaporation of the tool and the workpiece material [22]. The pulse energy provided in machining is about to few hundreds of micro joules, a small inter electrode gap of the order of few microns is to be maintained in between the tool and workpiece to sustain the spark discharges. The Micro EDM machining system is consists of two different types of driving devices for gap distance control. First one is stepping motor controlled stage and the second one is piezo electric tube [23]. The first one requires loutish adjustment while the second one requires fine adjustment. In this study, piezoactuated tool feed mechanism is considered for a economical Micro EDM equipment. Fig 1 sows the set up of a Micro EDM.

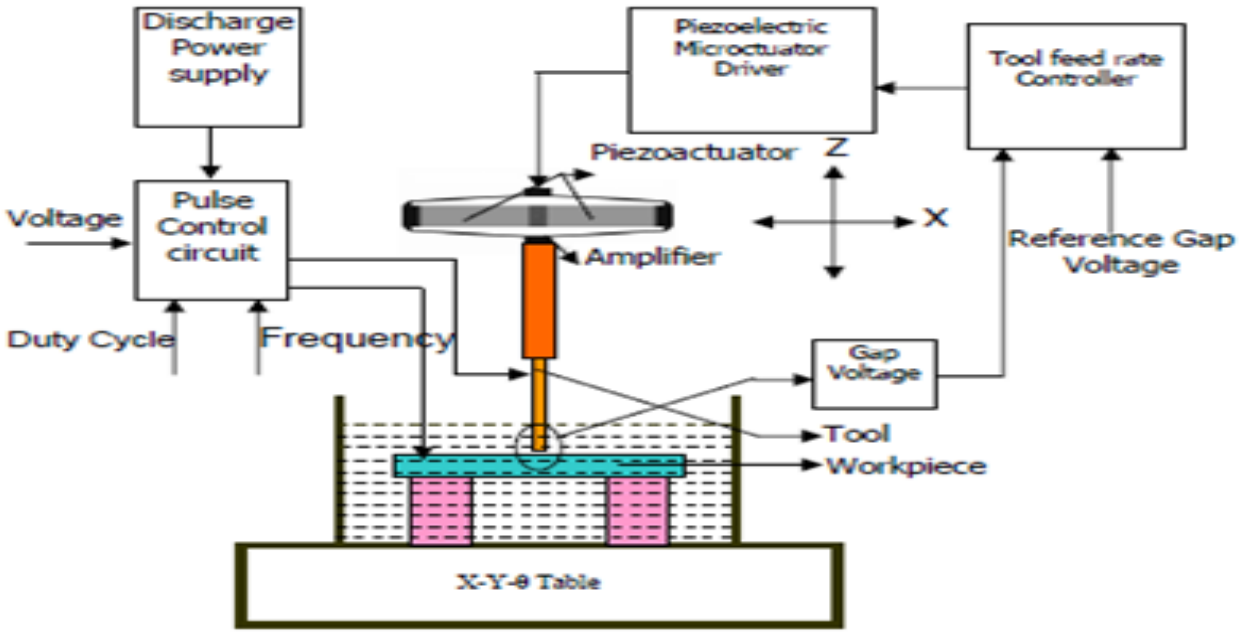

Fig.2 Micro EDM set up [22]

1.2.1 Tool feed control mechanism of the Micro EDM

Fig. 2 shows the block diagram of the tool feed control mechanism. Tool feed control is achieved based on the gap voltage as the response signal. In this set-up, the tool is moving at a low feed rate till the inter electrode gap between the tool and the workpiece reaches a inter electrode gap equivalent to the preferred spark gap. When the inter electrode gap equals to the spark gap, sparks are started to produced at the supplied pulse frequency, which results in melting and removal of materials. Because of this, spark gap and the average gap voltage also increases. At first the inter electrode gap voltage signal is to be filtered and then the DC component of this signal is to be compared with a reference voltage. After this the output, switches a generator to produce voltage signal with either positive or negative slope from the current voltage level. Then this signal is amplified and then supplied to the piezo actuator, which then moves the tool towards or away from the work piece i.e in Z –axis [23].Fig 2 shows the block diagram of tool feed control mechanism.

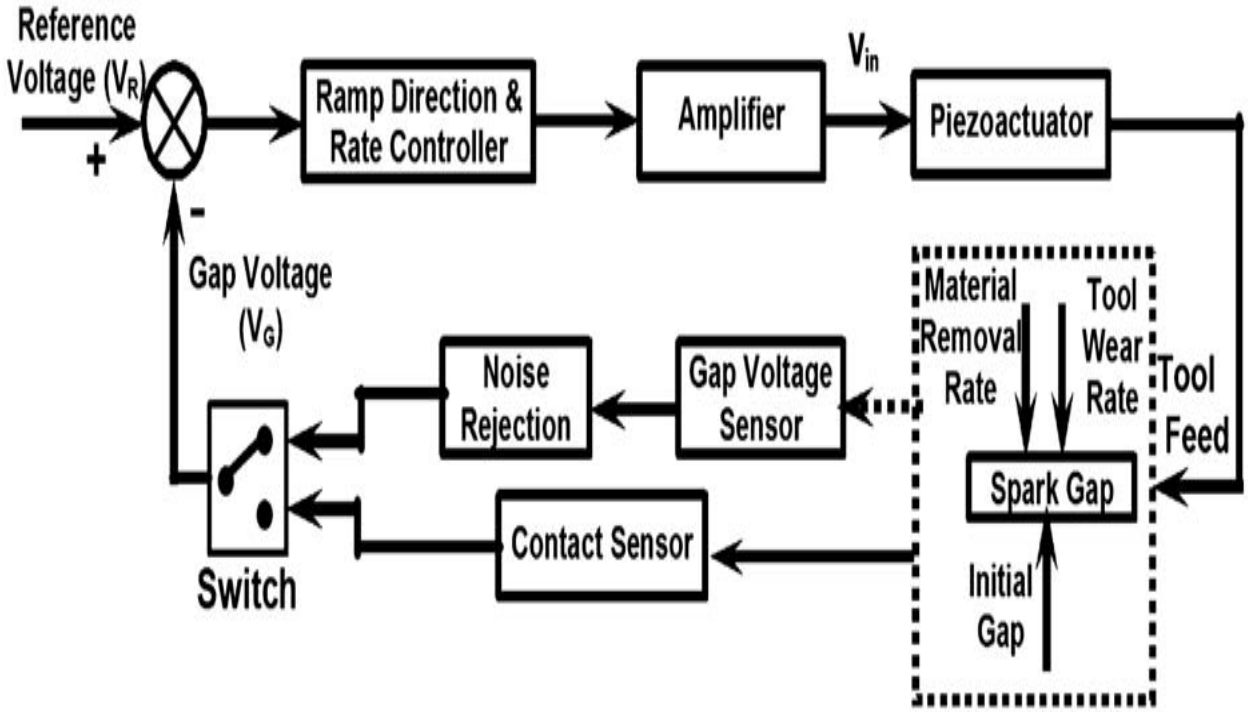

Fig.3 Block diagram of tool feed control mechanism [22]

1.2.2 Main components of the Micro EDM

1.Piezo Actuator and piezo actuator driver

As it can seen in fig 1 that the movement in Z- axis is achived by a piezo actuator. A precision drill chuck is mounted at the end of the actuator for holding electrodes. The micro piezo actuator is driven by a micro piezo driver .The movement of piezoelectric micro-actuator is to be controlled by monitoring the gap voltage between the tool and the workpiece. This piezo actuator driver is used to amplify the signal. Then this amplified signal is directly sent to the micro piezo actuator which feeds the tool. As a result of this the tool is moved towards the work piece (i.e along Z-axis) until the discharge takes place between tool and workpiece. Fig.3 shows the block diagram model of a piezo actuator. In Fig.4 its seen that the movement of the tool along the x, y and z axis respectively.

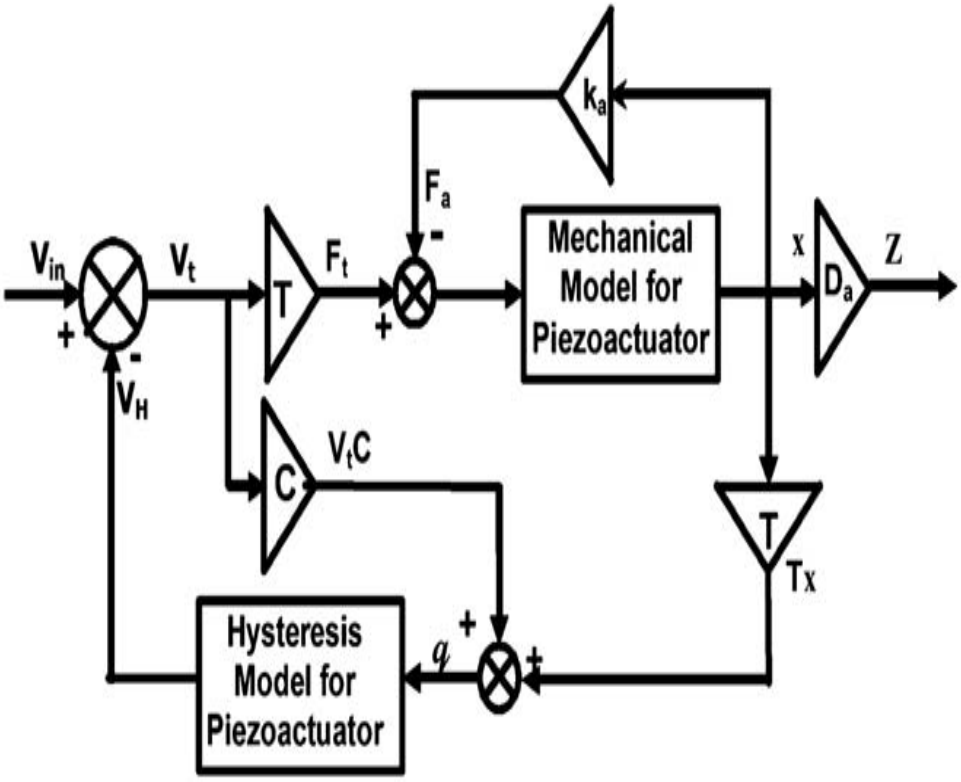

Fig.4 Block diagram of a piezo actuator [22]

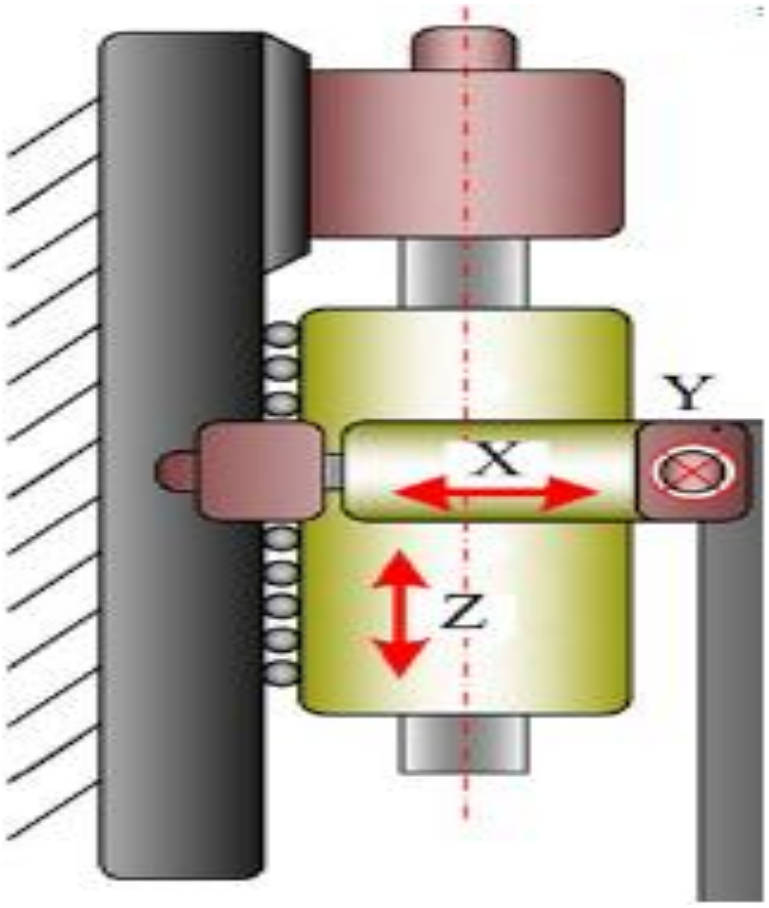

Fig.5 Movement at the x ,y and z axis at the head of the Micro EDM

2.Pulse control circuit

In Micro EDM Transistor-type pulse control circuit is using to generate high-voltage pulses between the tool and workpiece at the preferred frequency .It provides higher material removal rate due to its very high discharge frequency. In this Transistor-type pulse control circuit the pulse duration and discharge current can randomly be changed which mainly depending on the machining characteristics required. The Conventional transistor-type pulse control circuit should be modified to minimize the time delay. As a result of which the isolated DC power supply will drive the pulse generator circuit, so its reduces the delay occurs due to the voltage attenuator used in transistor-type pulse control circuit [24]. Fig.4 shows the schematic diagram of Transistor type pulsed control circuit.

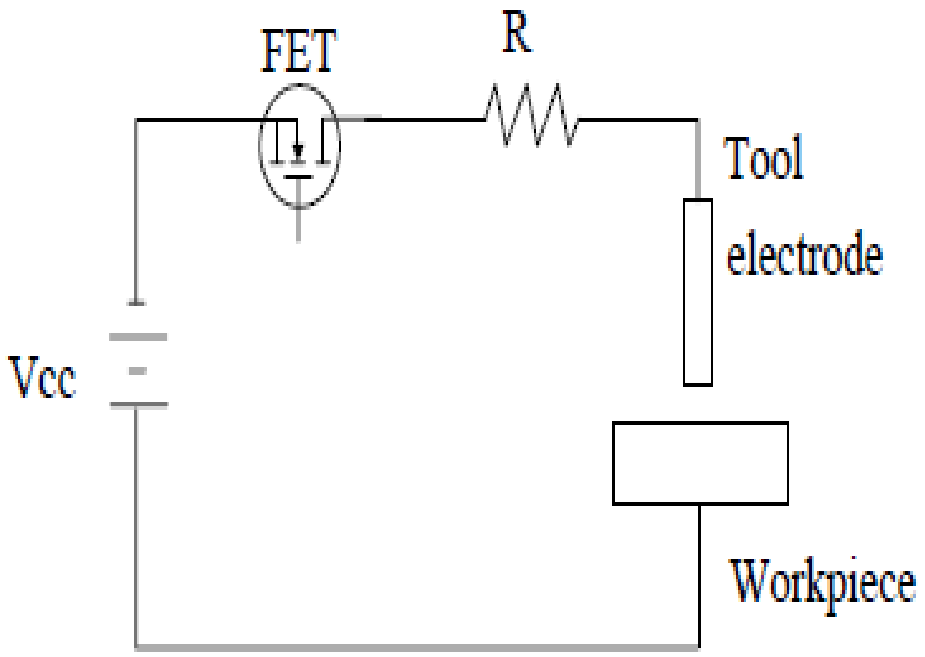

Fig.6 Transistor type pulsed control circuit [24]

3. Stepper Motor

The Micro-EDM machining center is based on a three-axis motor stage which is driven by five-phase stepping motors. This stepper motor is controlled with the help of micro step drivers that are capable of maximum 250 divisions. The control signals are fed as the clock wise and counter clock wise inputs for the stepping motors and to the piezo driver for the piezo actuator. The main function of this motor is to control the movement of the work table in x-axis and the y- axis direction. Sometimes this motor is used in coupled with the goniometer for proper controlling the movement.

4. Hydraulic pumping system

In Micro EDM set up its needed a hydraulic pumping system for flushing the dielectric at suitable rate to the tool and the work piece. A gear pump is suitable for this purpose as it supplies the dielectric at desirable pressure at the tool and work piece interface and flushes away the debris. The gear pump should comprises the appropriate flushing system through rotating spindles in addition to it there is needed needle valves for controlling the flow of dielectric.

5. Dielectric

. In Micro EDM the dielectric fluid acts as a cutting medium to improve the surface roughness and the corrosion resistance. In Micro EDM as dielectric fluid its can be used deionized water or kerosene oil. But in between these two the deionized water is best to use as a dielectric fluid because it has a high thermal conductivity, low viscosity coefficient and a high flowing rate it temperature is not affected by long working time so these characteristics improves the material removal rate. Sometimes for the proper cooling of the dielectric its used heat exchanger connected to the dielectric tank.

6. Dielectric Tank

For a compact micro EDM a dielectric tank of maximum capacity five litters is to be used .The dielectric tank is made of stainless steel or it also can built though fiber glass. The dielectric from the tank is supplied at a reasonable pressure through the hydraulic mechanism to the tool and work piece interface after which the dielectric returns back to the tank. This cycle continues till the end of the experiment.

Total Estimated cost of micro EDM set up

Sl.no	Component	source	cost Rs
1	Piezo electric micro actuator	http://www.thorlabs.com	18000
2	Piezo electric micro actuator driver	www.piezosystem.com	15000
3	5 phase stepping motor	http://catalog.orientalmotor.com	16000
4	Precision drill chuck	http://www.grizzly.com/products	3000
5	Contact sensor	http://www.robotshop.com/contact -sensors.html	3000
6	PLC unit	www.alibaba .com	30000
7	Needle valves	www.alibaba .com	4000
8	DC power supply unit	http://www.ebay.com	12000
9	Dielectric tank(5 liters capacity)		3000
10	Dielectric fluid (Deionized water)		
11	Miscellaneous(pumping system, electrical arrangements etc	www.ebay.com	10,000

1.3 Objective

The objectives of this project work are as follows:-

- To determine the significant parameters this influences the machining during Micro Electro-Discharge Machining (Micro EDM) of aerospace (Aluminium) material.

- For evaluating the performance of Micro Electro-Discharge machining (Micro EDM) on aerospace (Aluminium) material with respect to various responses such as
, material removal rate, overcut recast layer and spark gap.

- For Determining the temperature distribution of the tool and the work piece with the help of thermal electrical model developed.

- To compare the MRR from the experimental work and from the ANSYS modelling.

2. Literature Review

Allen et al. [2007] had replicated the process of single spark micro-EDM on molybdenum material to find the material removal rate. This model was used to calculate the effect of EDM parameters on the crater volume. Their study indicated the upsurge of tensile residual stresses near the crater boundary in all directions. The effect of machining parameters like pulse duration and pulse current on the residual stresses was further studied by Biswas et al. [24] using ANSYS software [28].

Han et al. (2006) had developed a new transistor-type iso pulse generator for micro-EDM. Their experiments show that the transistor type iso pulse generator is suitable for micro-EDM. Their experimental results expose that the transistor-type pulse train generator is unsuitable for micro-EDM due to its low removal rate. The material removal rate of the transistor-type iso pulse generator is three or four times higher than that of the conventional RC pulse generator [29].

Cao et al. (2007,) had suggested the effects of EDM machining conditions on micro-EDM characteristics. The pulse condition is focused particularly on the pulse duration and the ratio of on-time to off-time , and the machining properties are reported on material removal rate, tool wear, and machining accuracy. Their results (experimental) show that the current of the pulse and the voltage exert sturdily to the machining properties and the shorter EDM pulses is more proficient to make a precision part with a higher material removal rate [30].

Klocke et al. (2004) suggested the influence of the powder particles in micro-sinking-EDM on the influenced zone and the thermal spread in the dielectric . They have reported the physical properties of the powder additives play an significant role in varying the recast layer composition and morphology. Their experiments result gives two important conclusions; 1) Al powder leads to thinnest rim zone and the highest material removal rate. 2) Si powder produces a grey zone below the actual white zone [31].

Mahapatra et al. [2007] had suggested the adjustment of WEDM process parameters to achieve better material removal rate, cutting width and surface finish simultaneously. After calculating the metal removal rate through experiment, they have applied the Taguchi method to optimize the parameters and the output [32].

Liu et al. (2005) suggested that the material removal rate (MRR) for micro-hole machining over high nickel alloys is increasing stridently with increasing discharge current, and reached a maximum at discharge current of 500 mA when the pulse duration had fixed at 4 μs. This report divulges that a significant portion of total energy is used to vaporize the material at lower current resulting in reducing in material removal rate, however, when the discharge current is too large the explosive energy density is enormous, and the discharge spark is severe [33]

Yu et al. (1998) suggested a method based on the layer-by-layer machining with maintaining the original tool shape, which is called Uniform Wear Method. This method is very useful for micro electrical discharge milling process; complex shapes cavity can be machined with a accurate aspect ratio, it provides to permit wear compensation. They suggested that if a small depth of cut was used and a tool path was chosen that crossed over the previous path by the radius of the tool, the bulk of the wear would occur from the end of the tool. If the tool path is long, the tool will be appreciably shorter at the end of the path; therefore the next is reversed in order to attain a flat substructure [34].

Lim et al. (2003) studied the machining of high aspect ratio of micro-structures using micro-EDM. Parameters affecting the micro EDM were investigated and micro-structure has been sequentially fabricated. They suggested that the feed rate is inversely proportional to the machining dept. A micro slit die effortlessly manufactured using a micro electrical discharge machining is anticipated for micro heat sink fabrication (Wang et al. 2005).[34-35]

Prasad Bari et al (2012) had suggested that there are a number of ways to progress and optimize the material removal rate including some inimitable experimental models that depart from the conventional EDM sparking singularity. Despite a range of dissimilar styles, all the research works in those areas segments the same ideas of reaching more efficient material removal rate tied with decline in tool wear rate (TWR) and improved surface quality. They impending with outcome the best suitable dielectric fluid for a given work piece and tool material in order to increase material removal rate and reduce tool wear rate. Their paper also deals with the effects powder mixed dielectric fluid on material removal rate and tool wear rate. And the researchers concluded their study by the effect of powder mixed dielectric fluid

on MRR and TWR will be seen experimentally. MRR and TWR for various powders will be compared [36].

Pradhan et al. [2009] had suggested machining of titanium super alloys with micro EDM and then the process parameters were optimized by Taguchi analysis. In machining of TC4 alloy different parameters were studied and it was found that positive polarity machining is far better to negative polarity machining. It is more optimal when pulse width, open-circuit voltage, and pulse interval are 5 μs, 130 V and 15 μs respectively on the self-developed multi-axis micro-EDM machine tool. When the flushing method applied in micro-EDM, the machining efficiency is higher and relative wear of electrode is smaller [37].

Hargrove et al. [2007] had determined the cutting parameters in wire EDM based on surface temperature distribution of work piece. Like some other thermal machining process, WEDM can result in surface scratch of the work piece owing to heat of the spark. Hence they carried out an experiment to find the optimal machine parameters that will maintain a balance between cutting speed and minimum surface scratch. The analysis of three different surface layers formed due to WEDM – recast layer, white layer, and heat affected zone – was done. The optimum cutting parameters were at first calculated using FEM simulation and later on experimentally verified [38].

Satyanarayana et al. [2002], In this work they have analyzed the effect of EDM parameters namely Electrode material, polarity, current, and rotation of Electrode on metal removal rate (MRR), tool wear rate (TWR), and surface roughness (SR) in EDM of Al-SiC MMC. They concluded irrespective of the Electrode material, volume percentage of SiC, and polarity of Electrode the material removal rate increased with increase in discharge current, Increase in volume percentage of SiC had an inverse effect on MRR and positive effect on TWR and surface finish. By increasing the speed of rotation of Electrode it results in a positive effect with material removal rate tool wear rate and surface finish than stationary [39].

H.K. Kansala et al (2008) had suggested a simple reasonable model for an axi symmetric two-dimensional model for powder mixed electric discharge machining (PMEDM).This has been developed using the FEM. This model utilizes the several significant features such as

temperatures sensitive material properties, shape and size of heat source, % distribution of heat among work piece, tool and dielectric fluid, pulse on/off time, phase change (enthalpy) and material discharge efficiency etc. to predict the thermal behavior and material removal mechanism in PMEDM process. This developed model first calculated the temperature distribution in the work piece material using ANSYS software and then MRR was predictable from the temperature profiles. The effect of various process parameters on temperature distribution along the radius and depth of the work piece has been reported. Finally, the model has been validated by involving the theoretical material removal rate with the experimental one attained from a newly designed experimental setup developed in the laboratory [40].

G. L. Benavides et al (2008) had suggested that Micro-EDM is a subtractive meso-scale machining process. Agie Excellence 2F wire micro EDM is proficient of machining with a 25 micron diameter wire electrode and locates the work piece to within ±1.5 microns. This study was completed to study the machining performance of the wire micro EDM process by machining a high aspect ratio meso-scale part into a range of metals (e.g. 304L stainless steel, Nitronic 60,, Beryllium Copper, and Titanium). Machining performance factors such as, perpendicularity, profile tolerance, repeatability are related for the different materials. Applicable examination methods desirable for meso-scale value assurance tasks are also anticipated. Even though the wire EDM process is normally used to manufacture 2½ dimensional features, these features can be machined into a 3D part having other features such as chamfers and hubs to simplify assembly [41].

Ho and Newman (2003) reviewed the research work carried out from the inception to the development of die-sinking EDM within the past decade. It reported on the EDM research relating to improving performance measures, optimizing the process variables, monitoring and control the sparking process, simplifying the electrode design and manufacture. A range of EDM applications were highlighted together with the development of hybrid machining processes [42].

Puri and Bhattacharyya (2003) employed Taguchi methodology involving thirteen control factors with three levels for an orthogonal array L27 (313) to find out the main parameters

that affect the different machining criteria, such as average cutting speed, surface roughness values and the geometrical inaccuracy [43].

Saha et. al. (2004) developed a new approach using finite element modeling and optimization procedures for analyzing the process of wire electro-discharge machining. The results of the modeling and optimization showed that non uniform heating is the most important variable affecting the temperature and thermal strains [44].

Tzeng and Chiu (2003) conducted experiments on castek-03 for medium carbon steel material having excellent wear resistance. The most important factors affecting the EDM process robustness were pulse on time, applied electric current in low voltage and sparking current in high voltage. The most important factors affecting the machining speed were pulse on time and applied electric current in low voltage. The gain of 13.17 dB was able to decrease the variation range to 21.84%, which improved process robustness by 4.6 times. Huang and Liao (2003) presented the use of grey relational and S/N ratio analysis, for determining the optimal parameters setting of WEDM process. The results showed that the MRR and surface roughness are easily influenced by the table feed rate and pulse on time [45].

Masuzawa and Fujino [1980] were the first to study the application of the transistor-type generator in micro-EDM, and they have obtained a pulse-on time of 220 μs. Transistor-type pulse train generator is unsuitable for micro EDM due to its low removal rate: 80- μs and 30- μs pulse on-times of discharge current can be obtained by using the transistor-type iso pulse generator and the removal rate of this generator is two or three times higher than that of the traditional RC pulse generator [46]. In the study of pulse condition affecting MRR and surface roughness it has been found that the voltage and current of the pulse exert strongly to the machining properties and the shorter EDM pulse is more efficient to make a precision part with a higher material removal rate, in the measurement of the gap between a tool and machined surface, it is increased with an increase of voltage and current. But it is inversely proportional to the length of pulse-on time [47]. Transistor serves as a switching device but it has some limitations because of this reason an alternative needed, MOSFET (Metal Oxide Semiconductor Field Effect Transistor) was found to be a suitable alternative [48]. MOSFETs have the advantage of high input impedance and absence of thermal runaway and second

breakdown as compared to bipolar junction transistors [49]. A transistor-controlled power supply composed of a low energy discharge circuit and an iso-frequency pulse control circuit can provide the functions of high frequency and lower energy pulse control, by this the peak current decreases with an increase in pulse-control frequency with a 33.33% duty cycle [50].

Guha et al. [1995] evaluated MRRs for copper & beryllium alloys with graphite and copper & tungsten electrodes (negative polarity) and copper electrode (positive and negative polarity). MRR was higher when positive polarity was used for copper electrodes. For negative polarity the highest MRR were obtained with graphite electrodes. Yan et al. [51] observed in their investigation that using negative polarity in EDM caused a higher MRR under a higher discharge energy (Ip>3 A or ton>5 µs); in contrast, a positive polarity caused a higher MRR under lower discharge energy (Ip<3 A or ton<5µ s) [52].

Lin and Lin (2004) reported the use of an orthogonal array, grey relational generating, grey relational coefficient, grey-fuzzy reasoning grade and analysis of variance to study the performance characteristics of the EDM machining process. The machining parameters (pulse on time, duty factor and discharge current) with considerations of multiple responses (electrode wear ratio, material removal rate and surface roughness) were effective. The grey-fuzzy logic approach helped to optimize the electrical discharge machining process with multiple process responses. The process responses such as the electrode wear ratio, material removal rate and surface roughness in the electrical discharge machining process could be greatly improved [53].

Li et al. [1980] proposed inchworm electrode feed mechanism having features like, high feeding accuracy and quick response to keep micro gap between electrode and work piece during machining process. By integrating the transistor type iso pulse generator with the servo feed control system, removal rate can be increased by about 24 times than that of the conventional RC pulse generator with a constant feed rate in both semi finishing and finishing conditions [54].

Diver et al. (2004) investigated that the fabrication of reverse tapered holes in EDM systems. They emphasized that the existing EDM system is not fully qualified and produce low quality reverse tapered holes. According to their novel technique, tapered holes with a entry diameter

of 100 μm and exit diameter of 160 μm can be produced. The other alternative ways of producing tapered holes are listed below [55]

(a) "Modify the EDM parameters (e.g. voltage, frequency, current, gap, gain, or pulse width) during machining to remove more material radially as the depth of machining increases.

(b) Move the work piece relative to the electrode to achieve the desired hole taper.

(c) Change the electrode angle and position radially during drilling.

(d) Feed and rotate the electrode at the angle required to achieve the desired hole taper.

3. Modelling of Micro EDM

In this study at first it has been developed one ANSYS model by taking Shankar et al [56] and Pradhan (2012) as reference for EDM process, after corresponding results it is converted into a micro EDM model and in addition to Al thermal models for Inconel 718 also have been developed. The results obtained from the thermal analysis have been used for calculating and comparing MRR and also to study the effect of different process parameters.

3.1 Thermal models of EDM and Micro-EDM

The working principle of EDM and Micro EDM are same in this process, electrodes are submerged in dielectric and they are physically separated by a gap, called inter-electrode gap. It can be modelled as the heating of the work electrode by the incident plasma channel. Fig.7 shows the idealized case where work piece is being heated by a heat source with Gaussian distribution.

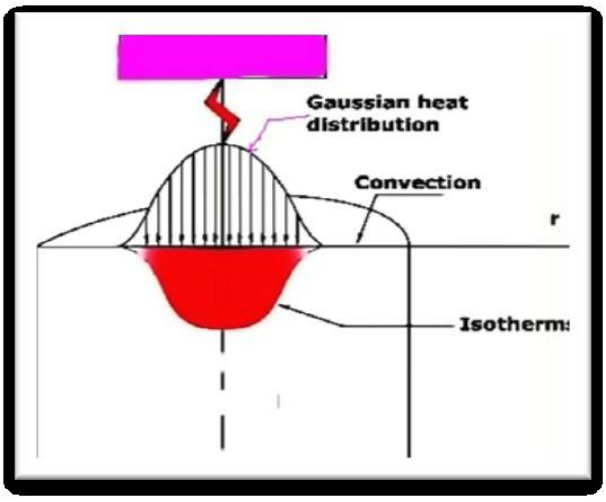

Fig: 7 Gaussian heat distribution in work piece [57]

Due to axisymmetric nature of the heat transfer in the electrode and the workpiece, a two-dimensional physical model is assumed. The following assumption is made in the thermal modeling of Micro EDM.

3.1.1 Assumptions

1. The modeling is done for a single spark.
2. The domain is considered as axisymmetric.
3. Work piece is being heated by a heat source with Gaussian distribution.
4. The material of the work piece is homogeneous and isotropic.
5. The ambient temperature was room temperature.
6. The work piece material properties are depending on the temperature.

3.1.2 Governing equation

Heating of work piece due to a single spark is assumed to be axisymmetric and governed by thermal diffusion differential equation considering boundary conditions for the temperature distribution in a cylindrical coordinate system is

$$\rho Cp\left[\frac{\partial T}{\partial t}\right] = \left[\frac{1}{r}\frac{\partial}{\partial r}\left(K_r\frac{\partial T}{\partial r}\right) + \frac{\partial}{\partial z}\left(K\frac{\partial T}{\partial z}\right)\right] \quad \text{.....(1)}$$

Where ρ is density, Cp is specific heat, K thermal conductivity of the work piece, T is the temperature, t is the time and r & z are coordinates of the work piece.

3.1.3 Boundary condition

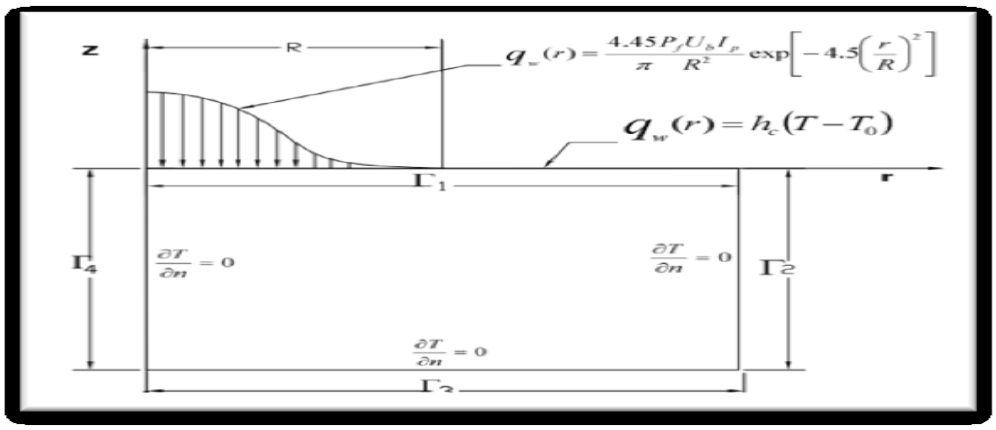

Fig.8 Boundary condition in work piece [57]

As shown Fig.8 the work piece is represented by a semi-infinite rectangle bounded by four boundaries Γ1, Γ2, Γ3 and Γ4. On the top surface the heat is transferred to the work

piece shown by Gaussian heat flux distribution. Heat flux is applied on boundary Γ1 up to spark radius R, beyond R convection takes place due to dielectric fluids. The coordinate axes are r and z, where z is the axis of symmetry. The process consists of heating period (Ton) and cooling period (Toff). The initial and final boundary conditions for heating period are listed below.

1. At boundary surface Γ1

Initial condition: when $0 > t \geq Ton$

$$K\frac{\partial T}{\partial z} = Q(r), \text{When } R<r$$

$$K\frac{\partial T}{\partial z} = h_f(T-T_0), \text{When } R\geq r$$

2. For boundary surfaces Γ2, Γ3 and Γ4

$$\frac{\partial T}{\partial p} = 0$$

Where hf is heat transfer coefficient of dielectric fluid, Q(r) is heat flux due to the spark, T0 is the initial temperature and T is the temperature.

3.1.4 Material properties

The Micro EDM process, huge thermal energy is generated. As a result the work piece temperature rises up to the boiling temperature of the materials. In this study the variation of material properties with respect to the temperature is examined. The materials properties of Inconel 718 and Aluminium, and are given in table 1, and 2 respectively.

Table 1 Material properties of Inconel 718

Thermal Conductivity, K(W/mK)	11.4
Specific Heat, C(J/kg K)	435
Density, ρ (kg/m^3)	8190
Melting Temperature (K)	1609
Young's Modulus, E (GPa)	205
Poisson's Ratio	0.29

Table 2 Material properties of Aluminium

Thermal Conductivity, K(W/mK)	205
Specific Heat, C(J/kg K)	910
Density, ρ (kg/m^3)	2700
Melting Temperature (K)	933
Young's Modulus, E (GPa)	70
Poisson's Ratio	0.33

3.1.5 Heat flux

The work piece is being heated by a heat source with Gaussian distribution [57] so a Gaussian heat flux distribution is assumed in present analysis. Total power of each pulse for single spark can be written as follows

$$Q_w(r)=\frac{4.45PVI}{\pi R^2}exp\left\{-4.5\left(\frac{r}{R}\right)^2\right\} \quad \text{(2)}$$

Where R is the spark radius, r is the radial distance from the axis of the spark, I is the current, V is the discharge voltage, P is the fraction of energy lost to the cathode .Dibitonto et al (1989) predicted that about 8% of the total heat supplied is absorbed by anode and about 18% is absorbed by cathode. Shankar et al (1997) [56] calculated that 40%−45% of the heat input is absorbed by the work piece. Yadav et al (2002) [58] also considered same 8 % which is also considered in this simulation. The Spark on time, for the micro EDM process, 2μs is divided into 10 sub steps, and the ambient temperature was room temperature. The Temperature distribution through single spark has been calculated using ANSYS 13.0, and element who possessing temperature above the melting temperature were killed, after that the MRR is calculated.

3.2 Thermal modelling process using ANSYS software.

For the solution of the model of the EDM process commercial ANSYS 13.0 software was used. An axisymmetric model was created treating the model as semi-infinite. ANSYS has many FEA (finite element analysis capabilities), ranging from a simple, static analysis to a complex, transient dynamic analysis in the fields such as structural mechanics, fluid mechanics, and electromagnetic. In EDM analysis the geometry size is to be taken as 500 μm × 500 μm in 2D, with an element size of 1 μm, but for micro EDM process workpiece domain taken as 100 μm × 50 μm, with element size of 1 μm. After EDM modelling the work is protracted for the micro EDM with different parameter setting as given in table 4.

Steps for Thermal Modeling

Step1. Start ANSYS 13 software.

Step2. Choose analysis method-Thermal, h method.

Step3. Create the geometry of the work piece domain by taking dimension as 100 μm × 50 μm, with element size of 1 μm. The spark radius is taken as 5 μm. Since its a 2D modelling, the thickness of the material will not be taken into consideration.

Step4. Define the type of element (Thermal Solid, Quad 4node 55 – PLANE55) from Preprocessor > Element Type > Add/Edit/Delete. Click on Options and switch to the axisymmetric view.

Step5. Enter the element material properties (thermal conductivity, specific heat, and density).

Step6. For FEM modelling it's needed to create a mesh. Here it has been chosen an element edge length of 1 μm.

Step7. Apply the proper boundary layer conditions and solve the problem.

Step8. Current load step is to be solved to get the desired result.

Step9. Read and plot the result for nodal solution.

Step10. Finish.

3.3 Modelling of MRR of Micro EDM for single discharge.

As a result of a single spark shallow shape crater has been formed which has a cavity with a concave shape on the workpiece surface. The volume of the crater equals that of the removed material by the spark. After thermal modelling nodes showing the temperature more than melting temperature is selected and to be killed from the complete mesh of the work domain for further analysis. A typical crater cavity generated by this analysis. Calculation is done for single spark only. To calculate the MRR due to single spark discharge, the crater cavity volume was divided into number of cylindrical discs (Fig. 9). The x and y coordinates of the nodal boundary generated by the ANSYS 13 software are used to calculate the crater volume.

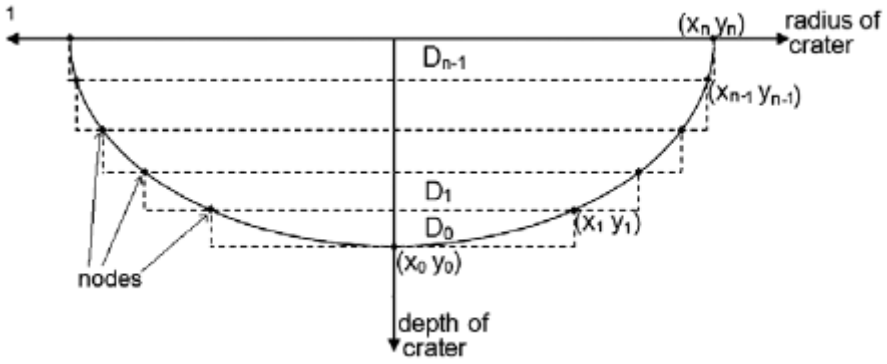

Fig.9 Crater cavity [59]

The total crater volume C_{vt} is given by :-

$$C_{vt} = \sum_{i=0}^{n-1} D_i$$

Where D_i is the individual volume of a disk ,which can be calculated as:-

$$D_{i=\Pi(X_i - X_0)^2 \times (Y_i - Y_{i-1})}$$

Where x and y are the coordinate generated by the ANSYS 13 software and n is the no of nodes.

Finally the material removal rate (mm3/min) is calculated by the following equation.

$$MRR = \frac{60 \times C_v}{(T_{on} + T_{off}) \times 10^3}$$

Where Cvt is the volume of material removed per discharge ,Ton is discharge duration and T off is the discharge off time.

3.4 MRR calculation of Micro EDM in case of multi discharge

In case of multi- discharge at first it has to find out the no of pulses.

$$\text{No of pulse} = \frac{\text{Time for machinning}}{T_{on} + T_{off}}$$

MRR in case of multi discharge =No of pulses×MRR in case of single discharge

3.5 Analysis of residual stress

Residual stresses are the stresses which are exist in a body in the absence of mechanical loads or thermal gradients. In other words it can be say that the residual stresses are stresses that remain after the original cause of the stresses (external forces, heat gradient) has been removed. Theses stresses are known to influence a material's mechanical properties such as creep or fatigue life. Sometimes, these effects are beneficial; but in sometimes, the effect is very deleterious. Therefore, it is necessary to control the residual stresses. Micro EDM generates residual stresses because of sharp temperature gradients and metallurgical transformations. These stresses are found more than the yield point of the material and cause twining and cleavage depending on the crystal structure. Investigation on

residual stresses exposed high tensile residual stresses around the crater, but they are not as large as those beneath the adjacent surface. There stresses reach a maximum value and then gradually decreases as the depth increases and become compressive in nature. On further increase of depth, these stresses asymptotically diminish to a zero value. These stresses are arises mainly as a result of the thermal contraction of the re solidified metal, which was not excluded from the craters, onto the relatively unaltered parent metal, imply plastic deformation and biaxial tensile stress.

Mamalis et al. [50] and Rebelo et al. [61] have suggested that the peak stresses are independent of the discharge energy and approaches the ultimate tensile strength of the material. Kruth and Bleys [62] have found that, the peak stress is not located at the surface, but somewhat below for machining under high pulse and current settings. Finite element methods ‘are also used to measure the residual stress, in this method it has use process parameters such as power input, pulse duration, etc., to predict the transient temperature distribution, liquid- and solid-state material transformation and residual stresses that are induced in the workpiece as a result of a single-pulse discharge. An attractive feature of this method is its ability to predict the shape of the crater that is formed as a result of the material removal.

3.5.1 Coupled thermal-structural FEM simulation of the micro-EDM process

In micro-machining process it is essential to control the Surface quality .As materials in case of micro machining are removed by means of cyclic spark discharges, because of this thermal action ,micro-EDM induces the residual stresses thus the surface integrity of a machined component is get affected. As a result small surface cracks and stress corrosion cracking may appear which will reduce the fatigue life of the components. The objective of this simulation is to find out the residual stress distribution on the work piece.

For determining the induced stress in the workpiece, by using a transient thermal analysis a time dependent temperature profile due to a spark discharge has to be determined first. A sequentially coupled thermal-structural analysis is performed using the commercial FEM package ANSYS.13 For this an axisymmetric model had employed with element type ‘Plane 55’ for the thermal analysis and ‘Plane 42’ for the structural analysis. For doing the structural analysis it has to keep displacement at boundary 2 and 3 to 0 (Fig.10) for all degree of freedom.

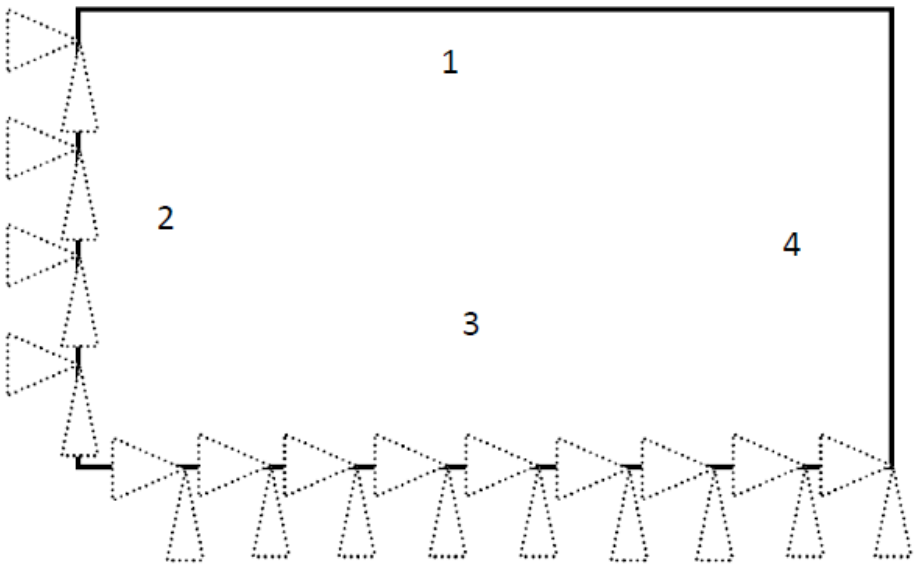

Fig.10 Boundary conditions in structural analysis

The procedure used to obtain the thermal and residual stresses is shown through a flow chat (Fig.11) below.

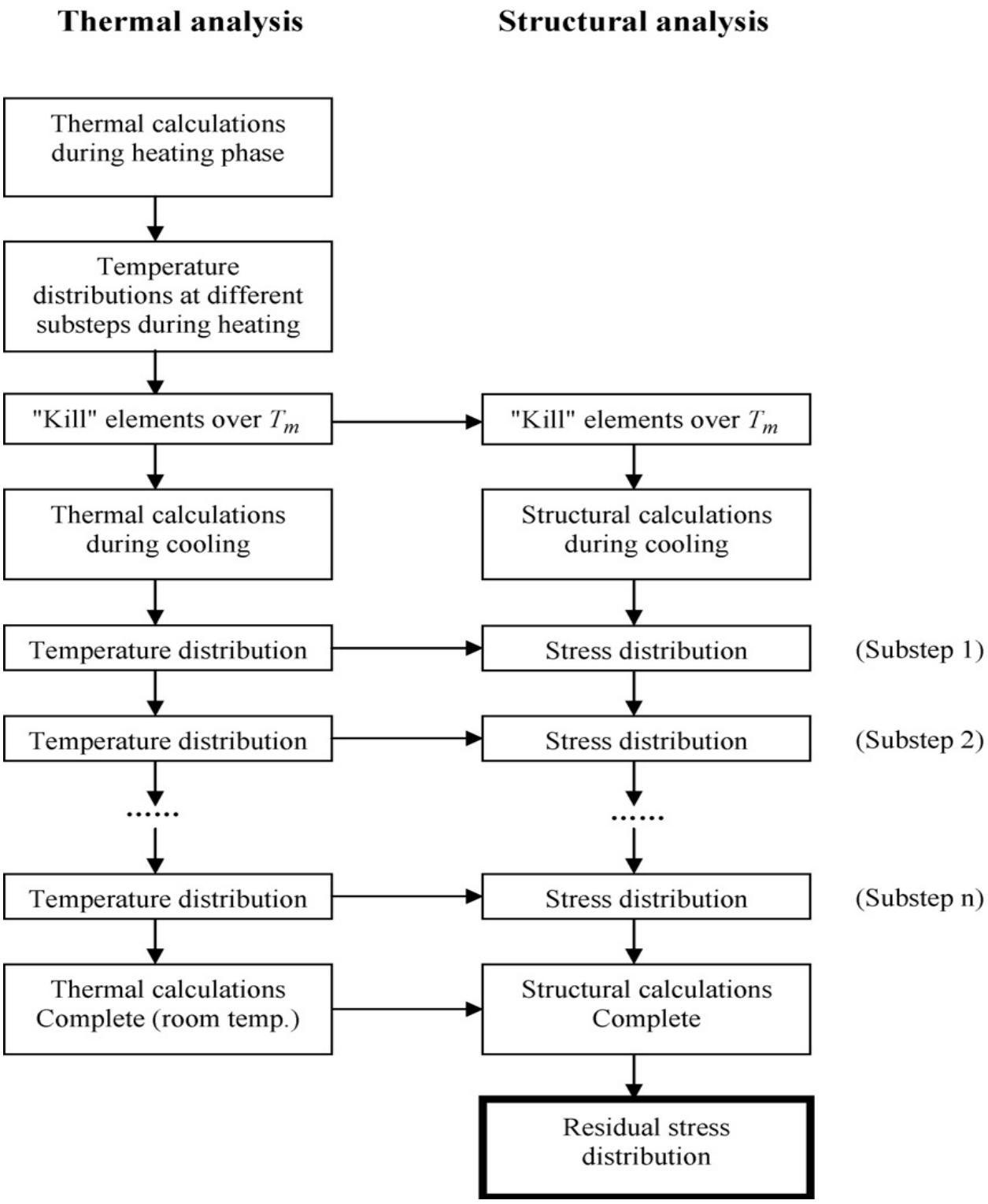

Fig.11 Flow chart to obtain the thermal and residual stresses [28]

3.5.2 Coupled thermal-structural modeling process using ANSYS 13 software

Analysis of any complex geometry can be easily done using ANSYS because It has many finite element analysis capabilities so in this study ANSYS 13 software has been used. In case of micro EDM the geometry size is to be taken as 100μm ×50 μm with element size is to be taken as 1 μm. Now the following procedures are to be followed for coupled thermal-structural modeling.

- At first start the ANSYS software and create the geometry with size 100μm ×50 μm, choose the thermal solid plane 55, 4 node quadrilateral element.
- Meshing is done with element size of 1 μm for micro EDM simulation.
- Define the material properties such as, thermal conductivity, density, and heat capacity.
- According to boundary conditions apply loads.
- Set the initial temperature at 298 K.
- Now solve the current L.S to get the desired result.
- Load title and loading has to change for the next solution.
- Now apply the necessary boundary condition as required in the structural analysis.
- Now transfer the thermal load data into the structural problem.
- Read the obtained result and plot the desired results.
- Finish.

4. Experimental details and optimization technique.

- For performing the experiment L_9 orthogonal array has been adopted. The experimental design has 3 levels and 3 factors.
- The experiment has been performed on ZNC270e of ELECTRONICA Company.
- SEM has been used to capture the image and measuring the dimensions of drilled holes.
- Process parameter has been optimized by grey based taguchi method and PCA (Principle component analysis) coupled with grey taguchi methods.
- The modelling of Micro EDM for different process parameters where done on ANSYS13 software.

Fig 12. Electronica Micro EDM machine

4.1 Specification of Micro EDM

table 3

Dielectric	Deionized water
Maximum work piece size	100×500×300
Maximum travel	500×300×450
Manufacture	Electronica

4.2 Process parameter used for experiment

Three response parameters are chosen

- Voltage
- Current
- Pulse on time

Table 4.Process parameter

Parameters	Units	Value
Voltage	V	8,9,10
Current	I	30,35,40
Pulse on time	µs	5,7,9

Table 5 Taguchi's L9 orthogonal array

S. No.	Voltage (V)	Current (A)	Ton (µs)
1	8	30	5
2	8	35	7
3	8	40	9
4	9	30	7
5	9	35	9
6	9	40	5
7	10	30	9
8	10	35	5
9	10	40	7
10	9	30	8

4.3 Test specimen

An Aluminium test specimen with dimensions of 7 × 2 cm and thickness of 0.2 mm. The holes were drilled with different parameter setting as given in Table 5 with a copper electrode having diameter 1mm. The workpiece were examined under SEM with zoom level of 200×.

4.4 Taguchi method

Genichi Taguchi a Japanese engineer has developed Taguchi methods which are statistical methods used to improve the quality of manufactured goods, and also applied to engineering, biotechnology, marketing and advertising [63]. In Taguchi method the quality of the value is measured by the deviation of a characteristic from its target value. So a loss function is developed from this deviation. The uncontrollable factors which are cause of the noise, such deviation are result into loss. Taguchi method tries to minimize the noise because the exclusion of noise factor is not viable. Taguchi method provides much compact variance for the experiment with optimum setting of process control parameters. That's why Taguchi methods are use in design of experiment with parametric optimization processes to get the desired results.

This method uses a statistical measure of performance which is called signal-to-noise ratio. The standard S/N ratios generally used are as follows:- 1. Higher the better. 2 lower the better 3 Nominal is best. The combination which have highest S/N ratio is the optimal setting.

To determine the target value Following three stage design operation is done in taguchi's method:-

- System design
- Parameter design
- Tolerance design

In this study its deals with the analysis of the experiment by the Taguchi method. L9 orthogonal arrays have been used to determine the importance of the factors.

In this experiment our main responses are:-

1. Machining time.
2. Circularity error.
3. Heat affected zone.

For FEA model optimization our main responses are:-

1. Material removal rate (MRR).
2. Residual stress.

4.5 Grey based Taguchi method

In solving multi objective problems, taguchi method is coupled with grey relational analysis, because taguchi alone cannot be able to solve multi-objective problems. Grey relational analysis is used to convert a multi-objective problem into a single objective problem and after that Taguchi method is applied. Following are the steps used in Grey based Taguchi method:-

Step.1 The first step in the grey relational analysis is to normalize the experimental data in the range of 0 to 1.This step is known as grey relational generation. After that Grey relational co-efficient are calculated to represent the relationship between ideal and the actual normalized data. In the normalization three types of data normalization are done:-

1. Lower is the better.
2. Higher is the better.
3. Nominal is the best

1. For lower the better criteria

$$x_i(k) = \frac{\max\ y_i(k) - y_i(k)}{\max\ y_i(k) - \min\ y_i(k)}$$

2. For higher the better criteria

$$x_i(k) = \frac{y_i\ (k) - \min\ y_i(k)}{\max\ y_i(k) - \min\ y_i(k)}$$

Where Xi (k) - value after the Grey relational generation.

Min Y_i (k) - Smallest value of Yi (k) for K^{th} Response.

Max Y_i (k) - Maximum value of Y_i (k) for K^{th} Response.

Step 2 .Calculation of Grey relational coefficient

$$\xi_i(k) = \frac{\Delta_{min} + \psi\Delta_{max}}{\Delta_{0i}(k) + \psi\Delta_{max}}$$

Where $\Delta_{0i}(k) = |X_0(k) - Xi(k)|$ = Difference between absolute values of $X_0(k)$ and $X_i(k)$

Step 3: After taking average of the Grey relational coefficients, the Grey relational grade can be calculated as:

$$\gamma_i = \frac{1}{n}\sum_{k=1}^{n} \xi_i(k)$$

Where n is the number of responses.

4.6 Grey relational analysis coupled with principal component analysis for optimization of parameters

In order to objectively reflect the relative importance for each performance characteristic in grey relational analysis, principal component analysis is used to determine the corresponding weighting values for each performance characteristic. In other words it can be say that, principal component analysis is used to determine the corresponding weighting values of each performance characteristics, when this method is coupled with grey relational analysis and used in problem with multiple performance characteristics, will reflect the relative importance for each performance characteristic. The steps used in Grey relational analysis coupled with principal component analysis are as follows:-

Step 1 The first step is to convert the experimental data into S/N values.

Step 2 Converted S/N value is normalized.

Step 3 After S/N value normalization calculate the corresponding grey relational coefficients.

Step 4 Calculate the grey relational grade using principal component analysis.

Step 5 Now perform the statistical analysis of variance and get the optimal levels of cutting

Parameters

For modelling the Micro EDM process the process parameters used are shown in table 6. And in the optimization of ANSYS model parameter setting has been shown in Table 7.

Table 6. Process parameters used for modelling in ANSYS 13 (Micro EDM)

Parameters	**Micro EDM process parameters**		
Voltage	8	9	10
Current	30	35	40
Heat input to the work piece	0.08	0.18	0.25
Spark radius	5μm		
Pulse-on time	2μs		
Pulse-off time	100μs		

Table 7. Taguchi L9 orthogonal array of process parameters for Micro EDM

S. No.	VOLTAGE	CURRENT	HEAT INPUT
1	8	30	0.08
2	8	35	0.18
3	8	40	0.25
4	9	30	0.18
5	9	35	0.25
6	9	40	0.08
7	10	30	0.25
8	10	35	0.08
9	10	40	0.18

For confirmation test 10^{th} process parameter is to be taken as V=9V,I=30A and heat input as 0.15

Results and discussion

5 Optimization of Micro EDM

In the present work ten holes were drilled according to design of experiment shown in Table 5.The process parameter setting has been shown in Table 7.While drilling the holes its seen the white color distribution around the circumference of the hole produced this white layer is called the recast layer which are always formed in holes done through Micro EDM .Recast layer thickness is defined as the thickness of the white layer formed on the work piece surface after the solidification. Recast layer is formed due to the spark whose thermal energy melts the metal and then the melted metal solidified and forms a white layer. The main responses in this analysis are machining time, heat affected zone and circularity error. It's taken the optimization criteria for all the response as Lower-the-Better.

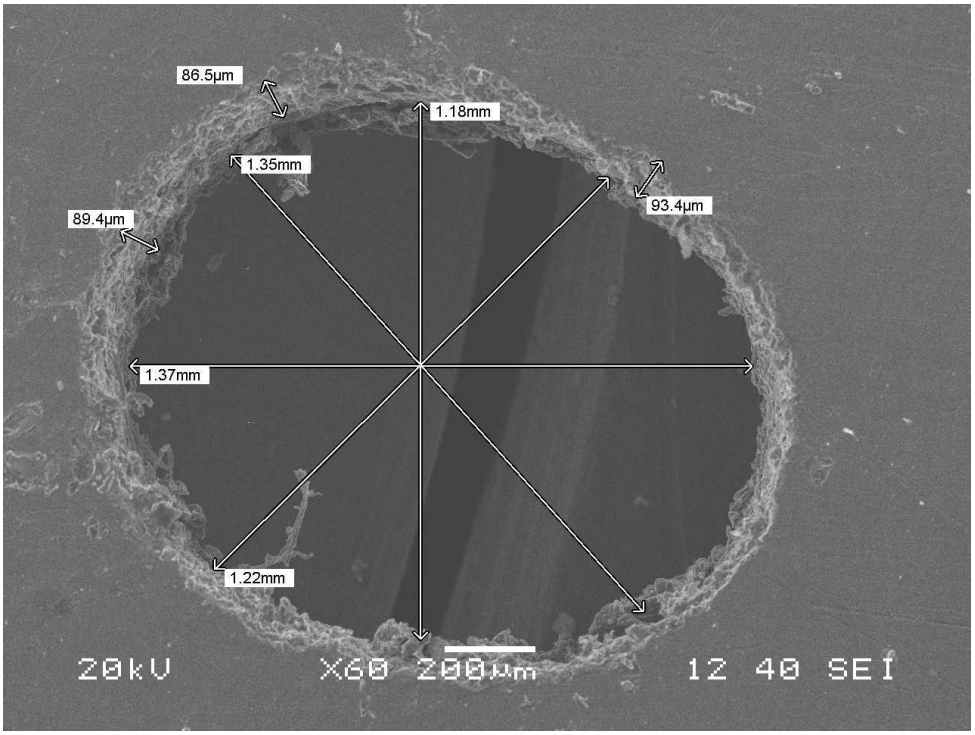

Fig.13 SEM image of the drilled micro hole at V=8V,I=30 and T_{ON}=5µs

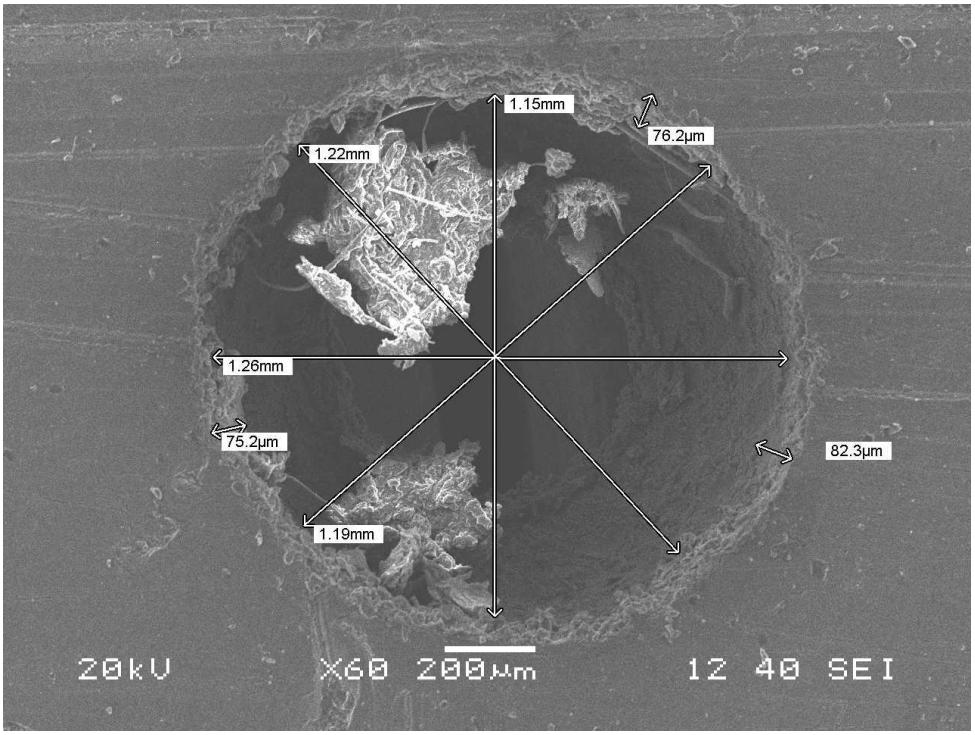

Fig.14 SEM image of the drilled micro hole at V=8V,I=35A and T_{ON}=7 µs

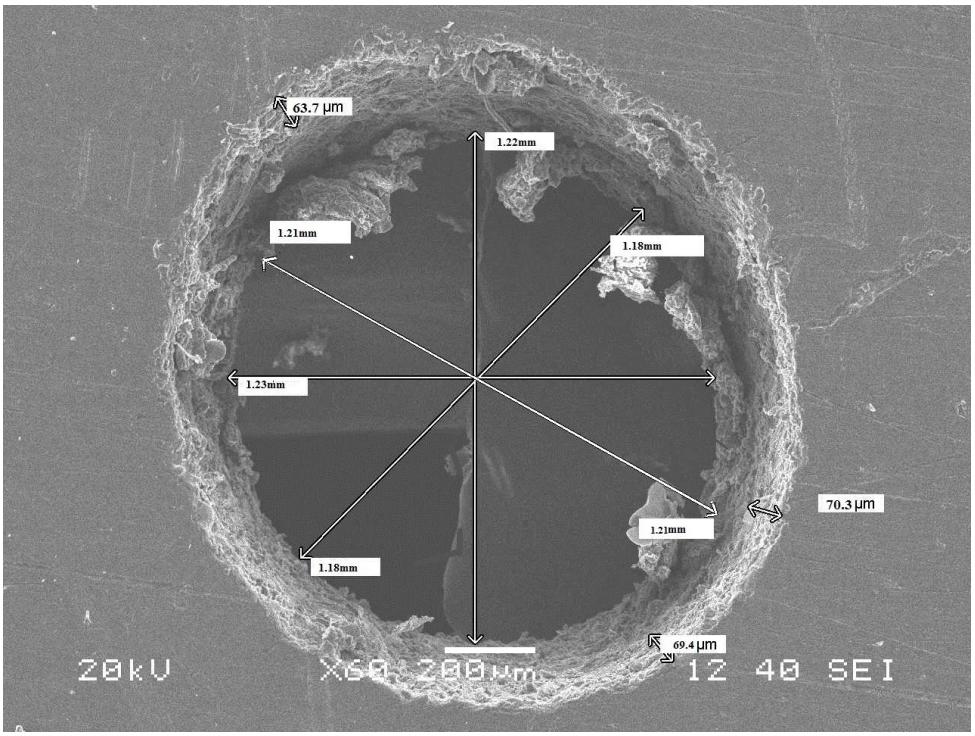

Fig.15 SEM image of the drilled micro hole at V=8V,I=40A and T_{ON}=9 µs

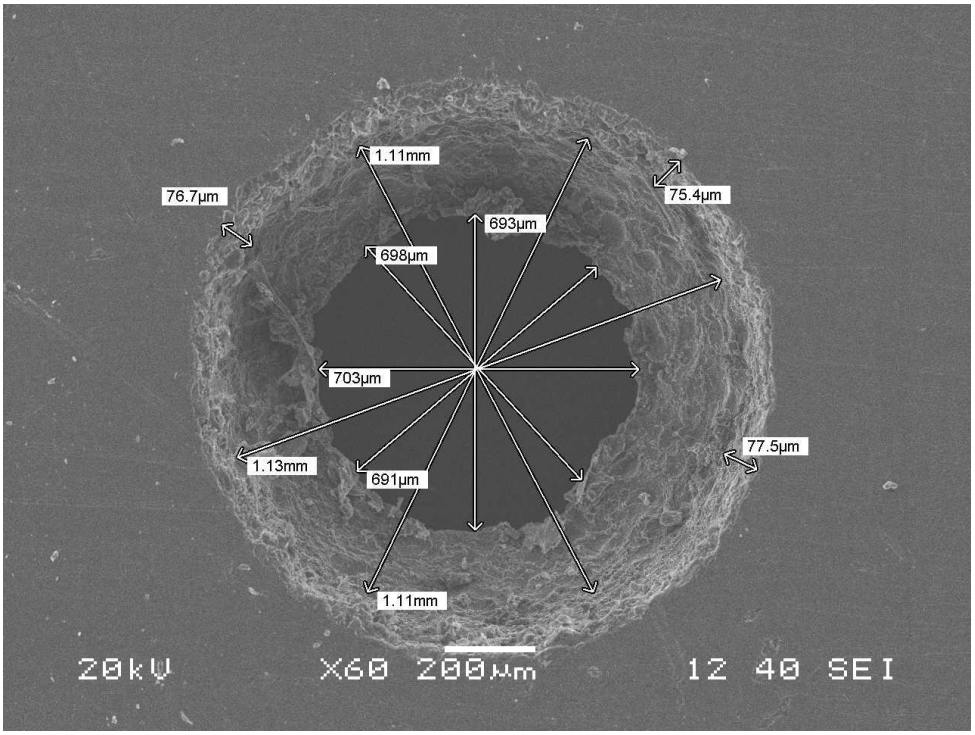

Fig.16 SEM image of the drilled micro hole at V=9V,I=30A and T_{ON}=7 µs

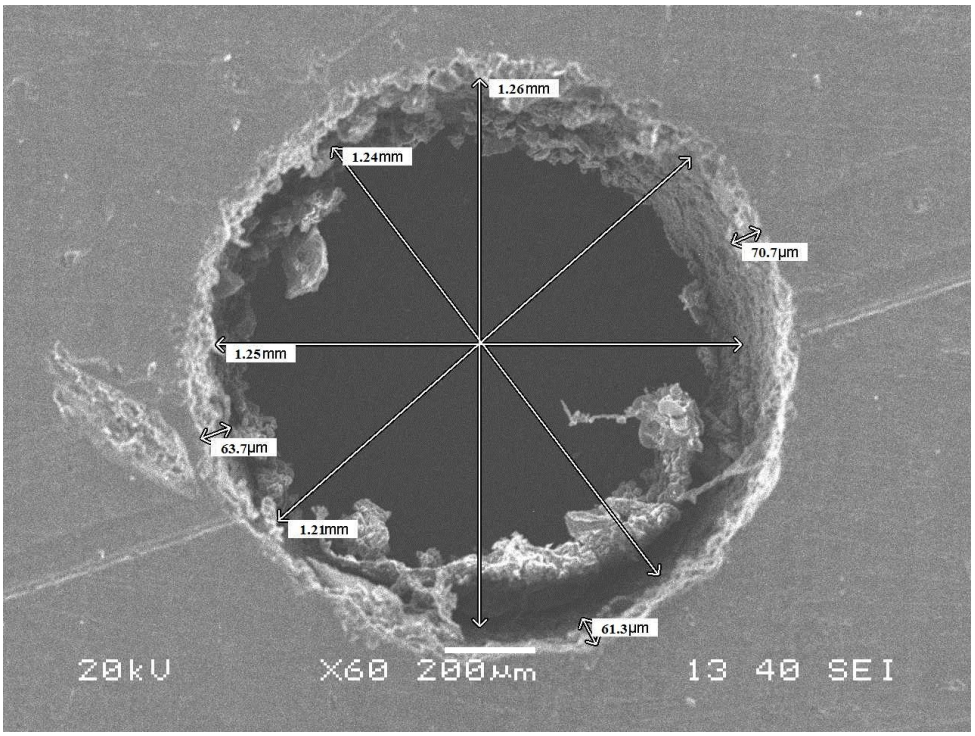

Fig.17 SEM image of the drilled micro hole at V=9V,I=35A and TON=9 µs.

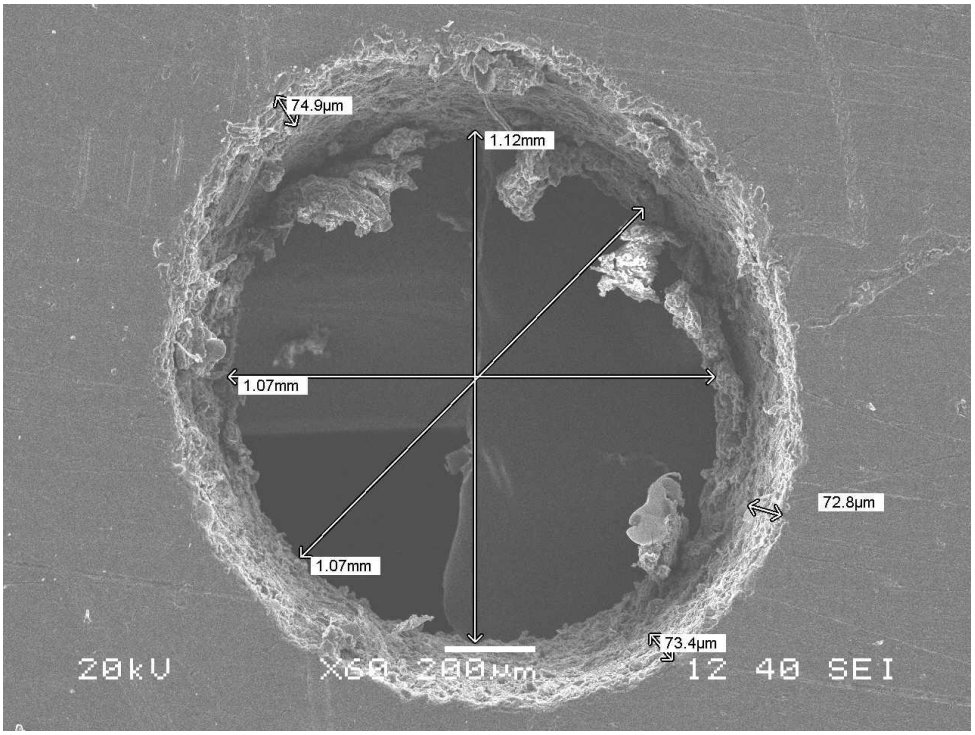

Fig.18 SEM image of the drilled micro hole at V=9V,I=40A and TON=5 µs

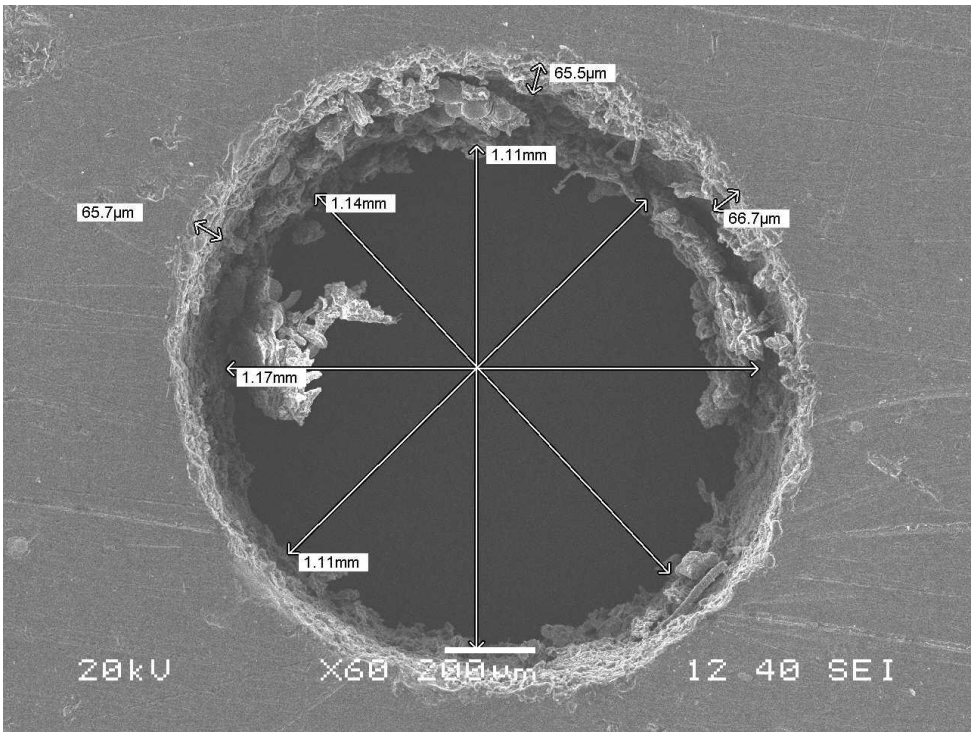

Fig.19 SEM image of the drilled micro hole at V=10V,I=30A and TON =9 µs

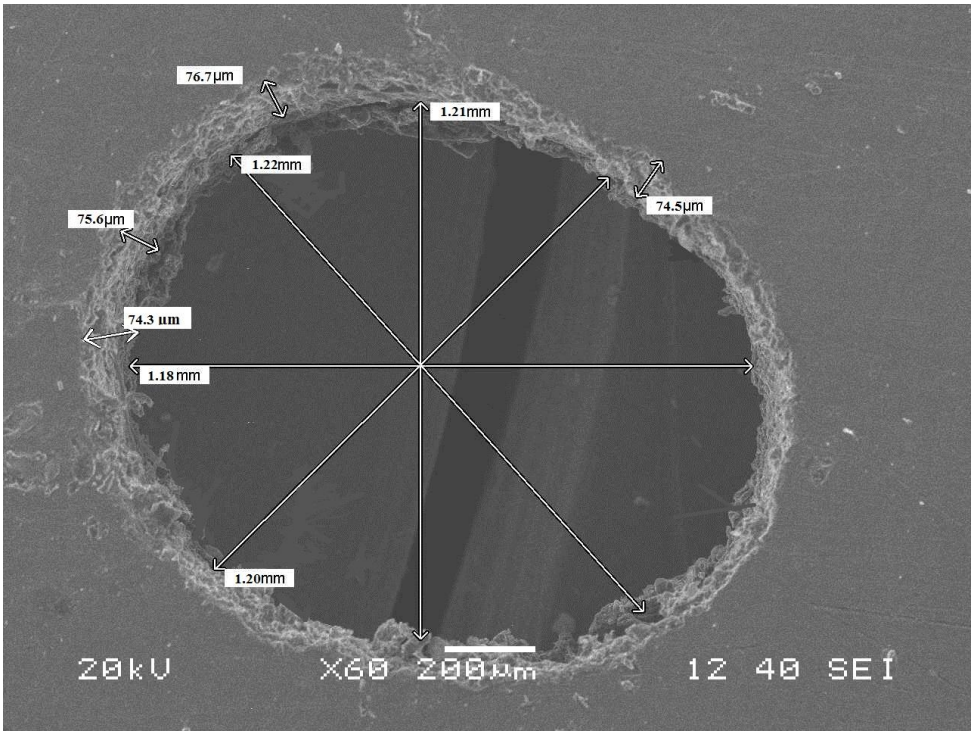

Fig.20 SEM image of the drilled micro hole at V=10V,I=35A and TON =5 µs

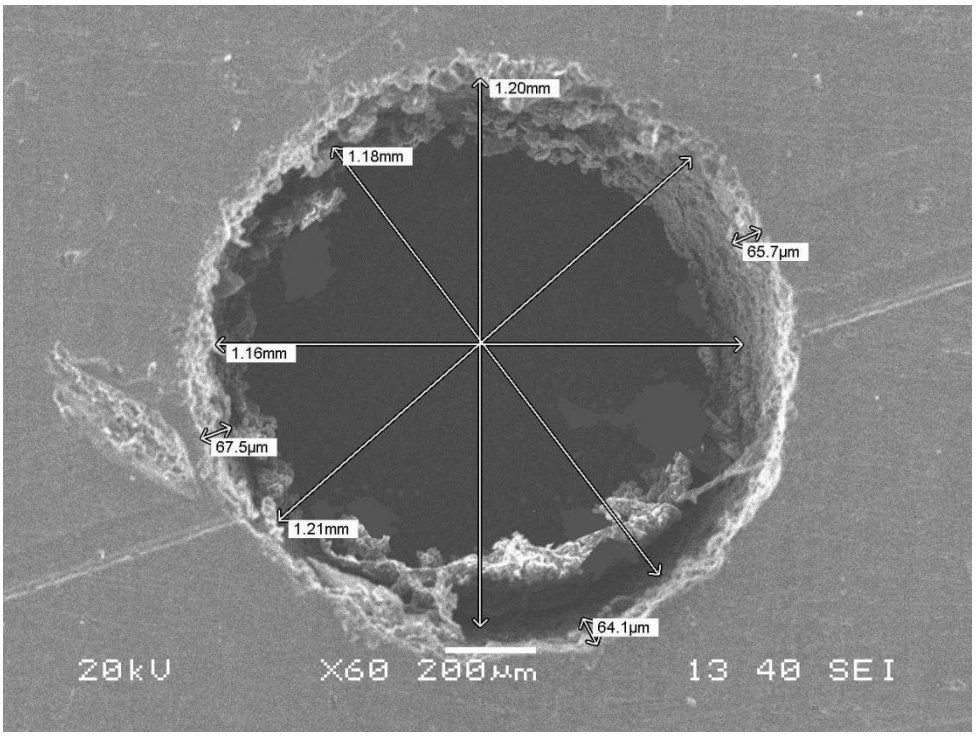

Fig.21 SEM image of the drilled micro hole at V=10V,I=40A and TON =7 µs

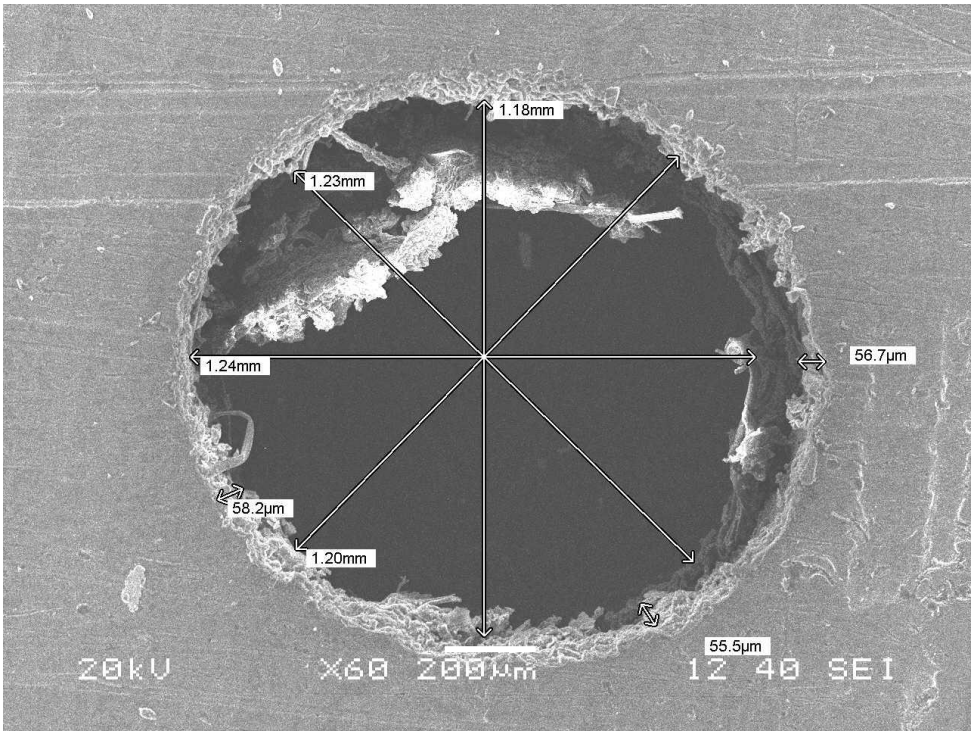

Fig.22 SEM image of the drilled micro hole at V=9 V, I=30A and TON =8 µs

Table 8. Circularity error

SL.No	Maximum dia(mm)	Minimum dia (mm)	Mean dia (mm)	Percentage circularity error
1	1.35	1.19	1.240	11
2	1.26	1.15	1.205	9
3	1.22	1.18	1.200	4
4	1.13	1.11	1.120	2
5	1.26	1.21	1.235	4
6	1.12	1.07	1.100	5
7	1.17	1.11	1.140	5
8	1.22	1.18	1.200	3
9	1.20	1.18	1.190	2
10	1.24	1.18	1.210	5

Table 9. Recast layer error

SL. NO	Maximum R.C.L	Minimum R.C.L	Mean R.C.L	Percentage error
1	93.4	89.4	4	4.28
2	76.2	74.2	2	2.62
3	70.3	63.7	6.6	9.38
4	77.6	75.6	2	2.57
5	63.7	61.5	2.2	3.45
6	74.9	72.8	2.1	2.80
7	66.7	65.5	1.2	1.79
8	76.6	75.6	1	1.30
9	65.7	64.1	1.6	2.43
10	56.7	55.5	1.2	2.11

5.1 Optimization by grey based taguchi method

Table 10. Grey relational generation

Machining time (sec)	**Circularity error (µm)**	**Recast layer (µm)**
0	1	0.8333
0.1111	0.6428	0.2777
0.1666	0.1428	1
0.0555	0	0.2877
0.0277	0.2142	0.3333
0.2778	0.2142	0.3055
1	0.2857	0.0556
0.8333	0.1428	0
0.2222	0.1684	0.1666
0.1111	0.2857	0.0557

Table.11 Grey relational coefficient of each performance characteristics (taking ψ=0.5)

Machining time (sec)	Circularity error (µm)	Recast layer (µm)	Overall grey coefficient
1	0.3333	0.3758	0.5694
0.8182	0.435	0.6429	0.6328
0.75	0.7778	0.3333	0.6203
0.8999	1	0.6429	0.8476
0.9473	0.7	0.6	0.7491
0.6428	0.7	0.6207	0.6545
0.3333	0.6364	0.8999	0.6232
0.3754	0.7778	1	0.7176
0.6923	0.5837	0.75	0.8141
0.1882	0.6366	0.7997	0.7849

Table.12 Response table (mean) for overall Grey relational grade

Level	V	I	Ton
1	4.337	3.478	3.818
2	2.542	3.122	2.399
3	2.925	3.205	3.588
Delta	1.795	0.356	1.420
Rank	1	3	2

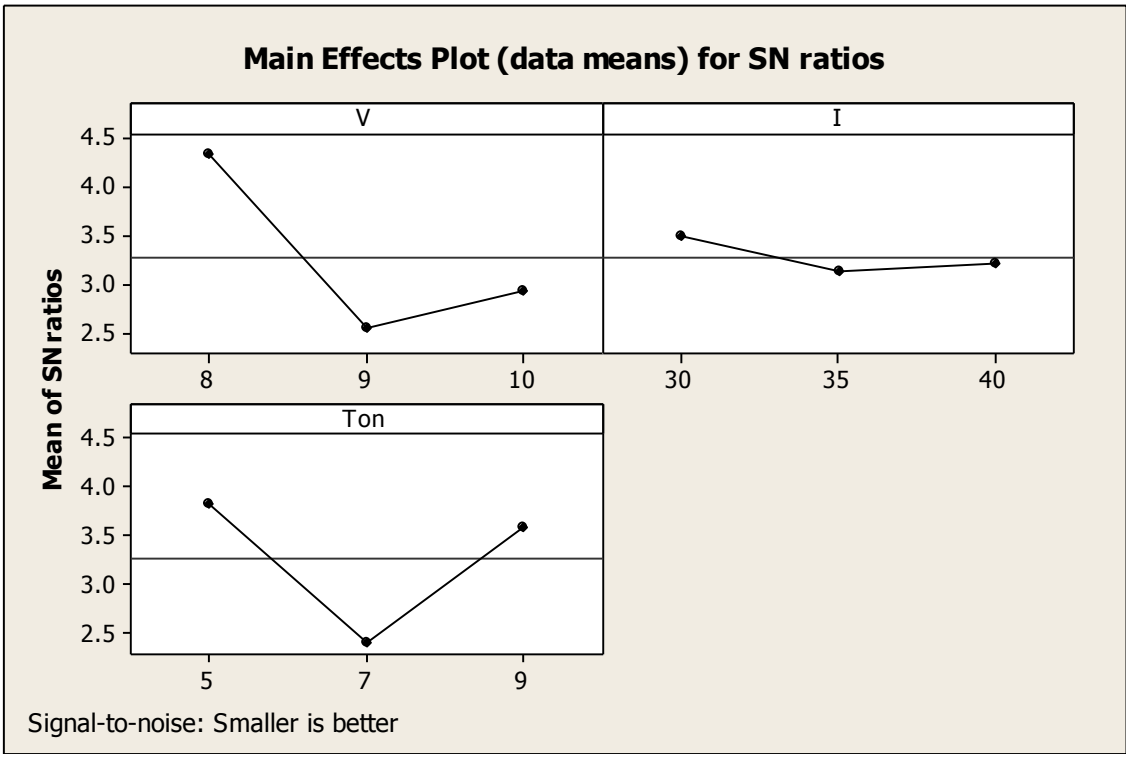

Fig.23 S/N ratio plot for overall grey relational grade

5.2 Optimization by grey relational analysis coupled with weighted principal component analysis

Table .13 Sequence of S/N ratio

v	I	Ton	SNRA1 (Machining time)	SNRA2 (circularity error)	SNRA3 (Recast layer Thickness)
8	30	5	40.8279	15.9176	12.0412
8	35	7	41.1381	19.1721	6.0206
8	40	9	41.2892	27.9588	13.2552
9	30	7	40.9844	33.9794	6.0206
9	35	9	40.9065	26.0206	6.8485
9	40	5	41.5836	26.0206	6.4444
10	30	9	43.2871	24.4370	1.5836
10	35	5	42.9226	27.9588	0.0000
10	40	7	41.4376	33.9794	4.0824

Table .14 Normalized S/N ratio

Machining time	Circularity error	Recast layer
1.00000	0.00000	0.10401
0.87384	0.18019	0.61985
0.81242	0.66667	0.00000
0.93636	1.00000	0.61985
0.96804	0.55936	0.54892
0.69268	0.55936	0.58354
0.00000	0.47168	1.00000
0.14822	0.66667	1.13568
0.75204	1.00000	0.78591

Table .15 grey relational grade using principal component analysis.

Machining time	Circularity error	Recast layer	Average	MEAN1
0.10401	1.00000	0.00000	0.367630	0.367630
0.61985	0.87384	0.18019	0.557402	0.557402
0.00000	0.81242	0.66667	0.492530	0.492530
0.61985	0.93636	1.00000	0.851217	0.851217
0.54892	0.96804	0.55936	0.691414	0.691414
0.58354	0.69268	0.55936	0.611248	0.611248
1.00000	0.00000	0.47168	0.490069	0.490069
1.13568	0.14822	0.66667	0.616239	0.616239
0.78591	0.75204	1.00000	0.845137	0.845137

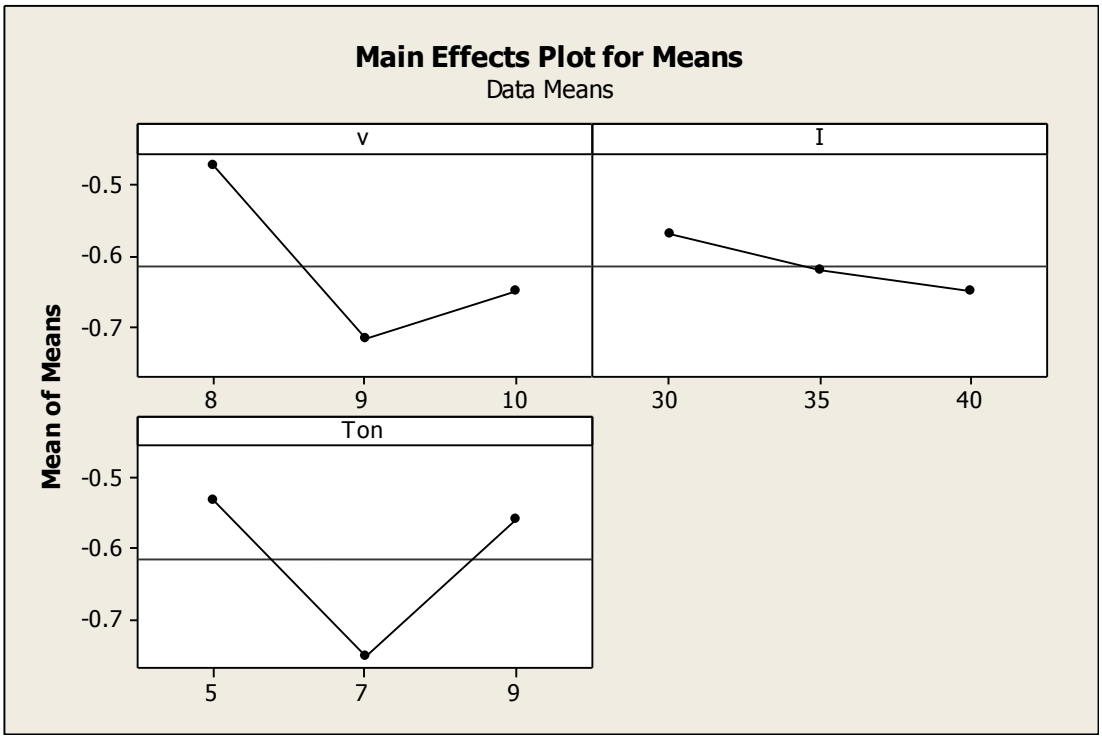

Fig.24 Main effect plot

5.3 ANSYS thermal model confirmation

In order to confirm the ANSYS thermal model at first it have to make an EDM model for AISID2 die steel with parameter setting as given in Table. 16 Later the value had been compared with M .K .Pradhan (Fig.3) (57). Fig 25 shows the plot for EDM process done for the AISID2 die steel. Element size is taken as 1 μm so it's getting the final temperature as shown in fig 25 is coming as 3720K which is approximately same as given by M.K.Pradhan [57].So it can be say that we are proceeding in right way.

Table 16.EDM process parameter

Parameters	Units	Value
Discharge voltage	V	25
Current	A	9
Percentage of heat input to the workpiece		0.08
Spark radius	μm	135
Pulse-on time	μs	100
Heat transfer coefficient	W/m^2 k	10,000

Table 17 Thermal and Mechanical Properties of AISID 2 steel

Thermal Conductivity, K(W/mK)	29.0
Specific Heat, C(J/kg K)	413
Density, ρ (kg/m^3)	7700
Melting Temperature (K)	1984
Young's Modulus, E (GPa)	208
Poisson's Ration	0.30

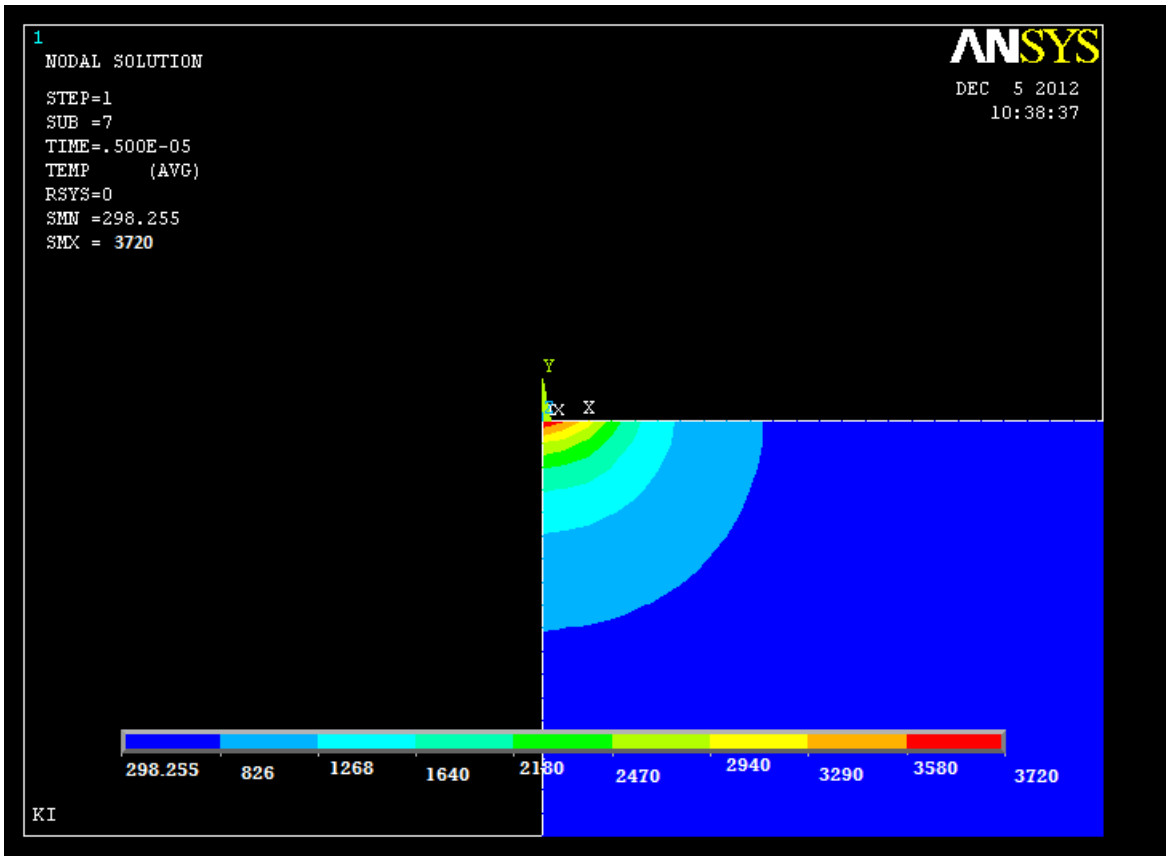

Fig.25 Temperature distribution for single spark EDM process

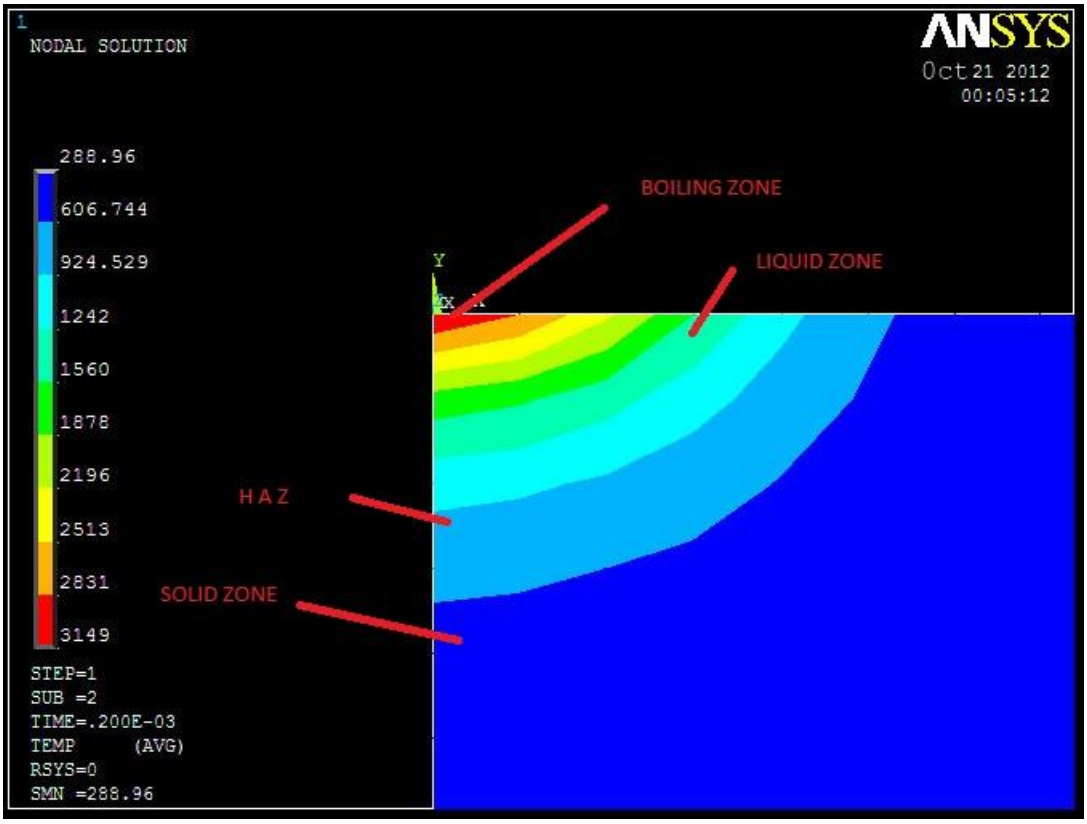

Fig.26 Interpretation of colors in the thermal modelling

5.4 Thermal modelling of micro EDM for single spark

After verification of the result of thermal model for EDM process now it can be analyze by the different process parameters from the table 7 by making the thermal model.

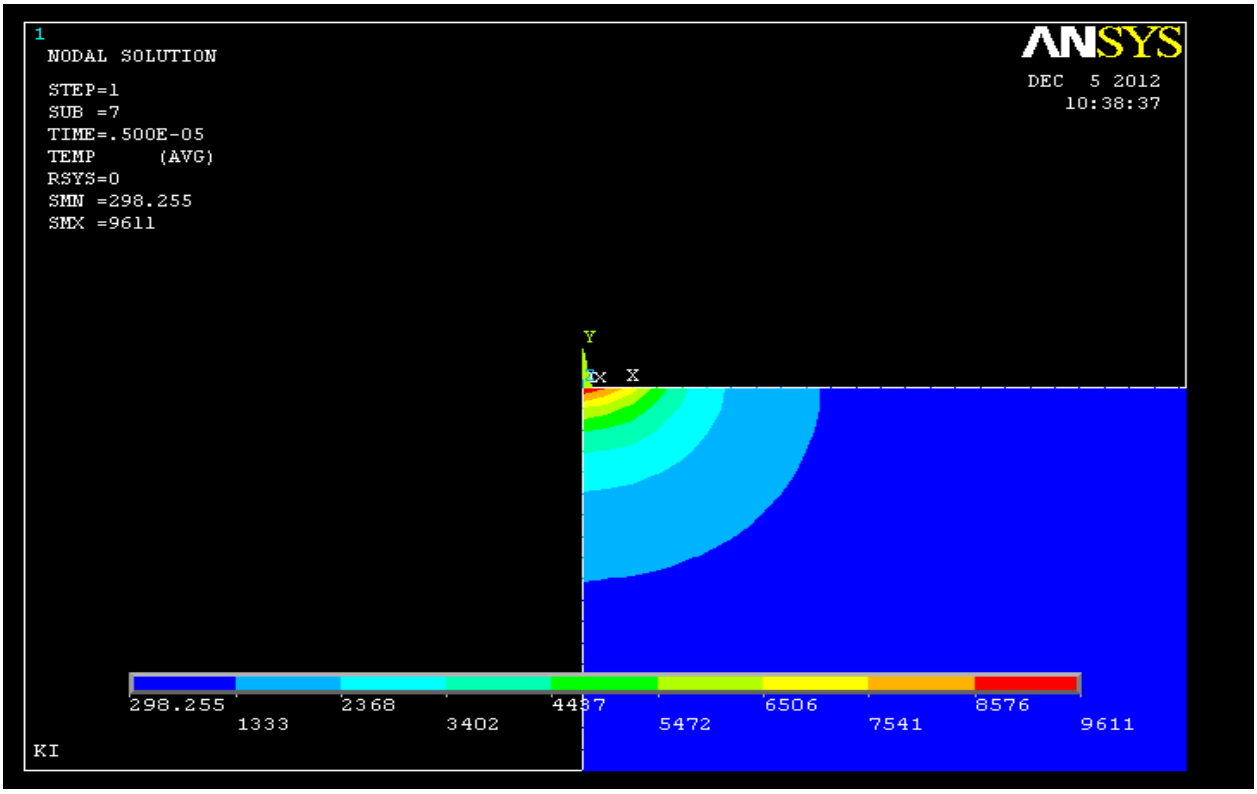

Fig.27 Temperature distribution in Al for V=8V,I=30A,Ton=5 µs,p=0.08

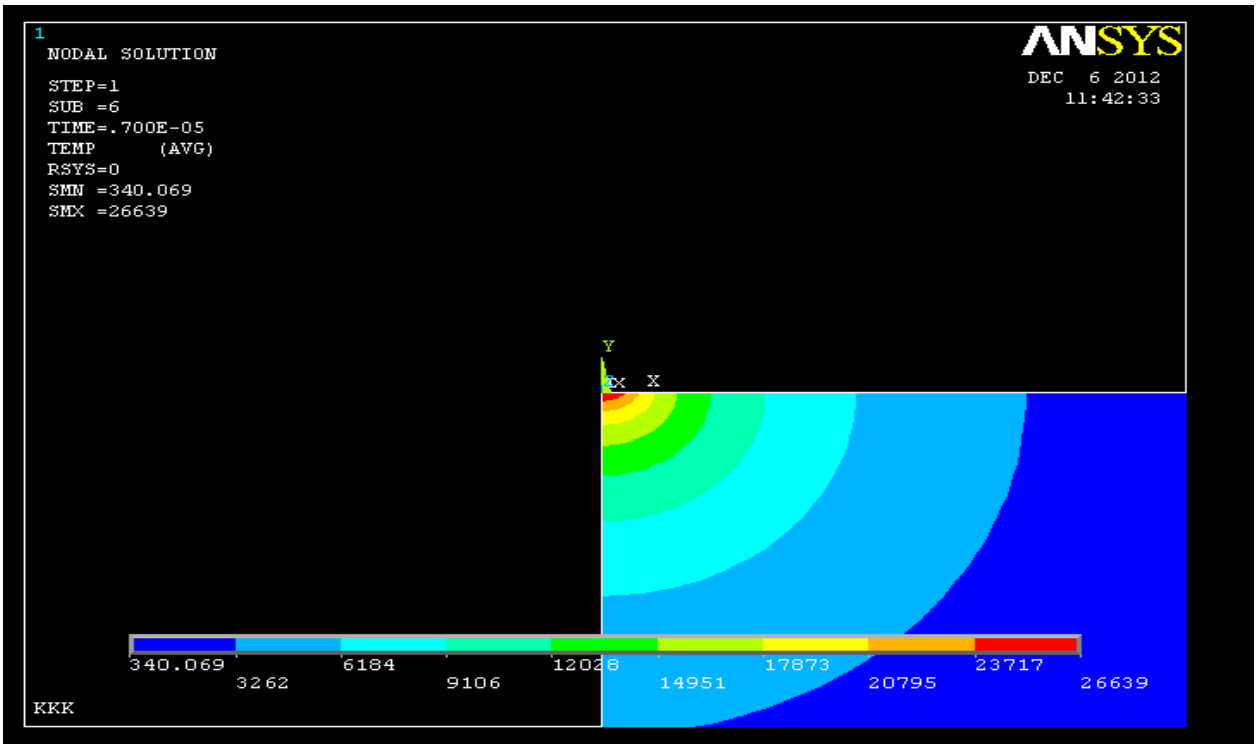

Fig.28 Temperature distribution in Al for V=8V,I=35A,Ton= 7µs ,p=0.18

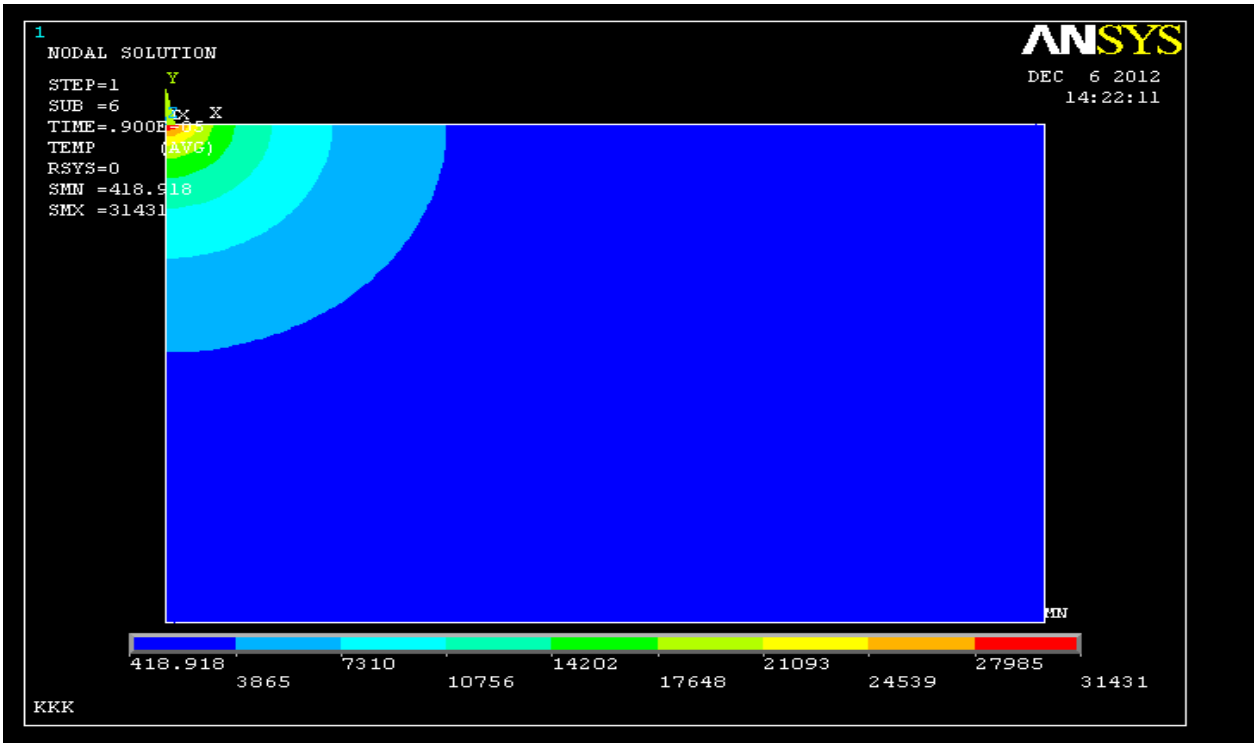

Fig.29 Temperature distribution in Al for V=8V,I=40A,Ton=9 µs ,p=0.25

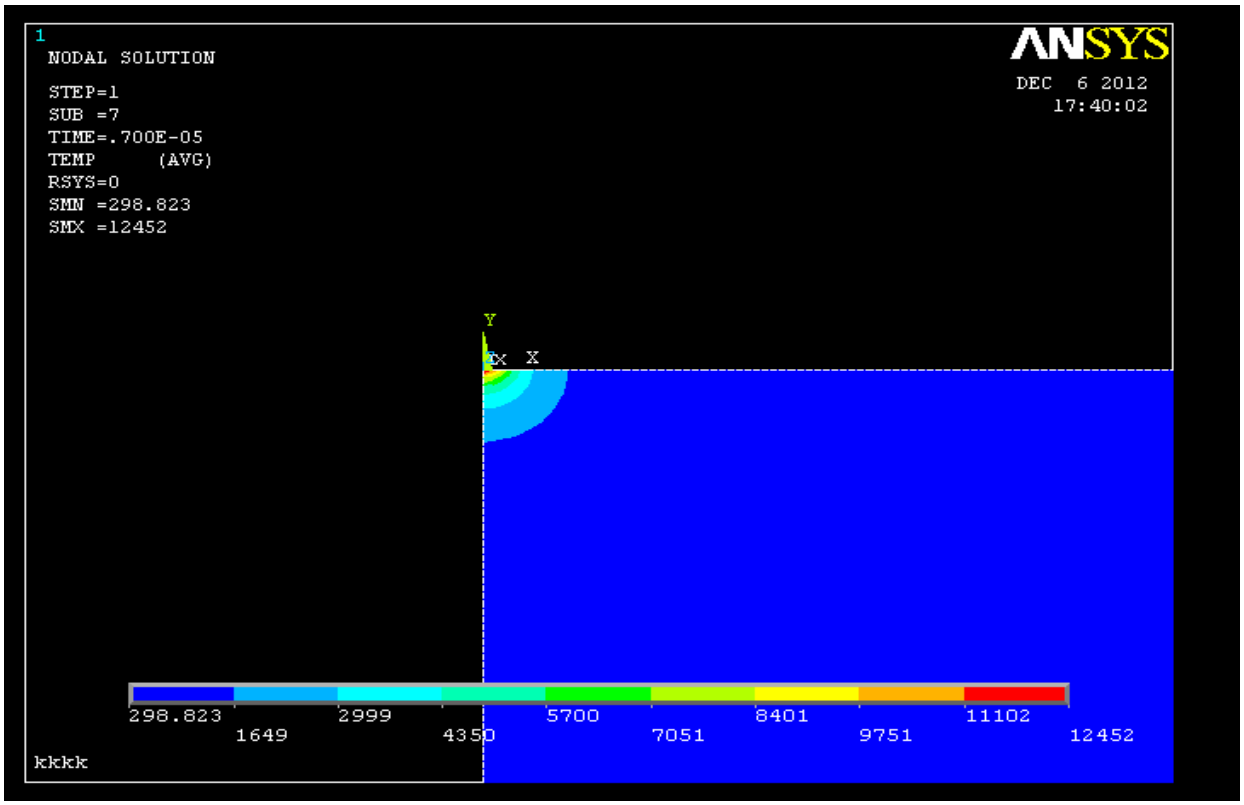

Fig.30 Temperature distribution in Al for V=9V,I=30A,Ton=7µs ,p=0.18

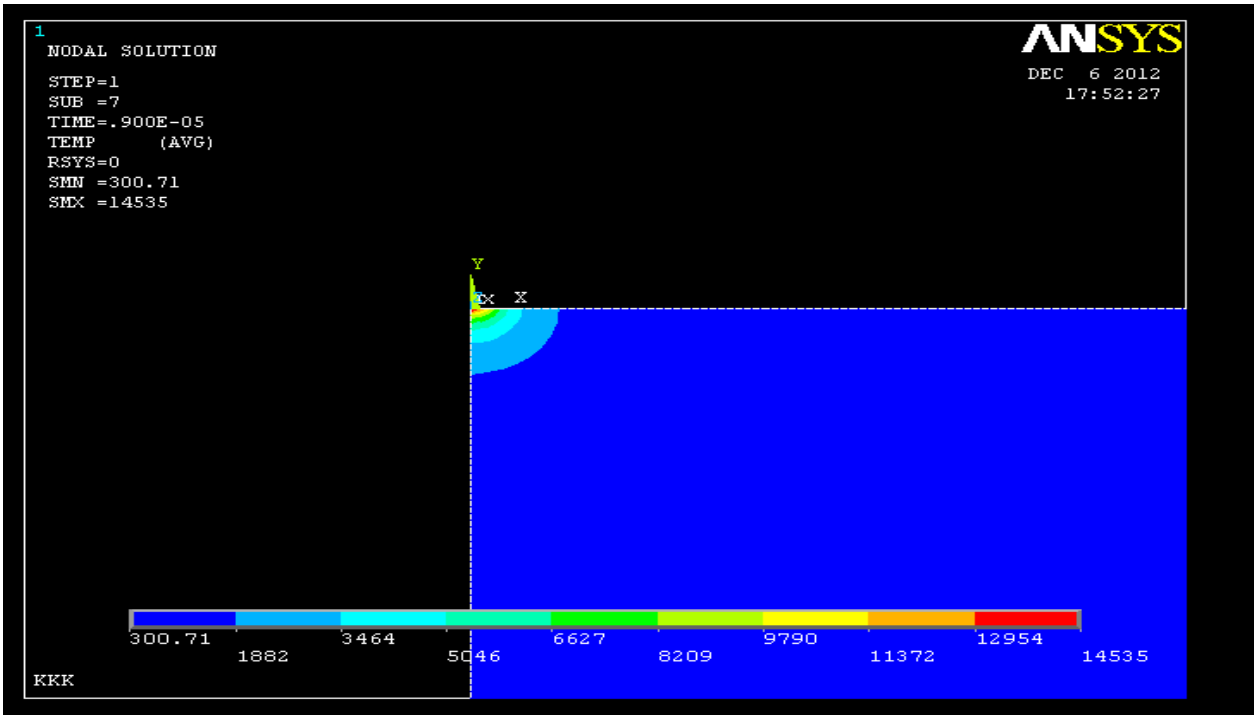

Fig.31 Temperature distribution in Al for V=9V,I=35A,Ton=9µs ,p=0.25

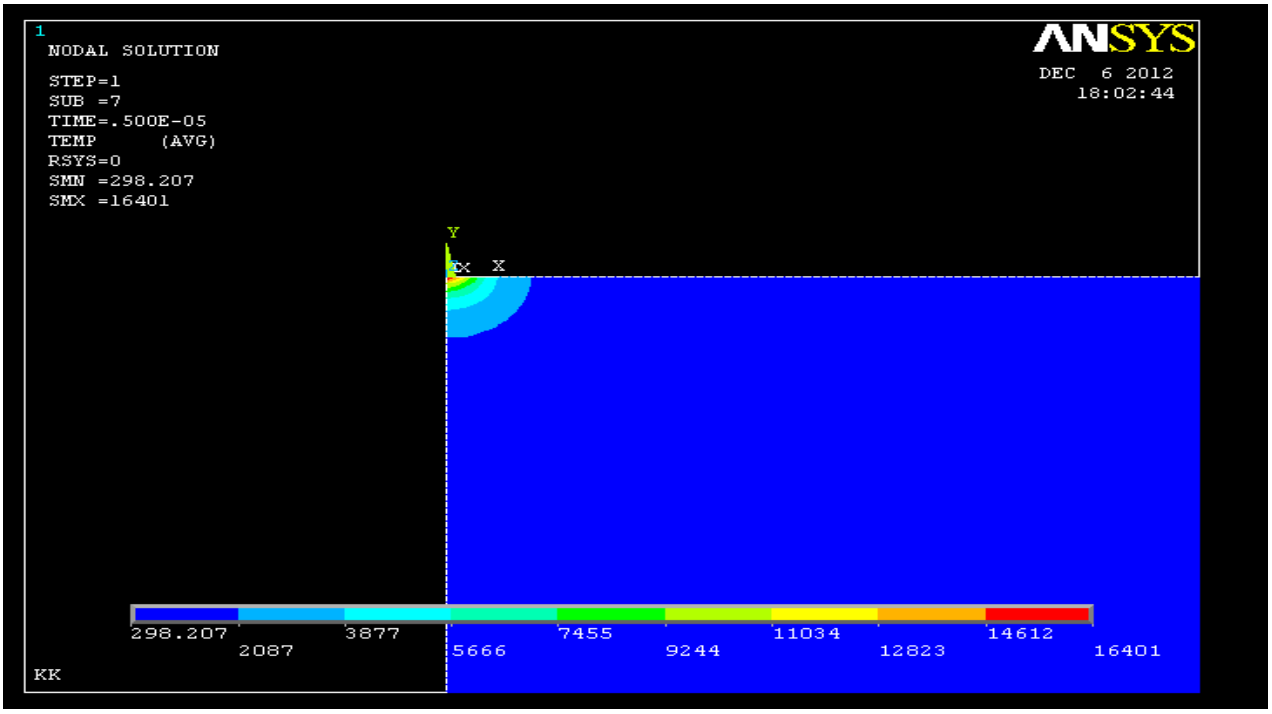

Fig.32 Temperature distribution in Al for V=9V,I=40A,Ton=5µs ,p=0.08

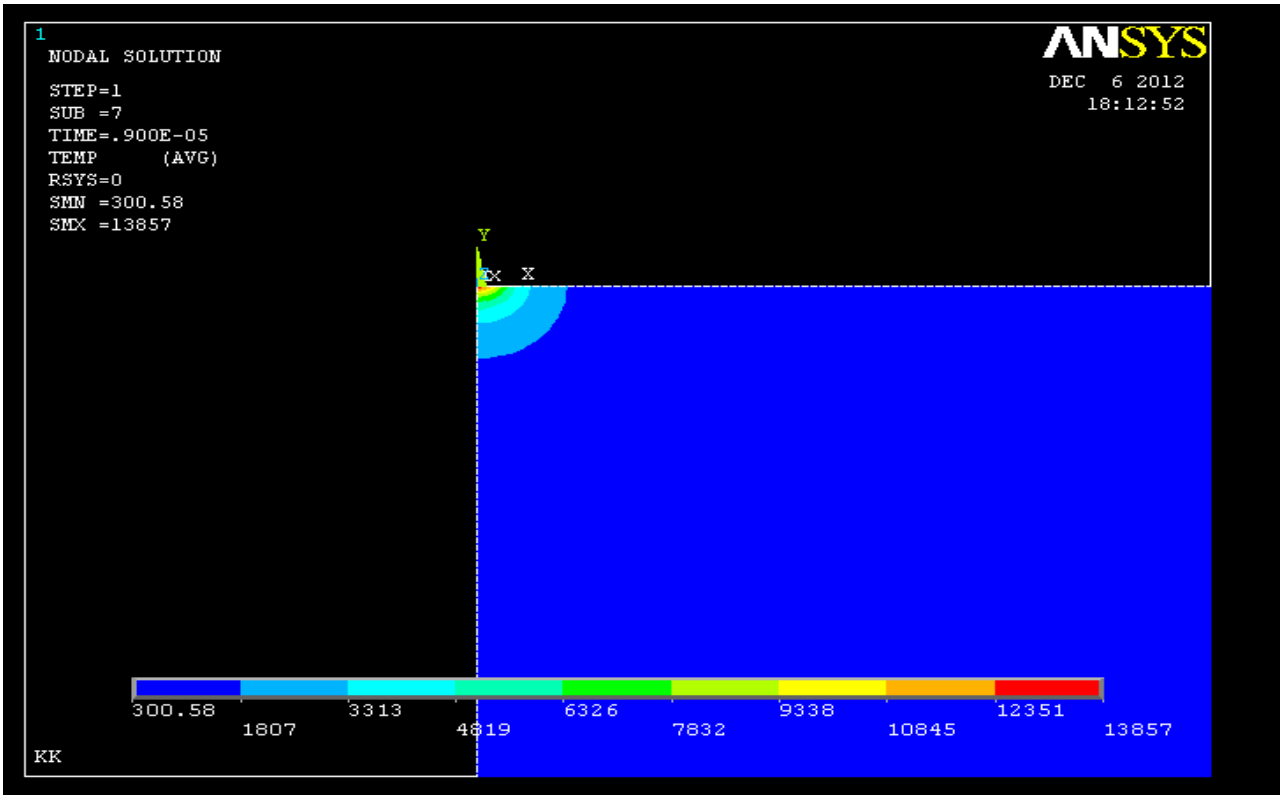

Fig.33 Temperature distribution in Al for V=10 V,I=30A,Ton=9µs ,p=0.25

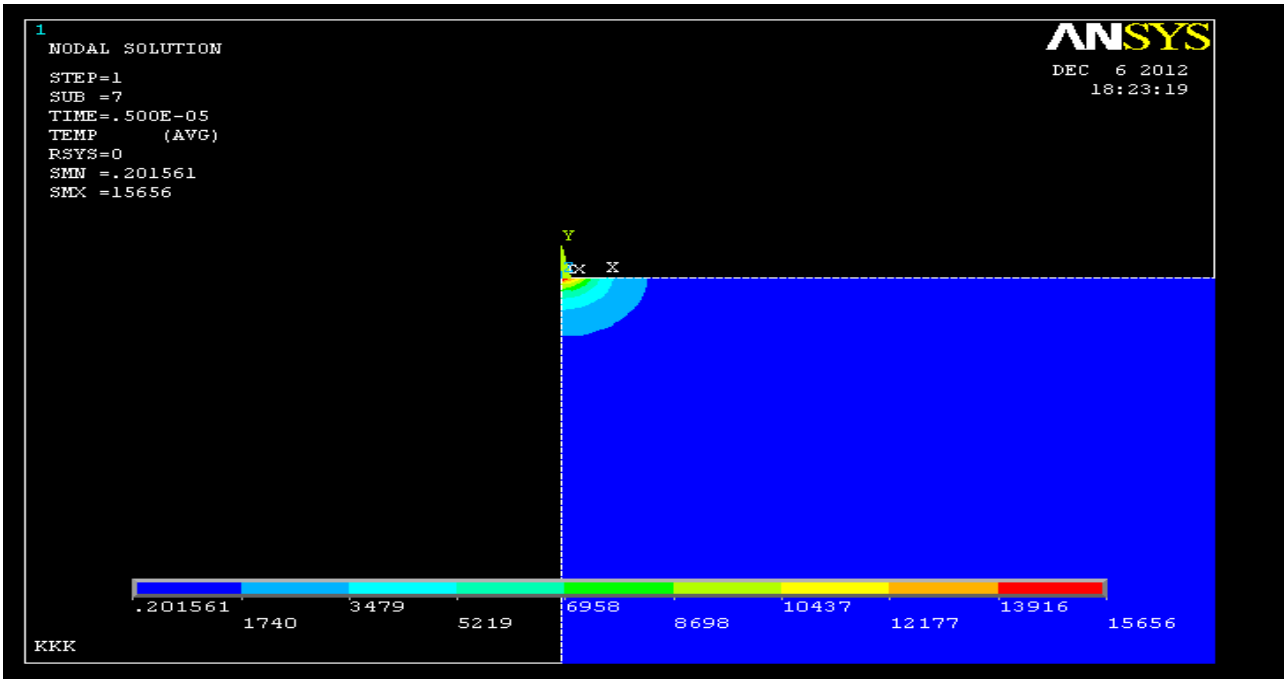

Fig.34 Temperature distribution in Al for V=10 V,I=35A,Ton=5µs ,p=0.08

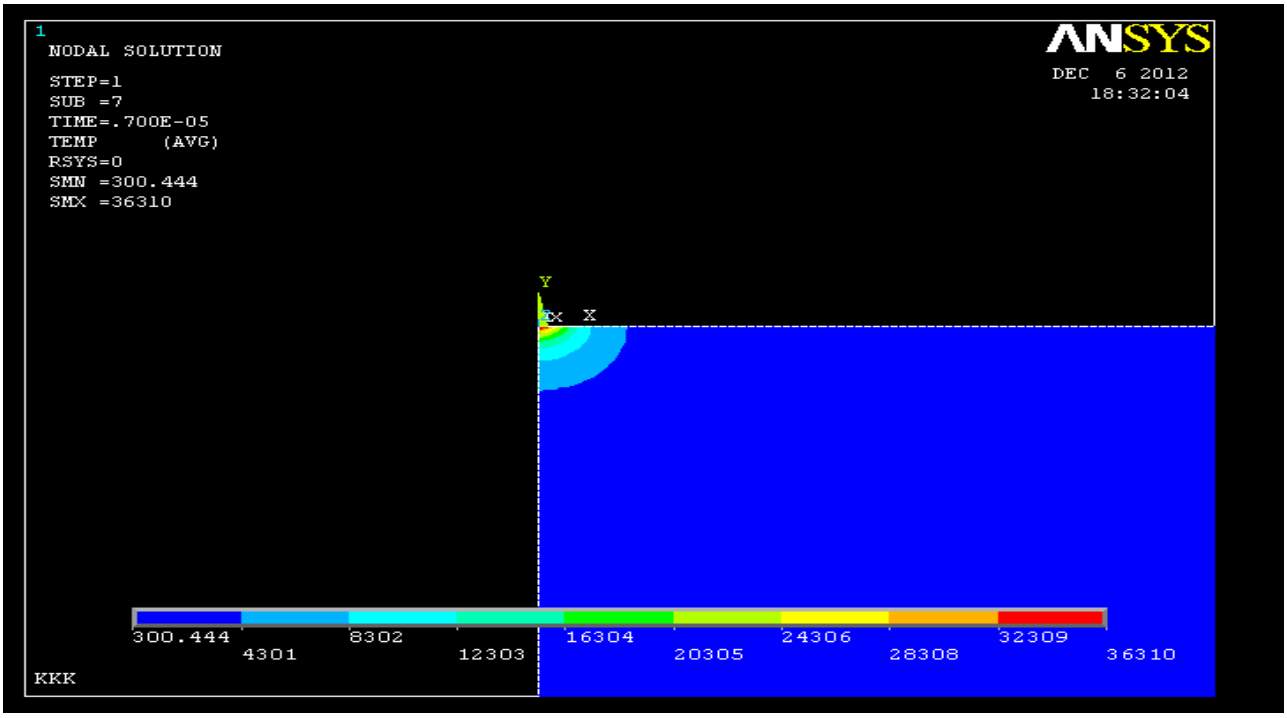

Fig.35 Temperature distribution in Al for V=10 V,I=40 A,Ton=7µs ,p=0.18

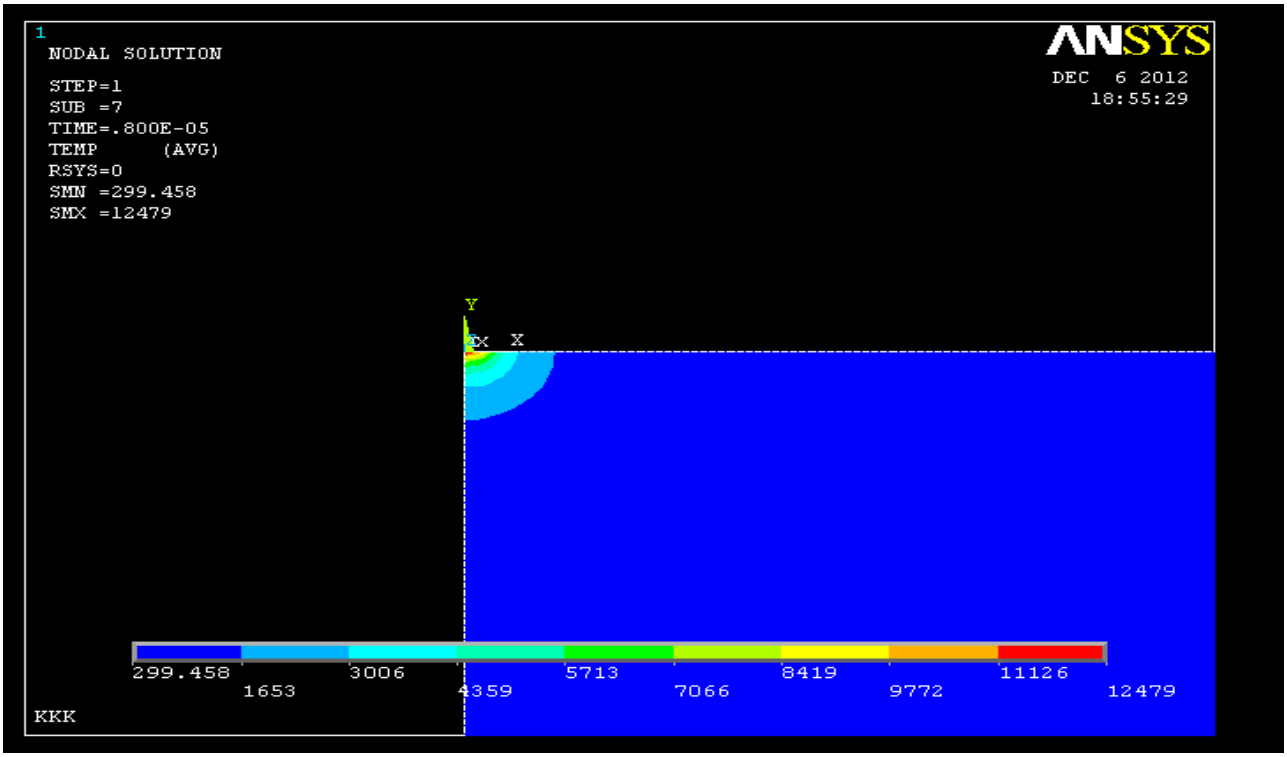

Fig.36 Temperature distribution in Al for V=9 V,I=30 A, Ton=8 µs ,p=0.15

5.5 MRR modelling of Micro EDM for single discharge

After doing the thermal modelling for single spark it has been done for the MRR modelling of Micro EDM for single discharge to calculate the modelled MRR for doing this modelling it have to kill all the elements above the melting temperature in the thermal model. Following are the MRR modelling in element view done for different process parameters as given in Table 7.

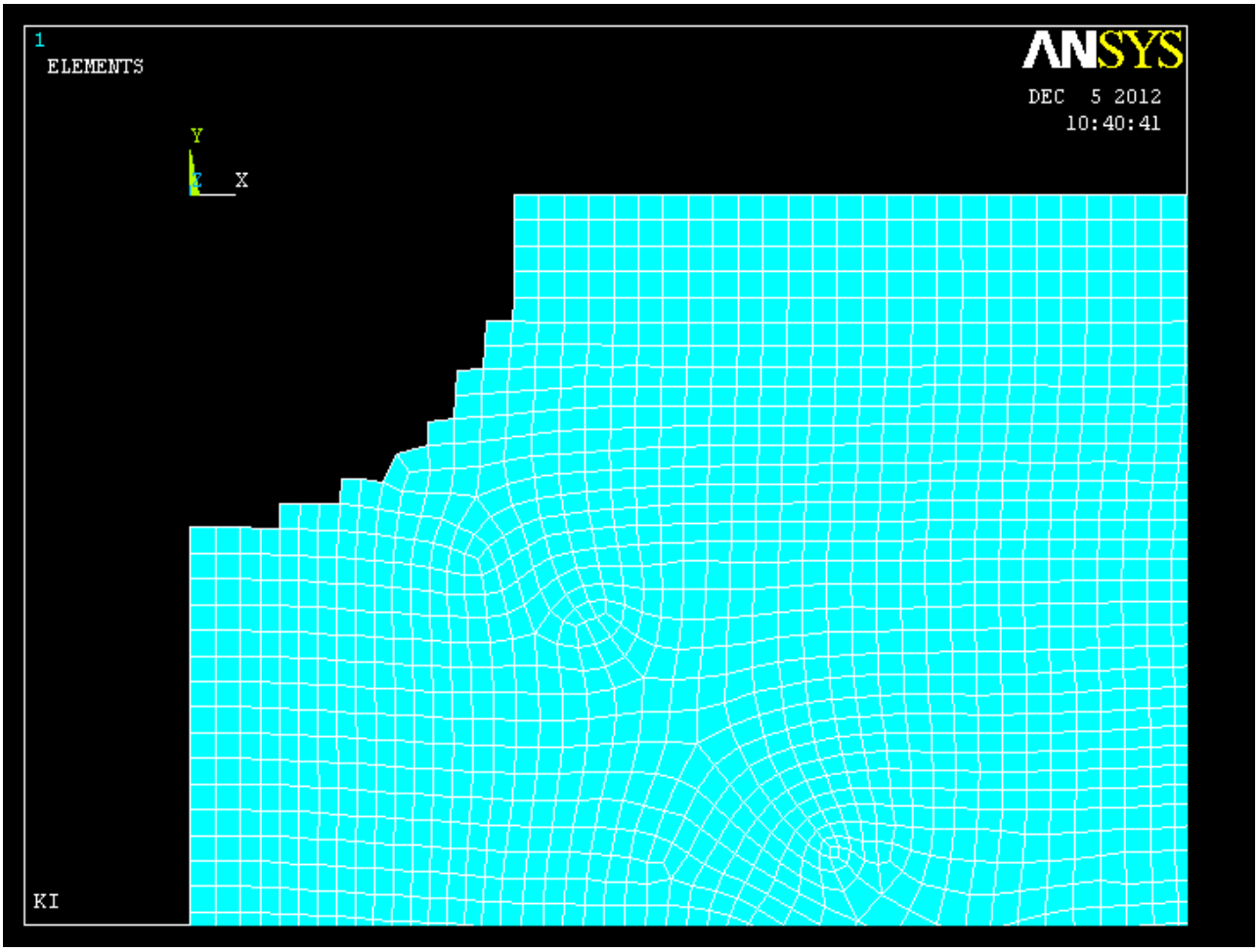

Fig.37 MRR modelling in Al for V=8V,I=30A,Ton=5 µs,p=0.08

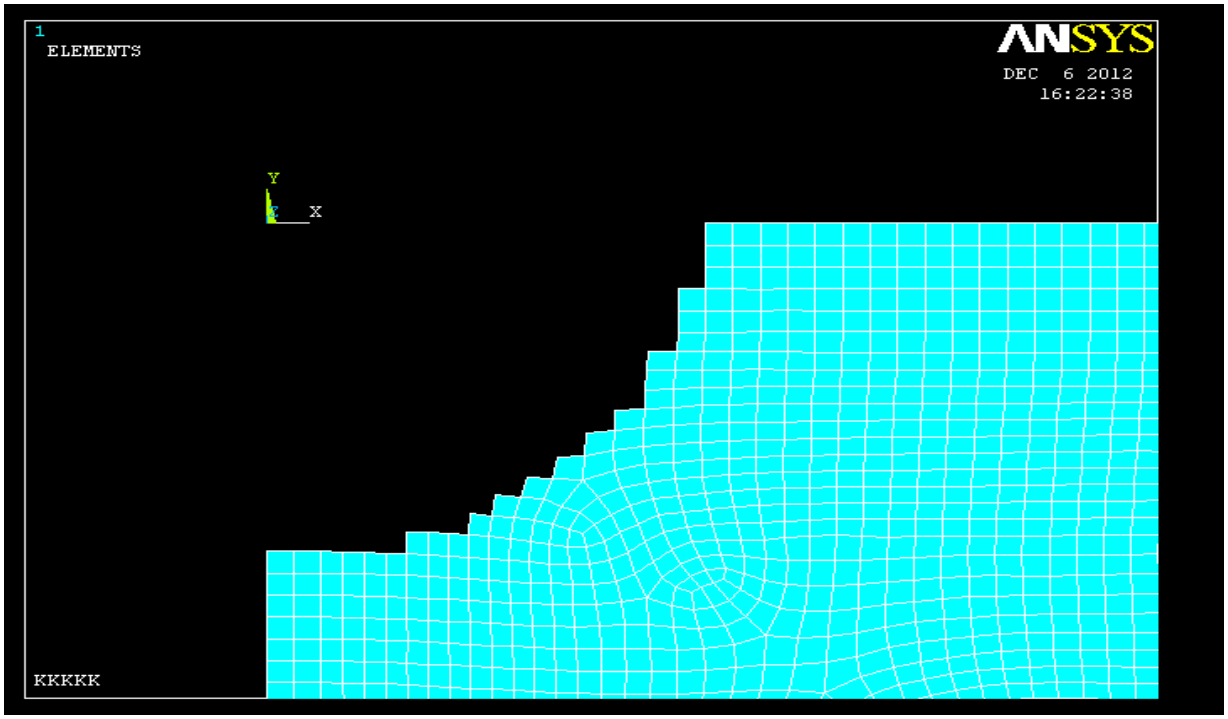

Fig.38 MRR modelling in Al for V=8V,I=35A,Ton= 7µs ,p=0.18

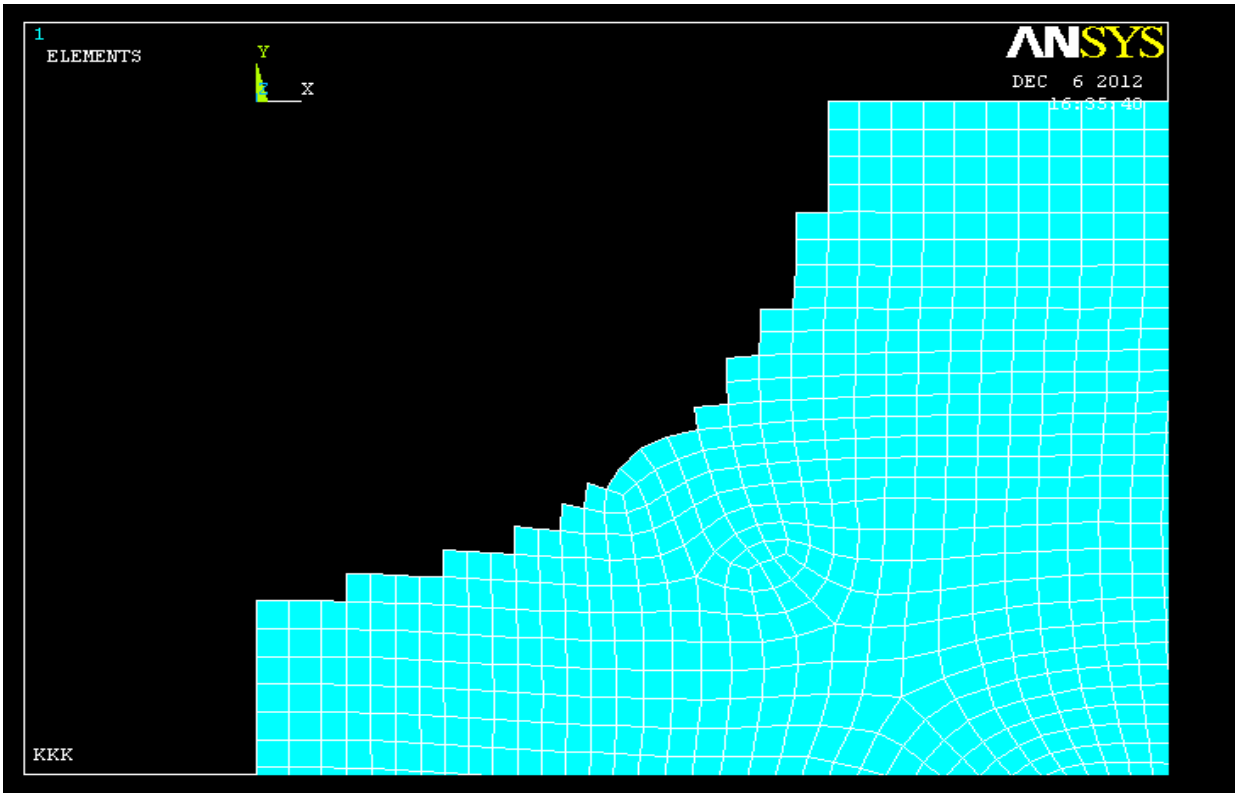

Fig.39 MRR modelling in Al for V=8V,I=40A,Ton=9 µs ,p=0.25

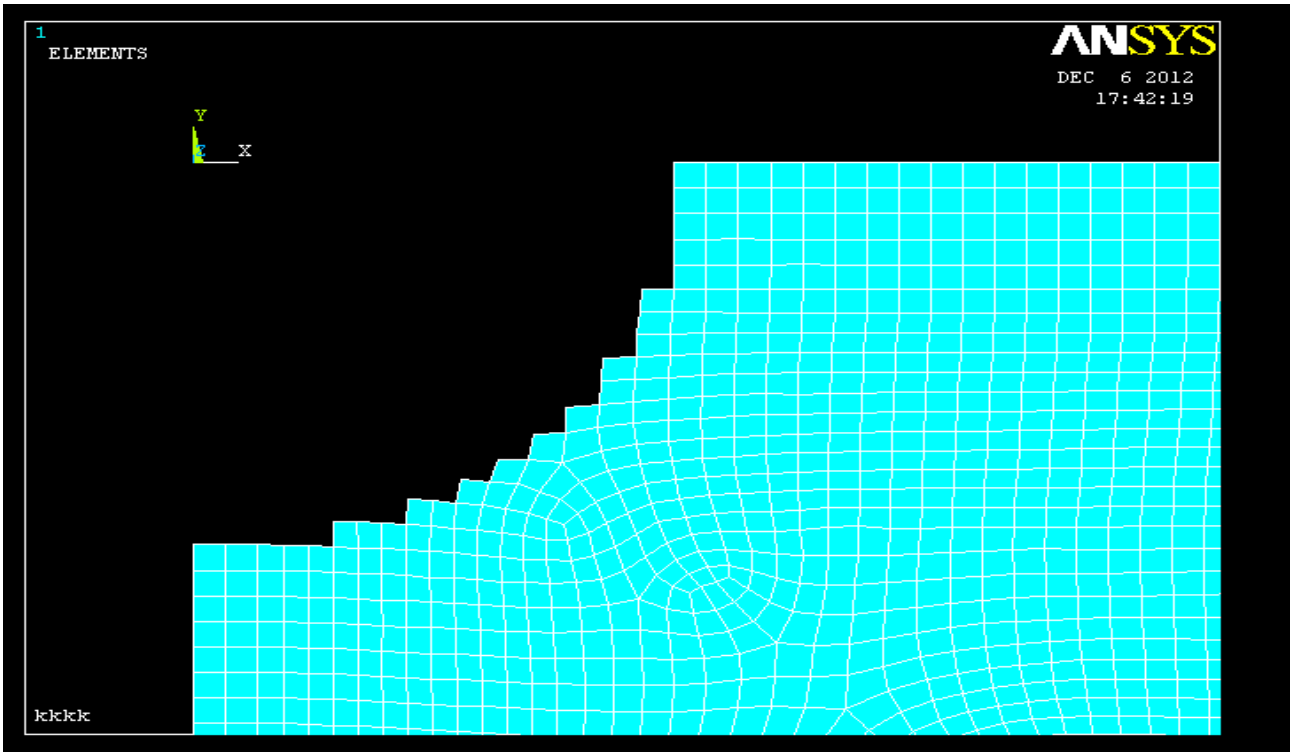

Fig.40 MRR modelling in Al for V=9V,I=30A,Ton=7µs ,p=0.18

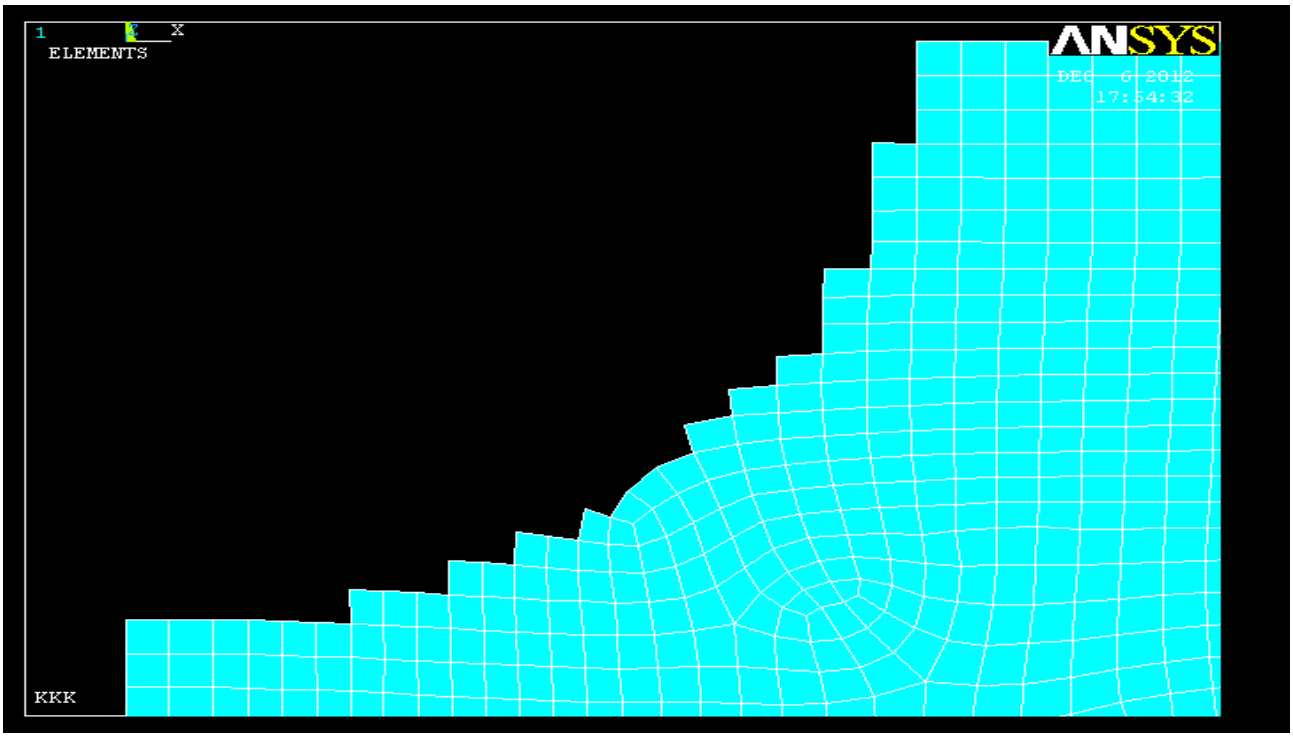

Fig.41 MRR modelling in Al for V=9V,I=35A,Ton=9µs ,p=0.25

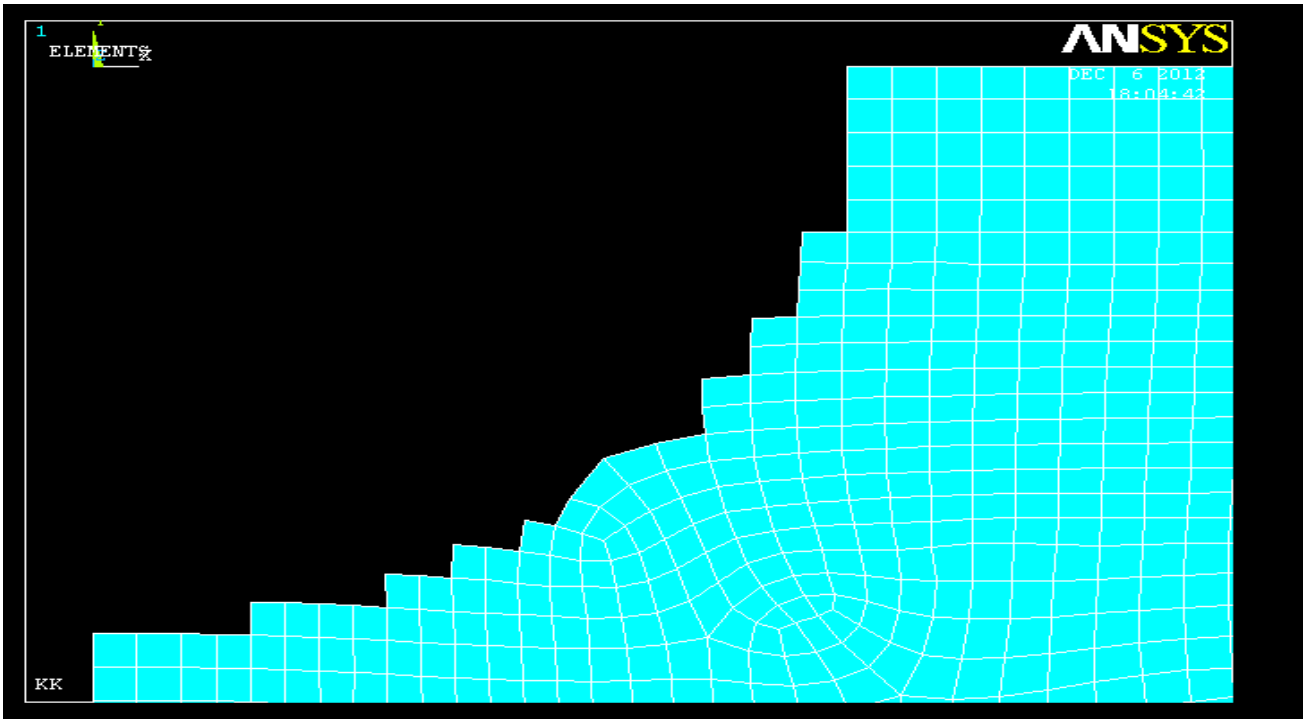

Fig.42 MRR modelling in Al for V=9V,I=40A,Ton=5µs ,p=0.08

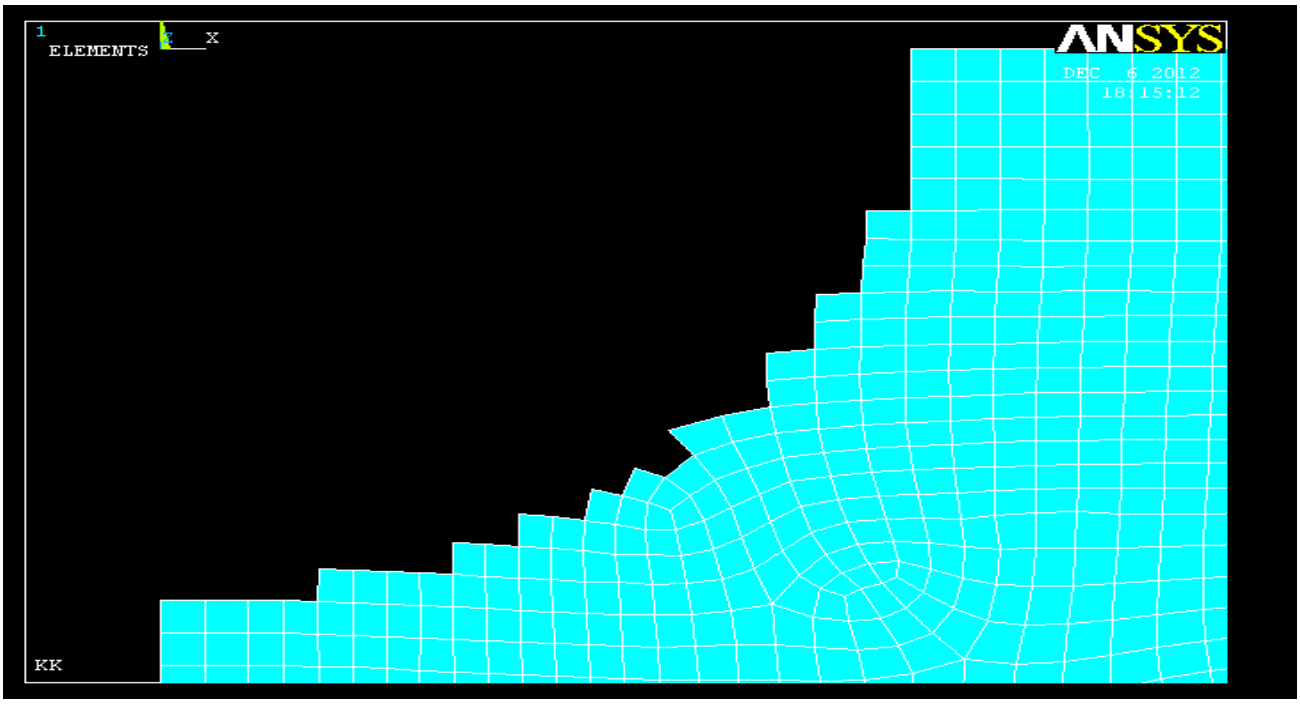

Fig.43 MRR modelling in Al for V=10 V,I=30A,Ton=9µs ,p=0.25

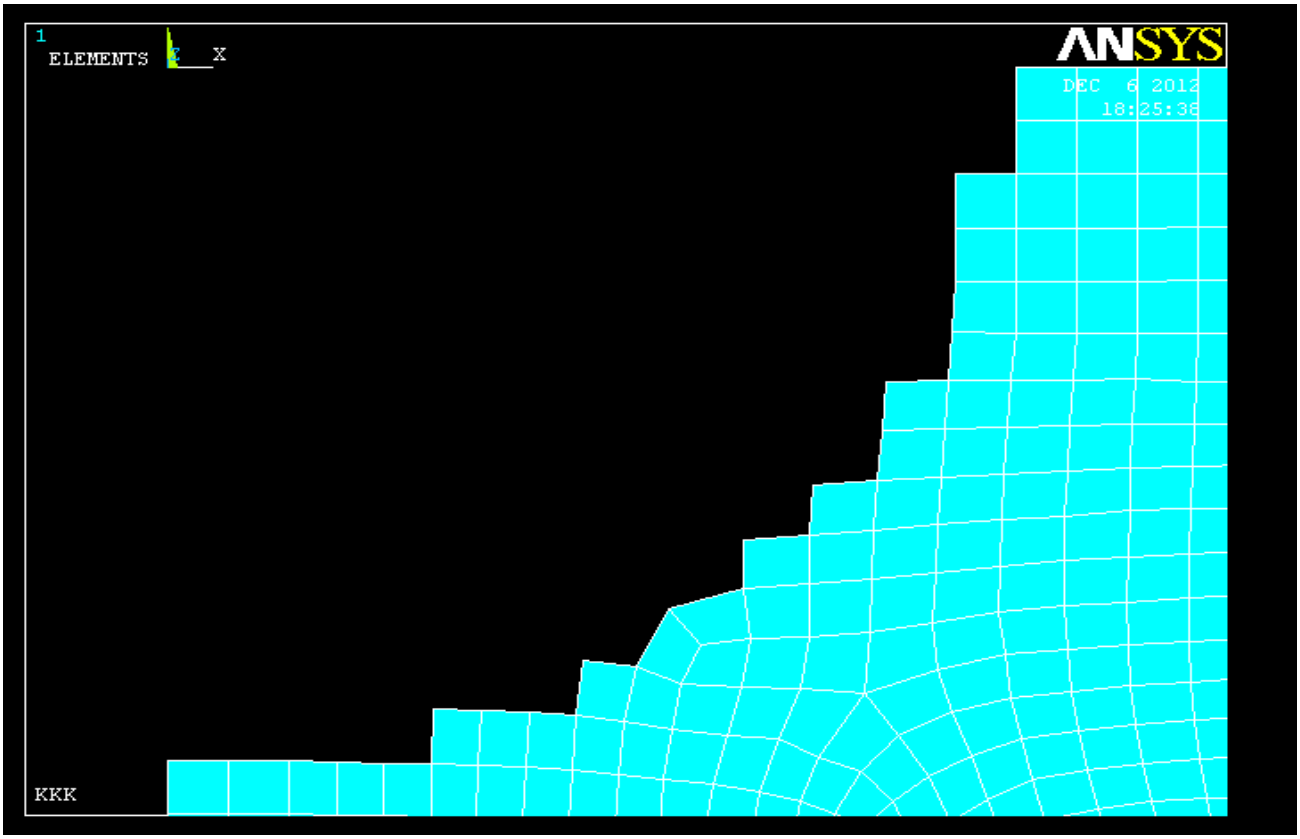

Fig.44 MRR modelling in Al for V=10 V,I=35A,Ton=5µs ,p=0.08

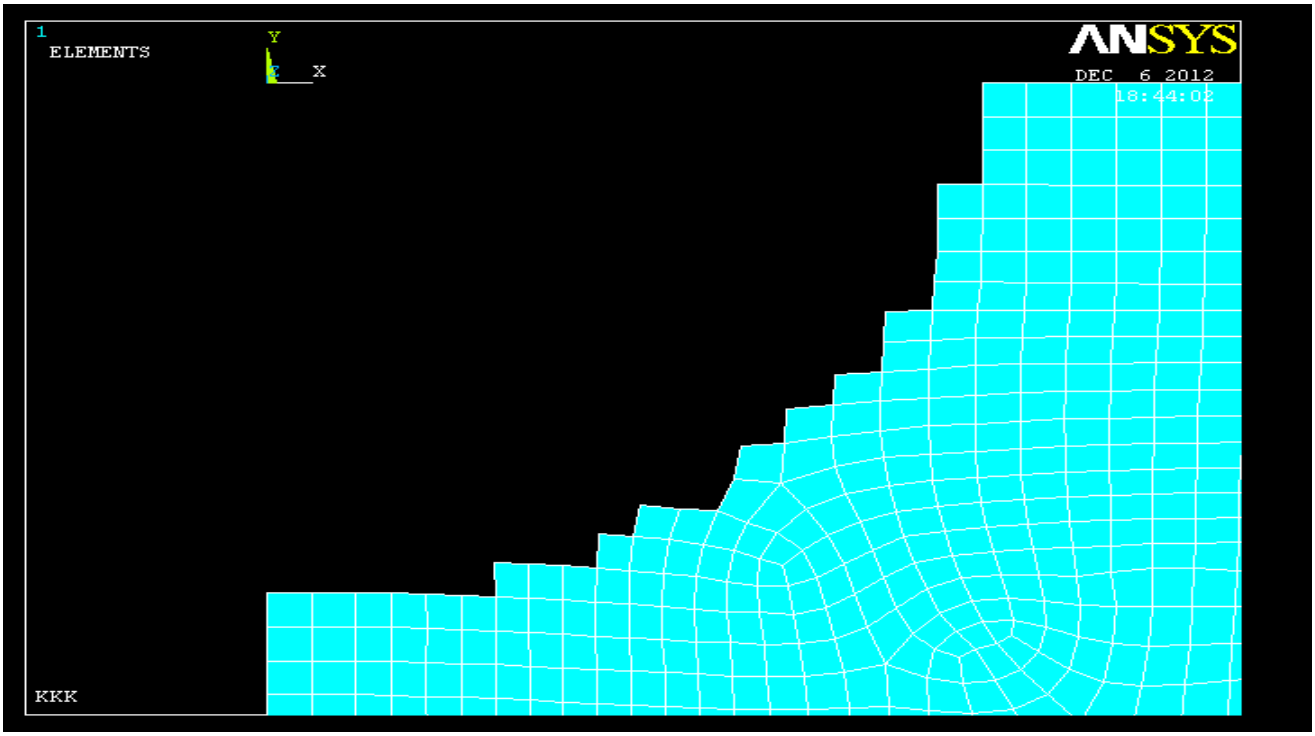

Fig.45 MRR modelling in Al for V=10 V,I=40 A,Ton=7µs ,p=0.18

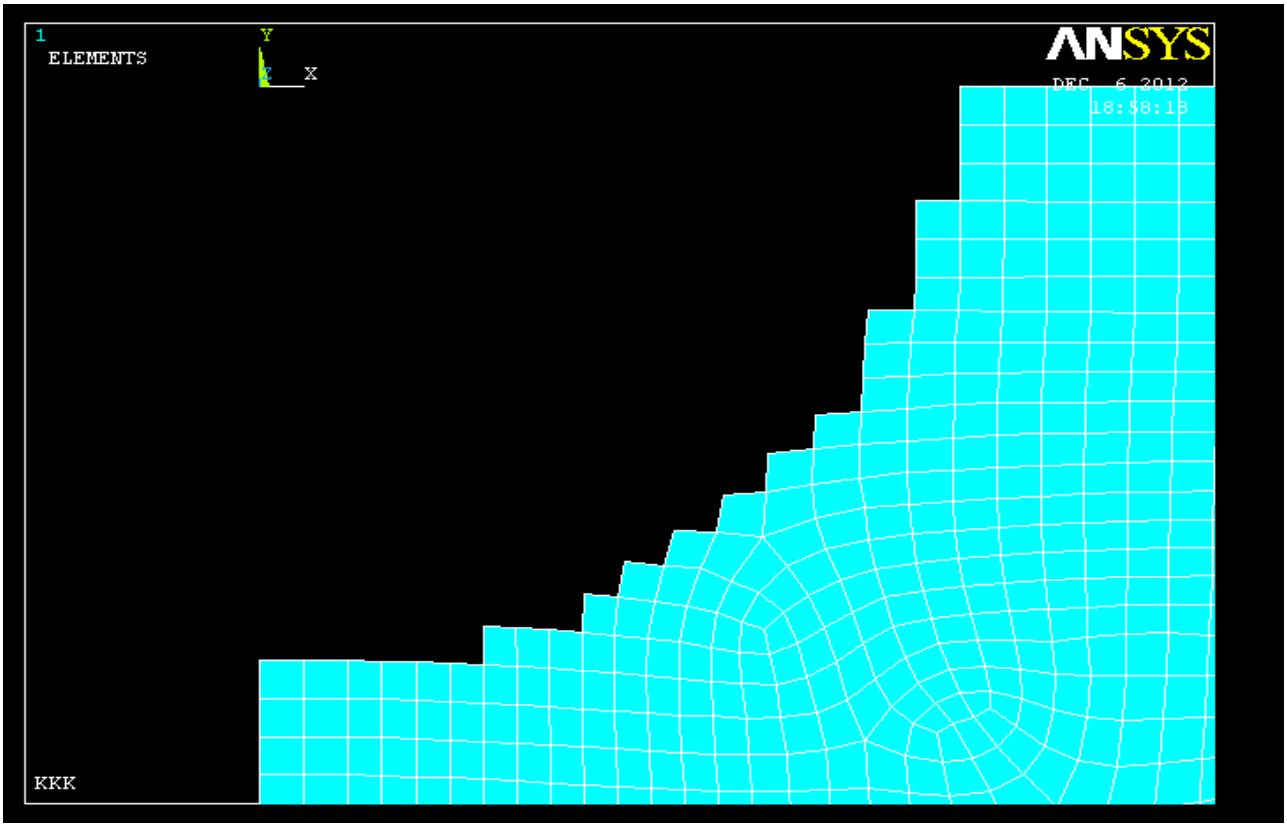

Fig.46 MRR modelling in Al for V=9 V,I=30 A, Ton=8 µs ,p=0.15

5.6 Calculation of MRR

Experimental MRR (mm^3/min) is calculated by:-

MRR=Volume of the hole ($\pi \times r^2 \times h$)/machining time

Where r is the mean radius,

h=thickness of work piece = 0.2 mm.

Table .18 Comparing the MRR, ANSYS Value Vs Experimental value

SL.NO	MRR THROUGH ANSYS ($mm^3/min)\times10^{-2}$	EXPERIMENTAL MRR($mm^3/min)\times10^{-2}$	%ERROR
1	6.53	5.68	12.82
2	5.76	5.05	12.35
3	6.20	5.62	9.35
4	5.96	4.98	16.44
5	6.28	5.65	17.15
6	5.94	4.75	20.00
7	5.86	5.04	13.9
8	5.49	4.67	15
9	5.93	5.15	13.1
10	6.48	5.80	10.5

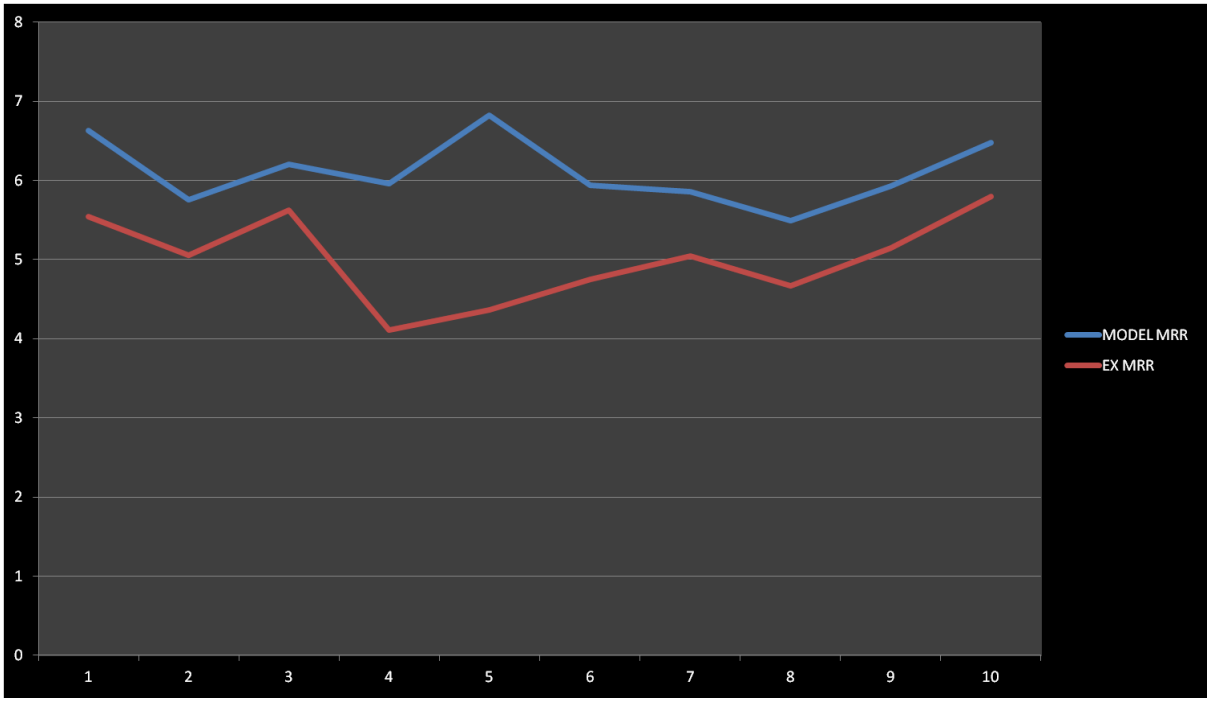

Fig.47 Graph between modeled and experimental MRR

5.7 ANSYS residual stress confirmation for Micro EDM

Residual stresses are stresses that remain after the original cause of the stresses (external forces, heat gradient) has been removed. Theses stresses are known to influence a material's mechanical properties such as creep or fatigue life. In order to confirm the ANSYS residual stress model at first it has to make a model for molybdenum with parameter setting as given in Table.19 Later the value had been compared with Philip Allen, (Fig.12) [28]. Fig 48 shows the residual stress model for EDM element size is taken as 10 μm so its getting the residual stress as shown in fig 48 is coming as 384 pa which is approximately same as given by Philip Allen [28].So it can say that we are proceeding in right way.

Table .19 Process parameters

Parameters	Units	Value
Discharge voltage	V	20
Current	A	1.5
Percentage of heat input to the workpiece		0.08
Spark radius	μm	5
Pulse-on time	μs	2
Heat transfer coefficient	W/m^2 k	680

Table.20 Thermal and mechanical properties of molybdenum

Thermal Conductivity, K(W/mK)	138
Specific Heat, C(J/kg K)	276
Density, ρ (kg/m^3)	10,220
Melting Temperature (K)	2896
Young's Modulus, E (GPa)	185
Poisson's Ration	0.30

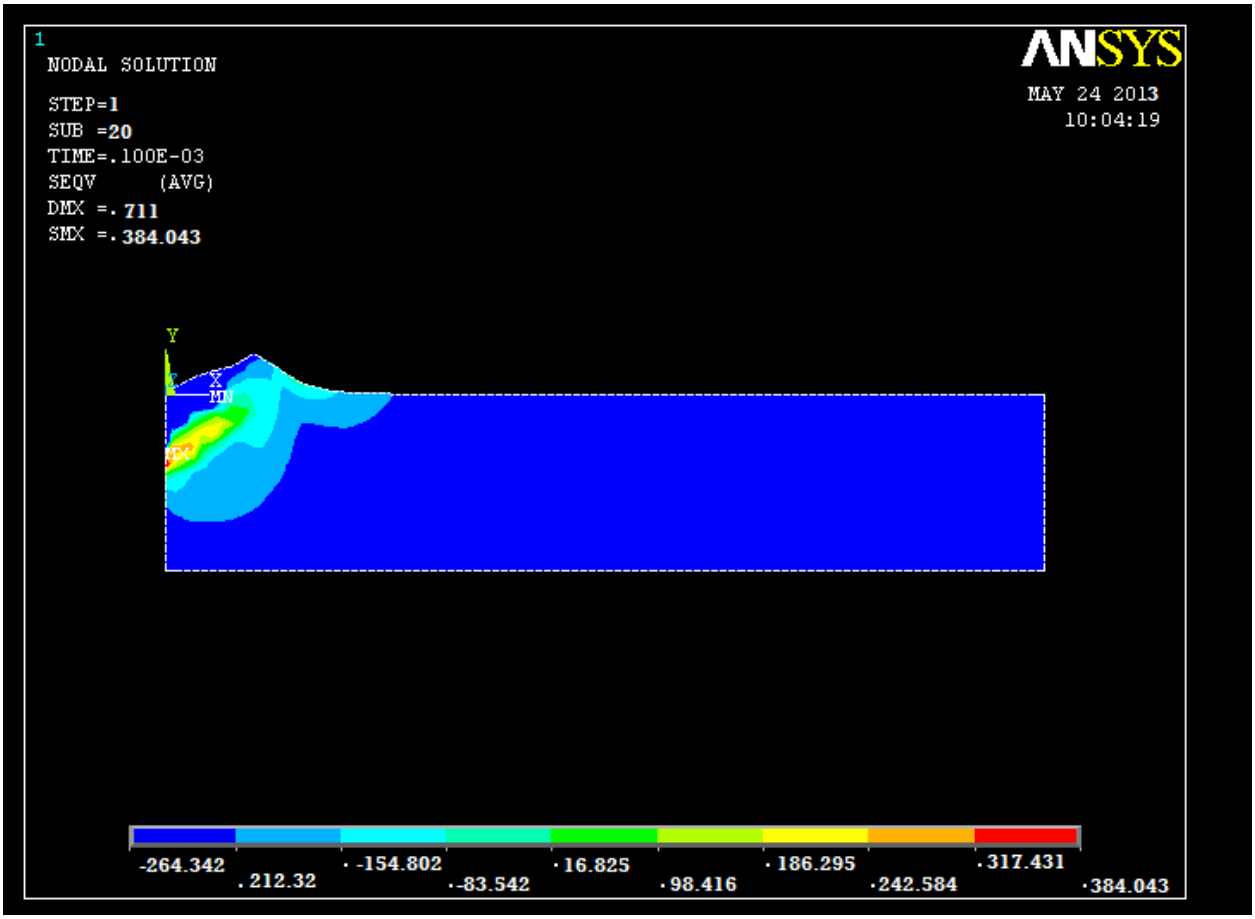

Fig.48 Residual stress distribution for single spark Micro EDM process

5.8 Optimization for Micro EDM process by Grey taguchi method

After getting the MRR and residual stress values through ANSYS 13 from the modelling for Micro EDM process its come to optimize the model there are two main responses of the model first one is MRR and second one is residual stress for MRR higher is the better criteria is adopted and for residual stress lower is the better criteria is adopted.

Table 21 Predicted data with ANSYS obtain from model of micro EDM for Al

S. No.	VOLTAGE	CURRENT	HEAT INPUT	MRR ($mm^3/min)\times10^{-2}$	Residual Stress (GPa)
1	8	30	0.08	6.53	3.85
2	8	35	0.18	5.76	4.36
3	8	40	0.25	6.20	5.72
4	9	30	0.18	5.96	4.82
5	9	35	0.25	6.28	6.28
6	9	40	0.08	5.94	5.33
7	10	30	0.25	5.86	3.47
8	10	35	0.08	5.49	6.87
9	10	40	0.18	5.93	5.84

Table 22 Grey relational generation

SL. No.	MRR	Residual Stress
1	0	0.111765
2	0.740385	0.261765
3	0.317308	0.661765
4	0.548077	0.414706
5	0.240385	0.826471
6	0.567308	0.547059
7	0.644231	0
8	1	1
9	0.576923	0.697059

Table 23 Grey relational coefficient for each performance characteristics (Taking ψ=0.5)

SL. No.	MRR (ψ=0.5)	Residual Stress (ψ=0.5)	Overall grade
1	1	0.817308	0.908654
2	0.403101	0.656371	0.529736
3	0.611765	0.43038	0.521072
4	0.477064	0.546624	0.511844
5	0.675325	0.37694	0.5261325
6	0.468468	0.477528	0.472998
7	0.436975	1	0.7184875
8	0.333333	0.333333	0.3333333
9	0.464286	0.41769	0.440988

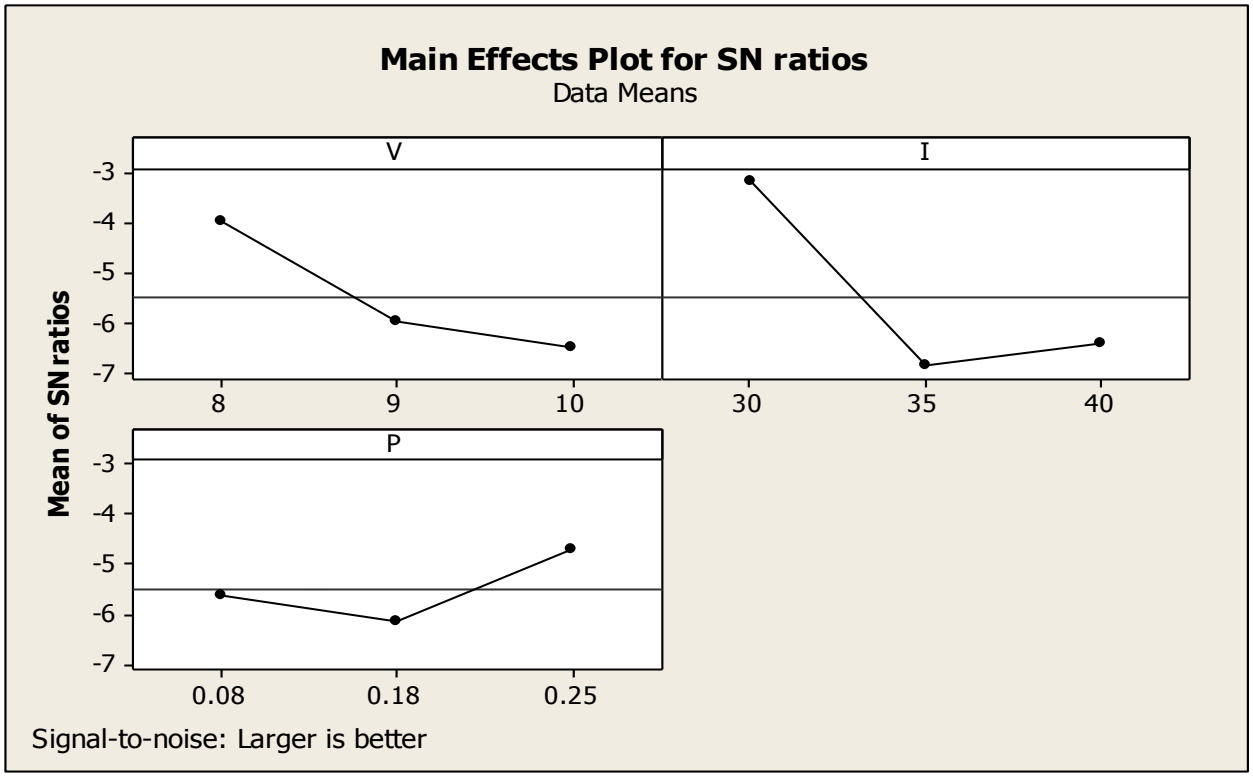

Fig 49.Mean effect plot

5.9 Optimization for Micro EDM process by Grey taguchi coupled with principle component analysis.

Table 24. Data preprocessing of each performance characteristics

Sl. no.	V	I	p	Normalisation 1 (MRR)	Normalisation 2 (R.stress)
1.	8	30	0.08	0	0.111765
2.	8	35	0.18	0.740385	0.261765
3.	8	40	0.25	0.317308	0.661765
4.	9	30	0.18	0.548077	0.414706
5.	9	35	0.25	0.240385	0.826471
6.	9	40	0.08	0.567308	0.547059
7.	10	30	0.25	0.644231	0
8.	10	35	0.08	1	1
9.	10	40	0.18	0.576923	0.697059

Table 25. Principal component analysis for L9 OA experimental observations

Sr. No.	Grey coefficient 1	Grey coefficient 2	overall grey grade	PC1 (Ψ1)	PC2 (Ψ2)	PC1square (Ψ12)	PC2 square (Ψ22)
1.	1	0.817308	0.908654	1.23387	0.381513	1.52243	0.145552
2.	0.403101	0.656371	0.529736	0.76974	-0.02689	0.5925	0.000723
3.	0.611765	0.43038	0.521072	0.69672	0.271869	0.48542	0.073913
4.	0.477064	0.546624	0.511844	0.71917	0.095331	0.51721	0.009088
5.	0.675325	0.37694	0.5261325	0.68738	0.354388	0.47249	0.125591
6.	0.468468	0.477528	0.472998	0.65684	0.126363	0.43144	0.015968
7.	0.436975	1	0.7184875	1.07483	-0.18872	1.15527	0.035617
8.	0.333333	0.333333	0.3333333	0.46202	0.093479	0.21346	0.008738
9.	0.464286	0.41769	0.440988	0.6046	0.155976	0.36554	0.024329

Table 26. (Analysis of covariance matrix), accountability proportion (AP)

Eigenvalue	0.057228	0.032774
Proportion	0.636	0.364
Cumulative	0.636	1.000

Table 27. Cumulative accountability proportion (CAP) computed for the two major quality indicators, Eigen analysis of the Covariance Matrix

Variable	PC1(Ψ1)	PC2(Ψ2)
normalisation 1	0.833	-0.553
normalisation 2	0.553	0.833

Table 28 Calculation of composite principal component (overall quality index) and corresponding S/N ratios

Sr.No.	composite principal component	S/N Ratio composite
1.	1.2915	2.22191
2.	0.77021	-2.26785
3.	0.74789	-2.52328
4.	0.72547	-2.78766
5.	0.77336	-2.23238
6.	0.66888	-3.49299
7.	1.09128	0.75869
8.	0.47138	-6.5326
9.	0.6244	-4.09079

Table 29 . Response Table for Signal to Noise Ratios (Larger is the better)

Level	V	I	p
1	0.85641	0.06431	2.60123
2	-2.83768	3.67761	3.04877
3	3.28823	3.36902	-1.33232
Delta	2.43183	3.74192	1.71644

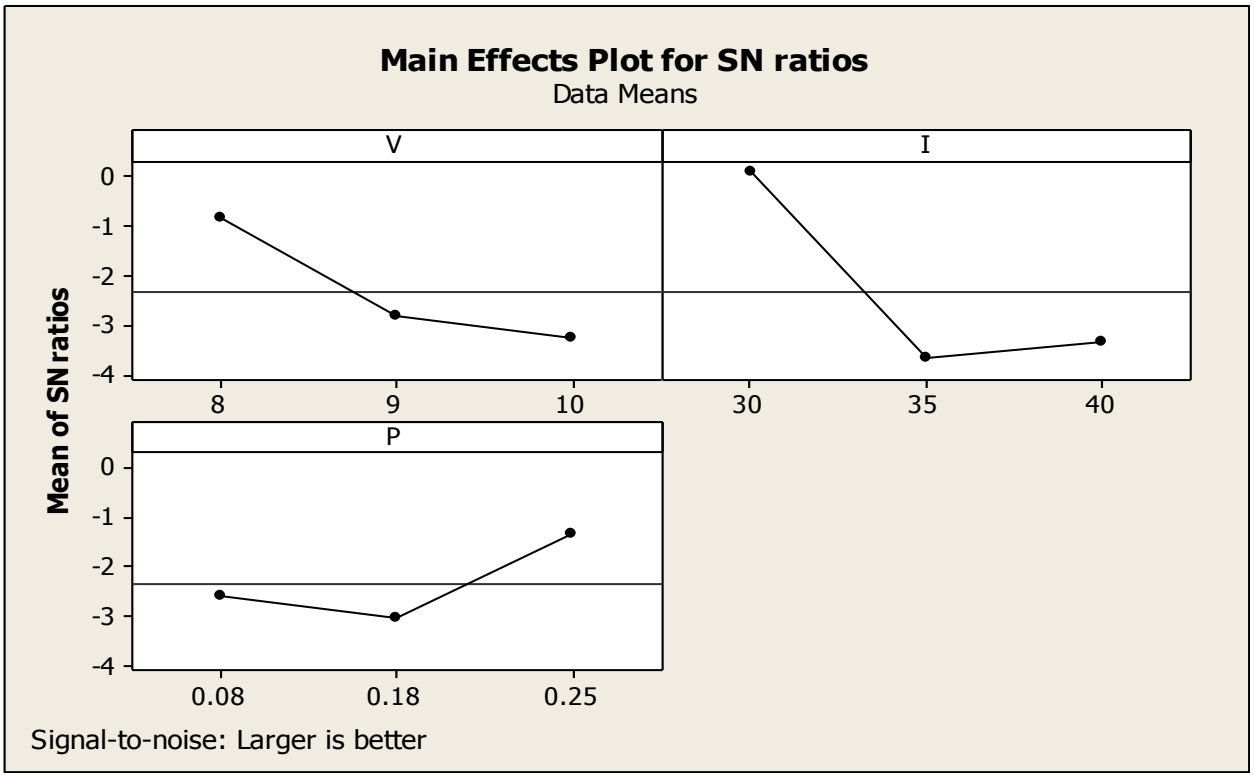

Fig.50 Mean effect plot for S/N ratio

5.10 Effect of different process parameters

5.10.1 Effect of current

From the graphs, Fig.51 and Fig.52 it is observed that the effect of current along the radius and depth of the work piece respectively. From the graph Fig. 51 it's seen that temperature on the top surface increases as the current increases. It happens because the heat flux equation is directly proportional to the current. Larger the value of current, larger the heat input hence higher the temperature. The considerable temperature gradient along the radial direction can be seen up to 8 μm.

In the graph Fig.52 it is observed that the effect of current along the depth of the work piece the maximum temperature is found at the surface and is going to decrease as proceed further.

No considerable variation in temperature is observed after a depth of 6 μm

Along the radius

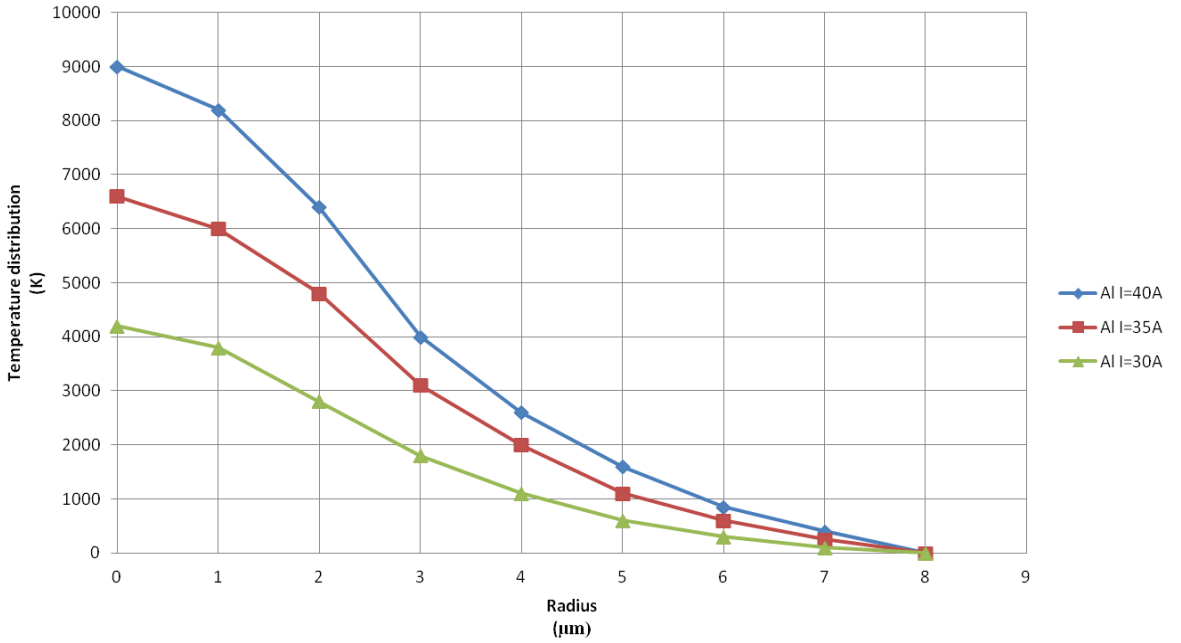

(a)

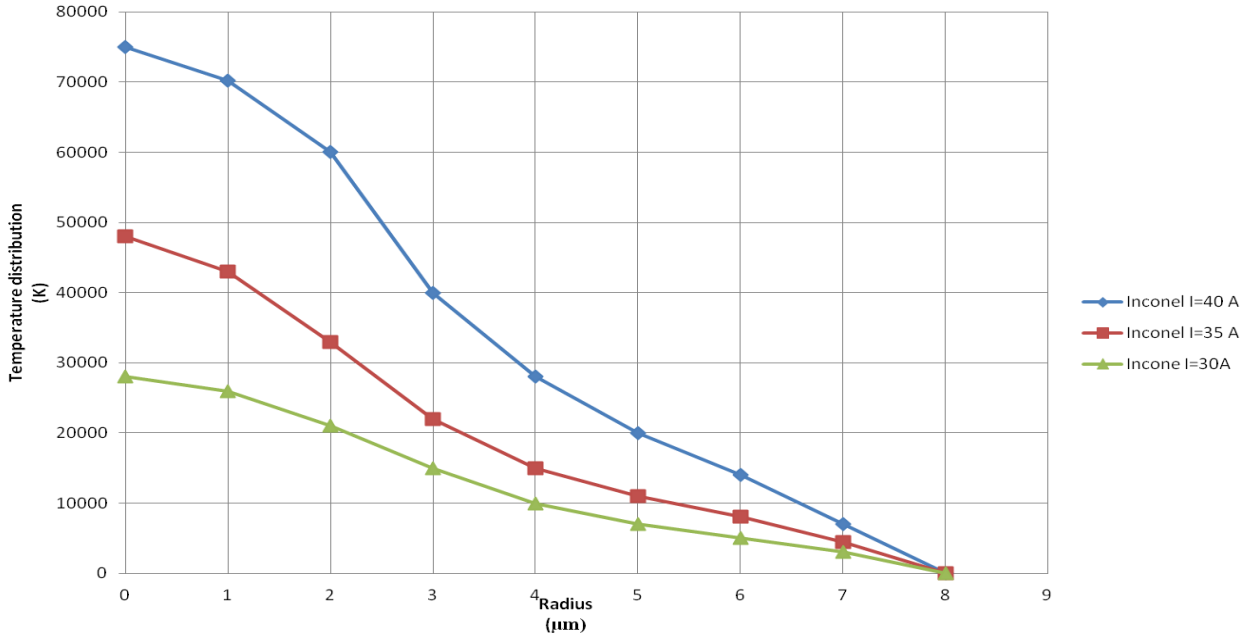

(b)

Fig. 51 The effect of current on the temperature distribution along the radius for micro EDM at P = 0.08, Ton = 5 µs, V = 8 V.(a) for Inconel 718 (b) for Al

Along the depth

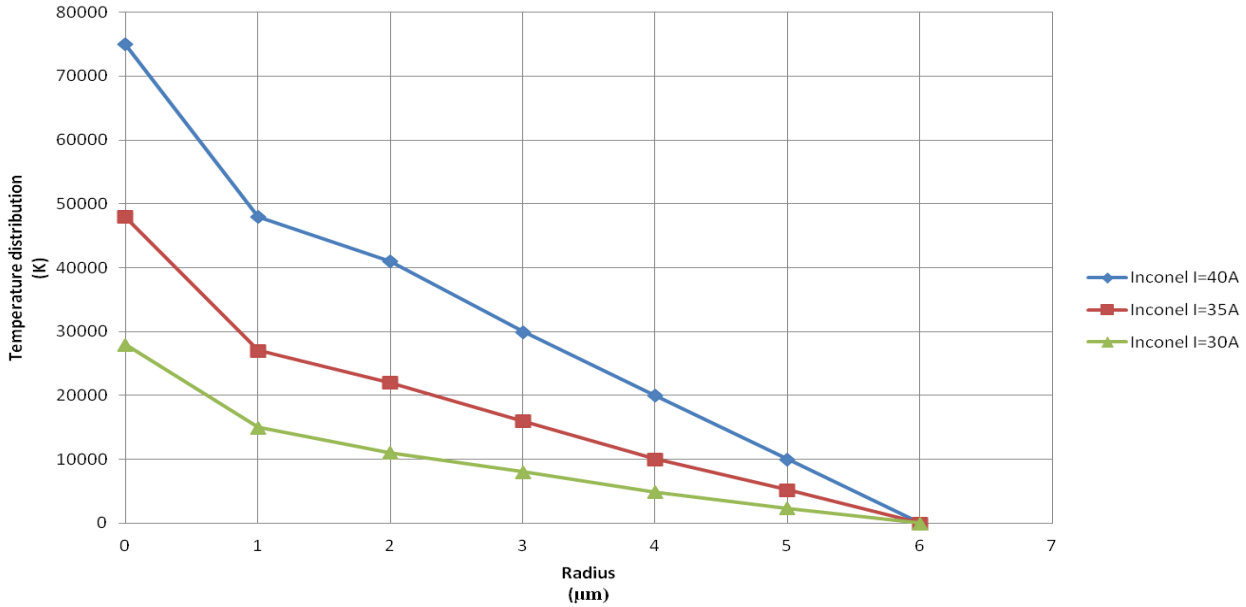

(a)

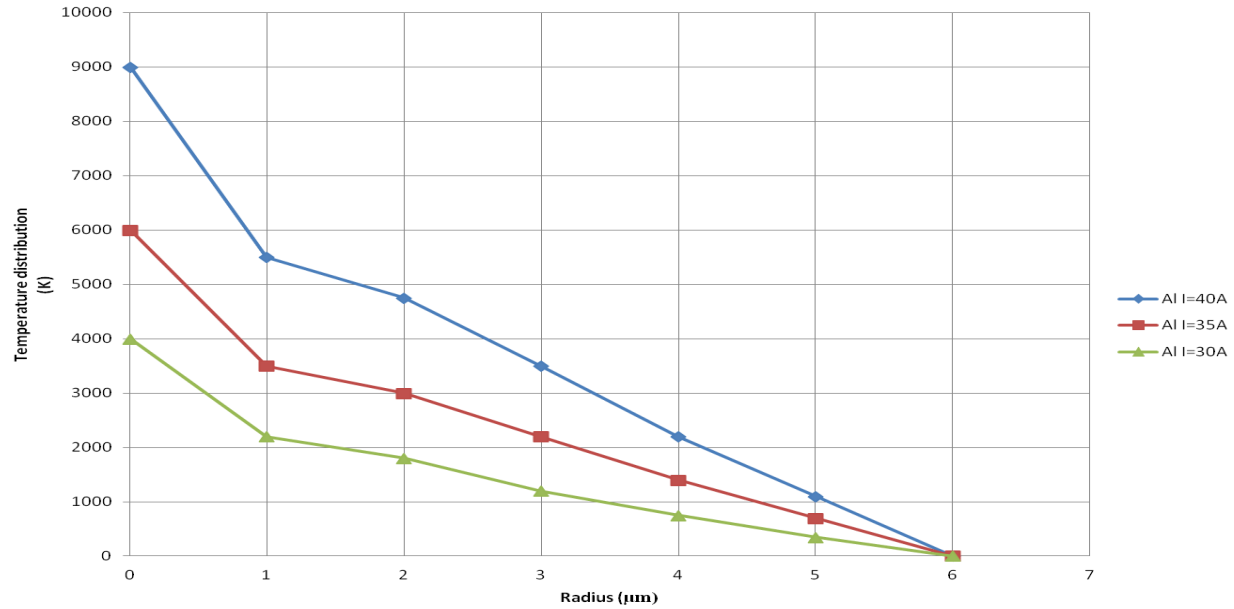

(b)

Fig. 52 The effect of current on the temperature distribution along the depth of workpiece for micro EDM at P = 0.08, Ton = 5 µs, V = 8 V.(a)Inconel 718 (b) Al

5.10.2 Effect of heat input

From the graphs, Fig.53 and Fig.54 it is observed that the effect of of heat input on the work piece along the radial and along the depth respectively. By observing both the graphs it can say that the temperature at the surface is going increasing as the heat input increases.

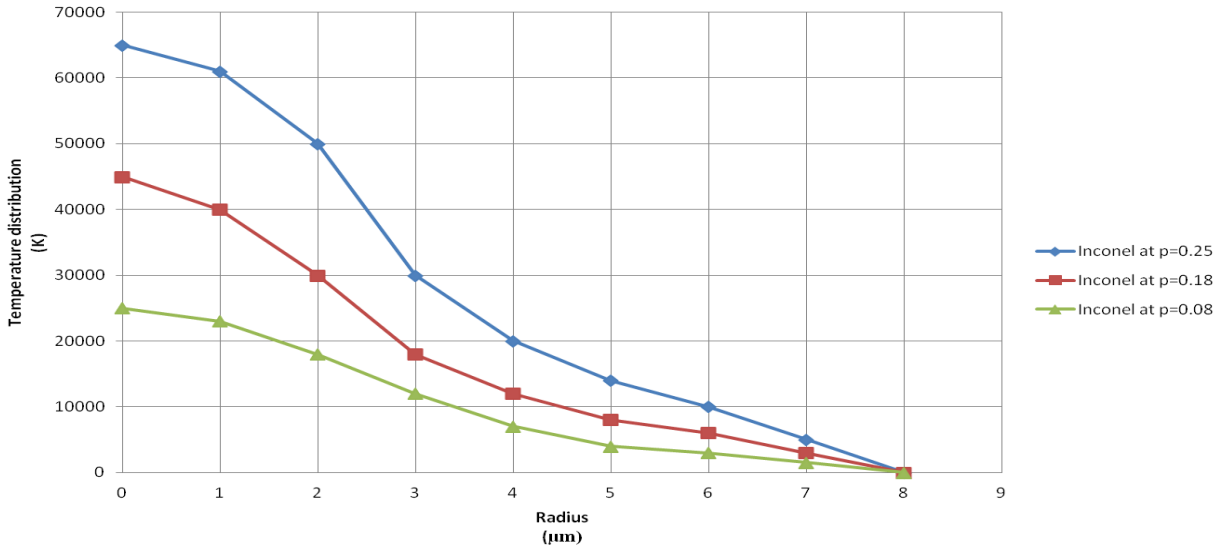

(a)

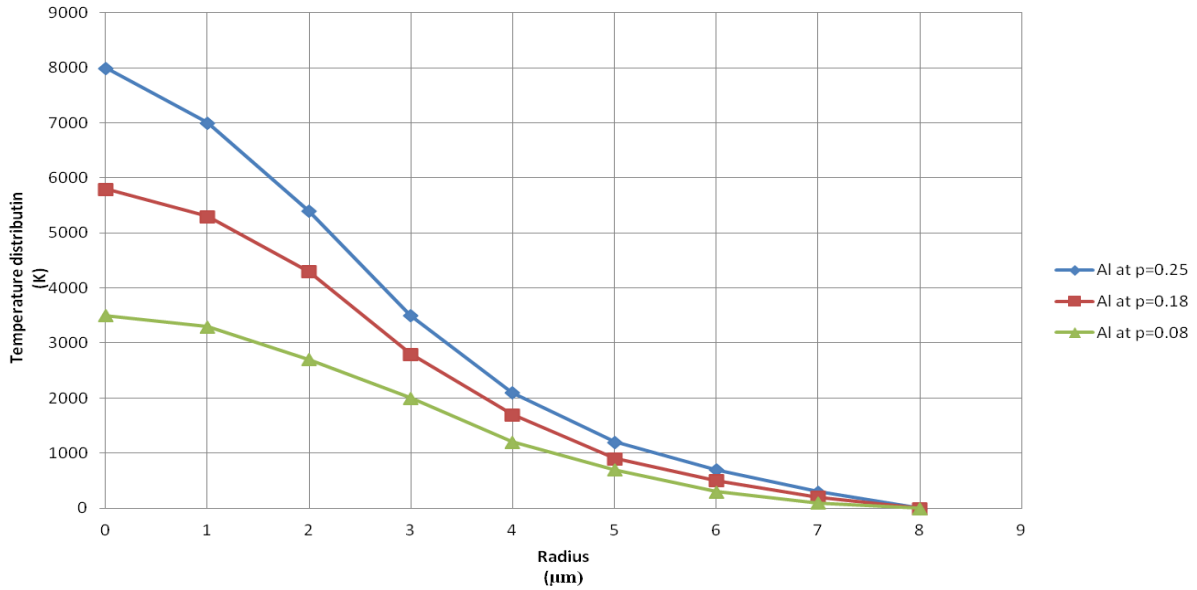

(b)

Fig.53 The effect of heat input to the workpiece on the temperature distribution along the radius for micro EDM at I = 30A, Ton = 5 µs, V = 8V.(a) inconel 718 (b) Al

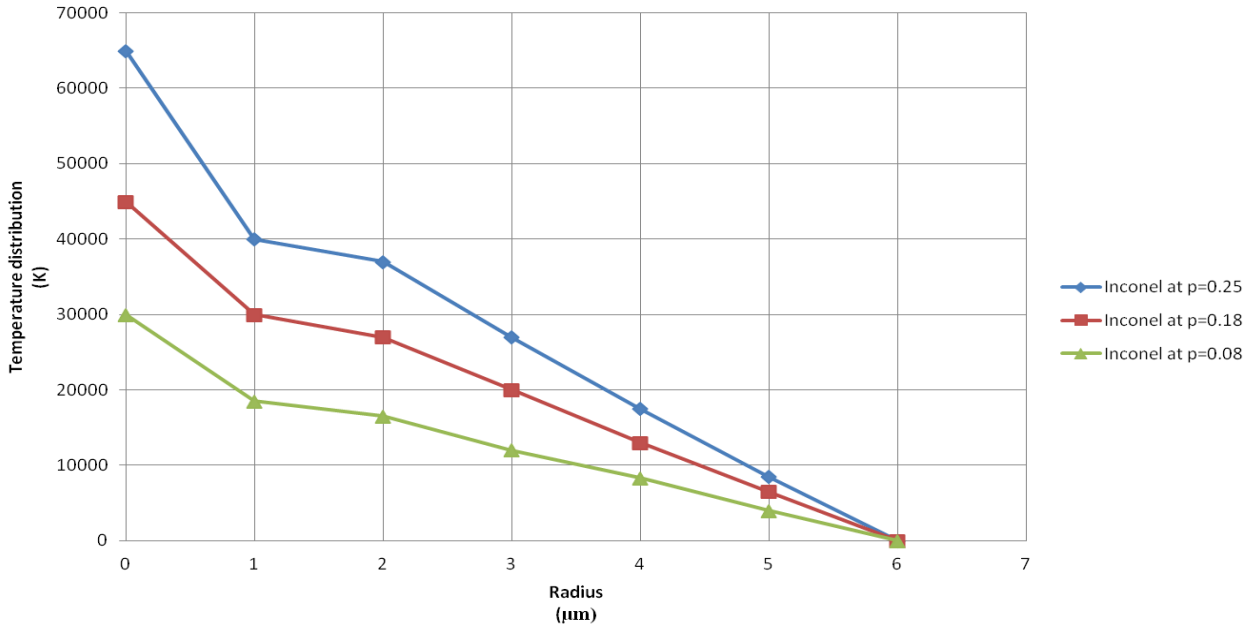

(a)

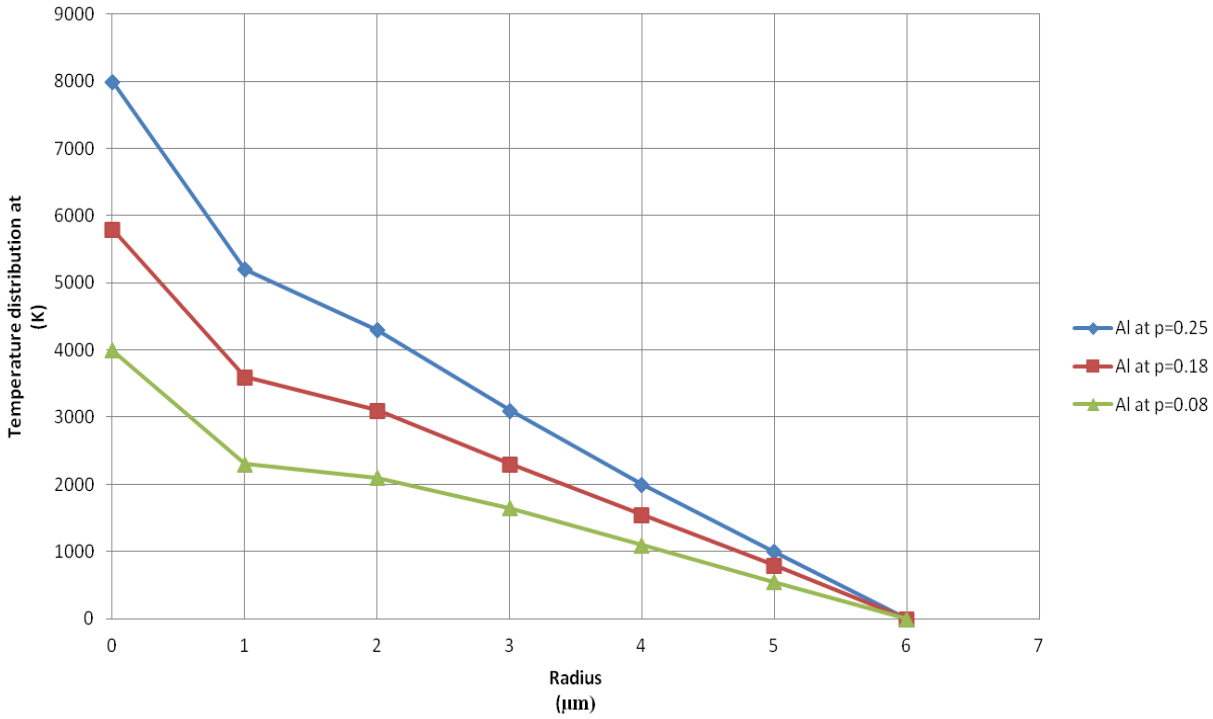

(b)

Fig 54.The effect of heat input to the workpiece on the temperature distribution along the depth of workpiece for micro EDM at I = 30 A, Ton = 5 µs, V = 8 V.(a) Inconel 718 (b) Al

6. Conclusions

- **From the Experiment**
  - From the S/N ratio plot the observed optimum parameter settings are V=9V,I=40A and Ton =7µs.
  - From the input parameters V is the most prominent factor which affects the responses.
- **From the ANSYS modelling**
  - We did the study of the effect of different process parameters. For micro EDM process MRR also have been calculated for Inconel 718 and Al. From the MRR analysis it is found that MRR in case of Al is higher than the Inconel material.
  - From the optimization it is found that the optimum parameter settings are V=8V,I=30A and p=0.25.
  - The MRR calculated through ANSYS model is closer to the experimental MRR except at few parameters this happens because of the p value i.e the heat input value.
  - From the graphs it is observed that the current significantly affects the heat flux .Because current is directly proportional to the heat flux.
  - From the residual stress modelling for both Inconel 718 and Aluminium it's found that residual stress is compressive in nature and it is found maximum in Al then Inconel 718.
  - From the graphs it is observed that with the increase in heat input value the temperature at the surface also increases.
  - From the input parameters current I is the most prominent factor which affects the responses.

References

- [1] J.F. Ready, Effects of High-power Laser Radiation, Academic Press, NewYork, 1971.
- [2] A. Erden, B. Kaftanoglu, Heat transfer modeling of electric discharge machining, Int. Mach. Tool Design Res. Conf. 21 (1980) 351–358.
- [3] M. Kunieda, B Lauwers, KP Rajurkar, BM Schumacher. Advancing EDM through fundamental insight into the process. Ann CIRP 2005;54(2):599–622.
- [4] T. Masuzawa, Micro-EDM. In: Proceedings of the 13th international symposium for electromachining. 2001. p. 3–19.
- [5] T. Masuzawa, State of the art of micromachining. Ann CIRP 2000;49(2):473–88.
- [6] Allen, Chen, Process simulation of micro electro-discharge machining on molybdenum, Journal of Materials Processing Technology186 (2007) 346–355.
- [7] D. Reynaerts, W. Meeusen, X. Song, H. V. Bruseel, S. Reyntjens, D. D. Bruyker, and R. Puers, Integrating electro-discharge machining and photolithography:Work in progress,‖ J. Micromech. Microeng., vol. 10, no. 2, pp. 189–195, June 2000.
- [8] Y. Honma, K. Takahashi, and M. Muro, Micro-machining of magnetic metal film using electro-discharge technique,‖ Adv. Inform. Stor.Syst., vol. 10, pp. 383–399, 1999.
- [9] C. A. Grimes, M. K. Jain, R. S. Singh, Q. Cai, A. Mason, K. Takahata, and Y. Gianchandani, Magnetoelasticmicrosensors for environmental monitoring,‖ in Tech. Dig. IEEE Int. Conf. Micro Electro Mechanical Systems (MEMS‘01), Interlaken, Switzerland, Jan. 2001, pp. 278–281.
- [10] K. Fischer, B. Chaudhuri, S. McNamara, H. Guckel, Y. Gianchandani, and D. Novotny, A latching, bistable optical fiber switch combining LIGA technology with micromachined permanent magnets,‖ in Tech. Dig., IEEE Intl. Conf. on Solid-State Sensors and Actuators (Transducers‘ 01), Munich, Germany, June 2001, pp. 1340–1343.
- [11] Z.Katz, C.J. Tibbles, Analysis of Micro-scale EDM process‖, International Journal of Advanced Manufacturing Technologies, 25 (2005) - 923-928.
- [12] T. Masuzawa, Micro EDM‖. Proceedings of the ISEM XIII (2001).3-19. Fundación Tekniker. ISBN 932064-0-7.
- [13] T. Masuzawa ―State of the Art Micromachining‖. Anals of CIRP Vol 49/02/2000. 473-488.

- [14] M. Albert. ―Fine Wire is just Fine‖, Moder Machine Shop On-line – Gardner Publications Inc.
- [15] S.H .Yeo, G.G. Yap, A Feasibility Study on the Micro Electro-Discharge Machining Process for Photomask Fabrication, The International Journal of Advanced Manufacturing Technology, 18 (2001), pp. 7–11.
- [16] F.T. Weng, M.G. Her, Study of the Batch Production of Micro Parts Using the EDM Process, The International Journal of Advanced Manufacturing Technology, 19 (2002),pp. 266-270.
- [17] B. Schacht, J.P. Kruth, B.Lauwers, P. Vanherck,., The skin-effect in ferromagnetic electrodes for wire-EDM, The International Journal of Advanced Manufacturing Technology, 23 (2004), pp. 794–799.
- [18] J. Fleischer, T. Masuzawa,., J. Schmidt, M. Knoll, New applications for micro-EDM,Journal of Materials Processing Technology, 149 (2004), pp. 246–249
- [19] Agie, From micro to nano EDM system performance, 10 July, 2006,

  http://www.agieus.com/PRs/Micro_to_Nano.asp.

- [20] G. Kibria & B. R. Sarkar & B. B. Pradhan & B. Bhattacharyya. ―Comparative study of different dielectrics for micro-EDM performance during microhole machining of Ti-6Al-4V alloy‖, Int J AdvManufTechnol (2010) 48:557–570.
- [21] S. Mahendran, R. Devarajan, T. Nagarajan, and A. Majdi, A Review of Micro-EDM ,international journal 2010 vol – 2,IMECS 2010.
- [22] Muralidhara, Nilesh Jayanthilal Vasa, and Singaperumal , a piezoactuated tool feed mechanism for micro edm Precision Engineering and Instrumentation Lab. International Journal of Machine Tools & Manufacture.
- [23] Hideki Takezawa , Naotake Mohri , Kouhei Asano , and Yasunori Kodama, Development of Micro Electrical Discharge Machine Int. J. of Automation Technology Vol.2 No.2, 2008.
- [24] Fuzhu Hana, Shinya Wachi , Masanori Kunieda Improvement of machining characteristics of micro-EDM using transistor type isopulse generator, Precision Engineering 28 (2004) 378–385.
- [25] ÖPÖZ, Tahsin, Tecelli manufacturing of micro holes by using micro electric discharge machining (MICRO-EDM), a master's thesis in Mechatronics Engineering Atılım University.

- [26] Mark T. Richardson, and Yogesh B. Gianchandani, ―Wireless Monitoring of Workpiece Material Transitions and Debris Accumulation in Micro-Electro-Discharge Machining‖, journal of microelectromechanical systems, vol. 19, no. 1, february 2010.

- [27] Chanda Kumar Biswas, Mohan Kumar Pradhan; FEM of residual stress of EDMed surfaces.

- [28] Philip Allen, Xiaolin Chen; Process simulation of micro electrodischarge machining of molybdenum, JMPT 186, 2007.

- [29] F. Han, Y.Yamada, T. Kawakami, M. Kunieda, 2006 "Experimental attempts of sub-micrometer order size machining using micro-EDM", Precis. Eng. 30 123-131.

- [30] D.M. Cao, J. Jiang, W.J.Meng, J.C.Jiang, W. Wang, 2007 "Fabrication of high-aspect-ratio microscale Ta mold inserts with micro electrical discharge machining", Microsystem Technologies 13 503-510.

- [31] F. Klocke, D .Lung, Antonoglou, G. Thomaidis, 2004 "The effects of powder suspended dielectrics on the thermal influenced zone by electrodischarge machining with small discharge energies" J. Mater. Process. Technol. 149 191-197.

- [32] H.S. Liu, B.H .Yan, F.Y.Huang, K.H. Qiu, 2005 "A study on the characterization of high nickel alloy micro-holes using micro-EDM and their applications" J. Mater. Process. Technol. 169 418-426.

- [33] Z.Yu, T. Masuzawa, M. Fujino, 1998 "Micro-EDM for Three Dimensional Cavities-Development of Uniform Wear Method", Ann. CIRP. 47 169-172.

- [34] H.S Lim, Wong, Y.S. Rahman, M. Edwin Lee, M.K., 2003 "A study on the machining of high-aspect ratio micro-structures using micro-EDM" J. Mater. Process. Technol. 140 318-325.

- [35] A.C Wang, B.H Yan, Y.X.Tang, F.Y .Huang,., 2005 "The feasibility study on a fabricated micro slit die using micro EDM", Int. J. Adv. Manuf. Tech. 25 10-16.

- [36] Prasad Bari et al (2005) "Dielectric Fluid in electro discharge machining" International Journal of Manufacturing Technology.

- [37] B. B. Pradhan, M. Masanta, B. R. Sarkar and B. Bhattacharyya, ―Investigation of electro discharge micro- machining of titanium super alloy‖, International Journal of Advance Manufacturing Technology (2009) 41:1094–1106.

- [38] S. Keith Hargrove, Duowen Ding; Determining cutting parameter in wire EDM based on workpiece temperature distribution, Int J AdvManuf Technol, 2007.

- [39] K.G. Satyanarayana, A. Rajadurai, and B. Mohan, Effect of SiC and rotation of electrode on electric discharge machining of Al-SiC composites, Journal of Materials Processing Technology 124 (2002) 297-304.

- [40] H.K. Kansala, Sehijpal Singh, Pradeep Kumar (2008). "Numerical simulation of powder mixed electric discharge machining (PMEDM) using finite element method"Mathematical and Computer Modelling 47 : pp 1217–1237.

- [41] G. L. Benavides et al "High aspect ratio meso-scale parts enabled by wire micro-EDM"Journal of Materials Processing Technology.

- [42] K.H.Ho and S.T. Newman, (2003), "State of the art in electrical discharge machining (EDM)", International Journal of Machine Tools & Manufacture, 43, 1287–1300.

- [43] A.B. Puri, and B. Bhattacharyya, (2003), "An analysis and optimization of the geometrical inaccuracy due to wire lag phenomenon in WEDM", International Journal of Machine Tools & Manufacture, 43, 151–159.

- [44] S .Saha, Pachon, M. Ghoshal, M.J. Schulz, (2004), "Finite element modeling and optimization to prevent wire breakage in electro-discharge machining", Mechanics Research Communications, 31, 451–463.

- [45] Y.F .Tzeng, and N.H Chiu, (2003), "Electrical-discharge machining process using a Taguchi dynamic experiment", International Journal of Advanced Manufacturing Technology, 21, 1005-1014.

- [46] Fuzhu Han, Li Chen, Dingwen Yu and Xiaoguang Zhou, ―Basic study on pulse generator for micro-EDM‖, International Journal of Advance Manufacturing Technology (2007) 33: 474– 479.

- [47] Seong Min Son, Han Seok Lim, A.S. Kumar and M. Rahman, ―Influences of pulsed power condition on the machining properties in micro EDM‖, Journal of Materials Processing Technology 190 (2007) 73–76.

- [48] Aditya Shah, Vishal Prajapati, Pavan Patel and AkashPandey, ―Development of Pulsed Power Dc Supply for Micro EDM‖, UGC National Conference on Advances in Computer Integrated Manufacturing (NCACIM) February 16-17, 2007.

- [49] P. Horowitz and W. Hill ―The Art of Electronics‖, Cambridge University Press, 1989, 0- 521-49846-5.

- [50] T.Masuzawa, M.Fujino (1980) Micro pulse for EDM. Proc Japan Society for Precision Engineering Autumn Conference,pp 140–142 .

- [51] B.H. Yan, H.C. Tsai and Y.C. Lin, ―Study on EDM characteristics of cemented carbides‖, in: Proceedings of the 14th National Conference on Mechanical Engineering, The Chinese Society of Mechanical Engineers, 1997, pp. 157 - 164.

- [52] A. Guha, S. Smyers, K.P. Rajurkar, P.S. Garinella and R. Konda, ―Optimal parameters in electrical discharge machining of copper - beryllium alloys‖, Proceedings of the International Symposium for Electro machining, ISEM XI, April 17 - 21, 1995, EPFL, Lausanne, Switzerland, pp. 217 - 224.

- [53] C. Diver, J. Atkinson,Helml, 2004 "Micro-EDM drilling of tapered holes for industrial applications", J. Mater. Process. Technol. 149 296-303.

- [54] T .Masuzawa, M. Fujino (1980) Micro pulse for EDM. Proc Japan Society for Precision Engineering Autumn Conference,pp 140–142 .

- [55] C. Diver, Atkinson, J. Helml, H.J., Li, L., 2004 "Micro-EDM drilling of tapered holes for industrial applications", J. Mater. Process. Technol. 149 296-303.

- [56] P. Shankar, V.K. Jain, T. Sundarajan, Analysis of spark profilesduring EDM process, Machining Science and Technology 1 (2) (1997) 195–217.

- [57] M K Pradhan, Process Simulation, modelling and estimation of Temperature and residual Stresses Electrical Discharge Machining of AISI D2 steel Department of Mechanical Engineering, Maulana Azad ISCI 2012.

- [58] V. Yadav, V. Jain, P. Dixit, Thermal stresses due to electrical discharge machining, Int. J. Mach. Tools Manuf. 42 (2002) 877–888.

- [59] S.N. Joshi and S.S. Pandey Thermo-physical modeling of die-sinking EDM process , Journal of Manufacturing Processes 12 (2010) 45_56.

- [60] A.G. Mamalis, N.M. Vosniakos, N.M. Vacevanidis, X. Junzhe, Residual Stress Distribution and Structural Phenomena of High-Strength Steel Surfaces Due to EDMand Ball-Drop Forming, CIRP Annuals, 37 (1) (1988) 531-535.

- [61] J.C. Rebelo, A.M.Diaz, D. Kremer, and J.L Lebrun,.: "Influence of Pulse Energy onthe Surface Integrity of Martensitic Steels" Journal of Materials Processing Technology,84 (1-3) (1998) 90-96.
- [62] J.P. Kruth, P. Bleys, Measuring Residual Stress Caused by Wire EDM of Tool Steel,International Journal of Electrical Machining, 5 (1) (2000) 23-28.
- [63] http://en.wikipedia.org/wiki/Taguchi_methods.